PREPARATION AND CHRACTERIZATION OF CELLULOSE NANOFIBRILS USING VARIOUS PRETREAMENT TECHNIQUES

by

HANSOL LEE

(Under the Direction of Sudhagar Mani)

ABSTRACT

Cellulose nanofibrils (CNF) has received a great attention due to its renewability, biodegradability and remarkable mechanical properties. This study investigated the effects of mechanical pretreatment using a shear cutting mill and low-concentration NaOH pretreatment on the production and properties of CNF. Three-cycle shear cutting of fluff pulp was suitable for producing CNF precursors, while consuming lower energy compared with other mechanical pretreatments by wet milling methods. Low-concentration NaOH (2wt.%) at low temperature (below 0 ℃) was a promising alternative condition to prepare CNF with improved thermal stability. CNF produced with 2wt% NaOH had comparable properties with the standard CNF produced at pilot scale. A life cycle assessment study on the CNF production concluded that the integration of mechanical and alkaline pretreatments potentially reduced the overall energy consumption and the global warming potentials. Further research is required to validate the proposed pretreatment techniques prior to commercialization.

INDEX WORDS: Cellulose nanofibrils, Shear cutting mill, Specific grinding energy, NaOH treatment, Life cycle assessment

PREPARATION AND CHRACTERIZATION OF CELLULOSE NANOFIBRILS USING VARIOUS PRETREAMENT TECHNIQUES

by

HANSOL LEE

B.S., Seoul National University, Republic of Korea, 2014.

A Thesis Submitted to the Graduate Faculty of The University of Georgia in Partial Fulfillment of the Requirements for the Degree

MASTER OF SCIENCE

ATHENS, GEORGIA

2016

PREPARATION AND CHRACTERIZATION OF CELLULOSE NANOFIBRILS USING VARIOUS PRETREAMENT TECHNIQUES

by

HANSOL LEE

Major Professor: Sudhagar Mani
Committee: Hitesh Handa
Peter Kner

Electronic Version Approved:

Suzanne Barbour
Dean of the Graduate School
The University of Georgia
August 2016

ACKNOWLEDGEMENTS

I would like to thank my advisor, Dr. Sudhagar Mani, who has guided me with patience and support throughout my graduate studies. The completion of this work would not be possible without his scientific insight and constant encouragement. I also would like to thank Dr. Hitesh Handa and Dr. Peter Kner for serving on my graduate advisory committee and offering helpful comments and suggestions. Thank to Dr. Eric Freeman for his generosity to allow me to work in his lab. Thank also to Dr. Jaya Sundaram for providing technical assistance at various stages of my research work. I am grateful to Dr. Hari P. Singh at Fort Valley State University for his financial support on electron microscopic studies, which made this work much more fruitful.

I would like to acknowledge my fellow lab members: Kamalakanta Sahoo, Yue Yang, Maryam Manouchehrinejad, Ikenna Joseph Okeke, and Thomas Brett Beery for their help over years. I will always cherish the memories we have mad together, and I hope there will be many more. I also appreciate the dedicated assistance of Lu Zhu, who provides a great deal of XRD data for this work. I would like to offer a special thanks to Natalia Bhattacharjee (née Shim), as she became one of my best friends. We shared every moment of happiness and sorrow with each other, and her friendship has been incredibly importance to me.

I would like to thank my parents, who have been my biggest supporters, encouraging me in every aspect of my life. I am thankful for everything that they have given me. Without their unconditional love and support, I could not finish this hard work.

Last but not least, thank you to Seungwon Ryu. As my fiancé, he has encouraged me not to give up on my goal. He has stayed by my side throughout everything, and I truly cannot imagine going through these last several years without him.

TABLE OF CONTENTS

Page

ACKNOWLEDGEMENTS iv

LIST OF TABLES ix

LIST OF FIGURES x

CHAPTER 1 INTRODUCTION 1

CHAPTER 2 REVIEW OF LITERATURE 11

1. Cellulose 11
2. Nanocellulose 12
3. Production of cellulose nanofibrils 15
4. Pretreatment methods 17
   - 4.1. Mechanical pretreatments for CNF production 17
   - 4.2. Chemical pretreatments for CNF production 20
5. Life cycle assessment (LCA) 26
   - 5.1. LCA of CNF production 27
6. Summary 28

CHAPTER 3 SHEAR CUTTING OF FLUFF PULP TO PRODUCE CELLULOSE PRECURSORS FOR CELLULOSE NANOFIBRILS 54

1. Introduction 56
2. Materials and Method 58
   - 2.1. Material and shear cutting process 58
   - 2.2. Shear cutting energy consumption study 58
   - 2.3. Characterization of knife-milled powders 59

2.4. Cellulose nanofibrils preparation 62
2.5. Characterization of cellulose nanofibrils 62
2.6. Statistical analysis 64
3. Results and discussion 64
3.1. Energy consumption for shear cutting process 64
3.2. Morphology of cellulose precursor/powder 66
3.3. Physical properties of cellulose precursors/powder 67
3.4. Effect of shear cutting on CNF production 69
4. Conclusions 71
CHAPTER 4 DEVELOPMENT OF THERMALLY STABLE CELLULOSE NANOFIBRILS USING LOW-CONCENTRATION ALKALINE TREATMENT 92
1. Introduction 94
2. Materials and Method 97
2.1. Materials and Chemicals 97
2.2. Alkaline treatment 98
2.3. Cellulose nanofibrils preparation 98
2.4. Characterization of alkali-treated cellulose 99
2.5. Characterization of fibrillated cellulose 100
2.6. Statistical analysis 103
3. Results and Discussion 103
3.1. Alkaline treatment 103
3.2. Characterization of fibrillated cellulose 105
4. Conclusions 112
CHAPTER 5 LIFE CYCLE ASSESSMENT OF PRODUCING CELLULOSE NANOFIBRILS WITH MECHANICAL AND ALKALINE PRETREATMENT 132
1. Introduction 134
2. LCA Scope and Functional unit definition 136
3. Process description 137

3.1. Pulp production 137
3.2. Valley beating route 137
3.3. Shear cutting route 138
3.4. Alkaline pretreatment route 138
3.5. Key assumptions 139
4. Life cycle inventory analysis (LCI) 140
5. Life cycle impact assessment (LCIA) 141
5.1. Fossil energy consumption 142
5.2. Global warming potential (GWP) 143
5.3. Water intake 144
5.4. Eutrophication potential 144
6. Sensitive analysis 145
6.1. Fossil energy consumption 146
6.2. Global warming potential (GWP) 147
6.3. Water intake 147
6.4. Eutrophication potential 148
7. Comparison to other carbon nanomaterials 148
8. Conclusions 150
CHAPTER 6 CONCLUSIONS AND RECOMMENDATIONS 161
APPENDIX A 164
APPENDIX B 171
APPENDIX C 177

LIST OF TABLES

Page

Table 3.1: Grinding rate and effective specific energy of shear cutting process with the different number of cycles 77

Table 3.2: Average width, length and aspect ratio of fluff pulp and one to three-cycle knife-milled powders 78

Table 3.3: Physical properties of one to three-cycle knife-milled powders 79

Table 3.4: Average fiber width and specific surface area (SSA) for samples 80

Table 4.1: Onset and DTG peak thermal degradation temperature of fibrillated cellulose fibers prepared with various NaOH solutions with or without CMC 118

Table 5.1: Input inventory for producing one kg of cellulose nanofibrils with three different processing routes 155

Table 5.2: Emissions to air per kg cellulose nanofibrils from three production routes 156

Table 5.3: Life cycle impact assessment of producing one kg of cellulose nanofibrils with three different processing routes 157

LIST OF FIGURES

Page

Figure 2.1: Chemical strucutre of cellulose 41

Figure 2.2: Schematic structure of (a) cotton fiber and (b) wood fiber 42

Figure 2.3: Cellulose fibrils surrounded by hemicellulose and lignin 43

Figure 2.4: Crystal structure of cellulose Iβ and cellulose II 44

Figure 2.5: A brief production process of cellulose nanofibrils (CNF) and cellulose nanocrystals (CNC) from lignocellulosic materials 45

Figure 2.6: Description of homogenizer systems 46

Figure 2.7: Description of microfluidizer systems 47

Figure 2.8: French pressure cell press 48

Figure 2.9: PFI Mill and Valley beater 49

Figure 2.10: TEMPO-mediated oxidation of cellulose at pH 10-11 50

Figure 2.11: Carboxymethylation of cellulose 51

Figure 2.12: Molecular rearrangement of cellulose chains in mercerization 52

Figure 2.13: Schematic conversion of cellulose I (a) into cellulose II (b) in a ramie fiber 53

Figure 3.1: A laboratory heavy-duty shear cutting mill 81

Figure 3.2: Complete flow diagram for shear cutting process 82

Figure 3.3: Fluff pulp (left) and three-cycle knife-milled powder (right) 83

Figure 3.4: Optical microscopic images of (a) raw fluff pulp at 5 times magnification and (b) one-, (c) two-, and (d) three-cycle knife-milled powders at 20 times magnification 84

Figure 3.5: Particle size distributions of one- to three-cycle knife-milled powders.....85
Figure 3.6: X-ray diffraction patterns of fluff pulp and knife-milled powders with one to three grinding cycles.....86
Figure 3.7: A photo of fibrillated cellulose gel after 15 passes through a French press (left) and standard CNF from University of Maine (right).....87
Figure 3.8: Optical microscopic images of the three-cycle knife-milled cellulose after passing through a French press with (a) 10 passes and (b) 15 passes.....88
Figure 3.9: Scanning microscopic images of (a) the fibrillated cellulose with 15 passes through a French press and (b) standard cellulose nanofibrils from University of Maine 89
Figure 3.10: The distribution of fiber width for the fibrillated cellulose passed through a French press with 15 passes (top) and standard cellulose nanofibrils from University of Maine (bottom).....90
Figure 3.11: Dispersion states of the 0.1wt% suspensions of (a) the fibrillated cellulose passed through a French press with 15 passes, and (b) standard cellulose nanofibrils from University of Maine at 0, 10 and 90 minutes (from left to right) 91
Figure 4.1: Summary of cellulose nanofibrils production procedure in this study.....119
Figure 4.2: Cellulose Solubility in various concentrations of NaOH solutions with or without CMC 120
Figure 4.3: Optical microscopic images of cellulose fibers treated with 2-6wt% NaOH solutions without (left) or with CMC (right) (a,b : 0wt%, c,d : 2wt%, e,f : 4wt%, g,h : 6wt% NaOH solutions).....121
Figure 4.4: Fibrillated cellulose samples treated with 2-6wt% NaOH solutions without (left) or with CMC (right) (a,b : 2wt%, c,d : 4wt%, e,f : 6wt% NaOH solutions).....122

Figure 4.5 Dispersion states of the 0.1wt% fibrillated cellulose suspensions at 0, 10, 60 minutes and 24 hours (a: standard CNF, b: H-CMC-CNF, c: 2NaOH, d: CMC-2NaOH, e: 4NaOH, f: CMC-4NaOH, g: 6NaOH, and h: CMC-6NaOH) 123

Figure 4.6: Optical microscopic images of alkali-treated cellulose without (left) or with CMC (right) after the fibrillation process through a French cell press 10 times (a,b : 2wt%, c,d : 4wt%, e,f : 6wt% NaOH solutions) 124

Figure 4.7: Optical microscopic images of fibrillated cellulose samples treated with 2-6wt% NaOH solutions without (left) or with CMC (right) (a,b : 2wt%, c,d : 4wt%, e,f : 6wt% NaOH solutions) 125

Figure 4.8: SEM images of fibrillated cellulose samples treated with 2-6wt% NaOH solutions without (left) or with CMC (right) (a,b: 2wt%, c,d : 4wt%, e,f : 6wt% NaOH solutions), (g) standard CNF and (h) H-CMC-CNF 126

Figure 4.9: Diameter distribution of (a) the fibrillated cellulose treated with 2wt% NaOH solution containing CMC, (b) standard CNF and (c) H-CMC-CNF 127

Figure 4.10: STEM images of (a) the fibrillated cellulose treated with 2wt% NaOH solution containing CMC, (b) standard CNF and (c) H-CMC-CNF 128

Figure 4.11: Specific surface area of cellulose powder, the fibrillated cellulose treated with 2wt% NaOH solution containing CMC, standard CNF and H-CMC-CNF 129

Figure 4.12: XRD patterns of fibrillated cellulose treated with 2-6wt% NaOH solution (1) without or (2) with CMC (a,d :2wt%, b,e : 4wt%, c,f : 6wt% NaOH solution), (g) cellulose powder, (h) standard CNF, (i) H-CMC-CNF 130

Figure 4.13: TG (top) and DTG (bottom) curves of fibrillated cellulose treated with 2-6wt% NaOH solution with or without CMC, standard CNF and H-CMC-CNF 131

Figure 5.1: A flowchart of CNF production with three different production routes: (1) the Valley beating route (to the left), (2) the shear cutting route (in the middle), and (3) the alkaline pretreatment route (to the right).....158
Figure 5.2: Comparative life cycle impact assessments of three different routes; Valley beating route, shear cutting route and alkaline pretreatment route (left to right).....159
Figure 5.3: Sensitive analysis of four different factors on global warming potential (top), water intake (middle) and cumulative energy demand, total (bottom).....160

CHAPTER 1

INTRODUCTION

Cellulose is the most abundant natural biopolymer derived from wood, cotton and other non-wood fiber sources (agricultural residues and grasses). Paper and pulp industries are converting woody biomass into various formats of cellulose fibers for manufacturing papers, tissues, moisture absorbents and several cellulose derivatives for chemical and pharmaceutical applications. For example, ethylcellulose is commercially used in coating, binder, and controlled-release drug systems, and other ether derivatives (carboxymethyl cellulose, hydroxyethyl cellulose) are also used as a viscosity modifier, gelling agent, foaming agent, and binding agent (Dufresne, 2013). Cellulose nanofibrils (CNF) is one type of nanocellulose, which typically has a diameter in range of below 100 nm and a length of several micrometers. The process of producing CNF was first developed by Turbak et al. (1983a) and Herrick et al. (1983). CNF has many desirable characteristics that make it a promising material for a wide range of applications, such as food, packaging, electronic, and biomedical applications. Firstly, CNF has exceptional mechanical properties as it can form extensive network structures due to its nano-scale dimensions. Yano and Nakahara (2004) reported that a pure CNF film had tensile strength of 250 MPa, but the value varied widely (222-310 MPa) as reported in the literature (Abe and Yano, 2009; Fukuzumi et al. 2009; Saito et al. 2009). The tensile strength of CNF is much higher than that of commercial polymers, such as polyethylene, polystyrene, and polycarbonate (up to 70 MPa) and also higher than that of high performance polymers, such as polyimide and polyetheretherketon (70-100 MPa) (Stevens, 1999). CNF is also lightweight (0.81-1.53 gcm-3)

and has a very good ability to form a transparent film (Yano and Nakahara, 2004; Abe and Yano, 2009; Syverud and Stenius, 2009). In addition, the cost of CNF could be reduced to relatively low compared with that of petroleum-based polymers since forest biomass and energy grasses are abundantly renewable feedstock and potential raw materials for manufacturing CNF.

Cellulose nanofibrils is manufactured from cellulose materials using a mechanical disintegration process, such as high pressure homogenization, microfluidization, and micro-grinding. In these approaches, cellulose fibers are delaminated by high shearing forces or/and impact forces. However, the mechanical disintegration process requires a vast amount of energy because the numerous processing cycles are necessary to obtain well-fibrillated cellulose nanofibrils. More specifically, the energy needed for the high pressure homogenization reaches as high as 70,000 kWh/ton (Eriksen et al. 2008).

To address this energy problem, various pretreatment processes have been developed using mechanical, chemical or/and enzymatic methods. Mechanical pretreatment process reduces cellulose fiber size and pre-fibrillates cellulose fibers. PFI mills and Valley beaters are commonly used as mechanical pretreatment methods (Chakraborty et al. 2005; Zhang et al. 2012; Spence et al. 2011; Sharma et al. 2015). Chemical pretreatment process introduces negatively charged functional groups on the cellulose surface, leading to repulsive forces between cellulose fibers; thus facilitating the disintegration of cellulose fibers easily. TEMPO-mediated oxidation and carboxymethylation are the common approaches for chemical pretreatment (Saito et al. 2006; Wagberg et al. 2008; Eyholzer et al. 2010; Besbes et al. 2011a and 2011b). However, each pretreatment technique achieved limited success because of its own disadvantages.

Firstly, the mechanical pretreatment process needs a certain amount of energy, potentially increasing the overall energy consumption for cellulose nanofibrils production. For instance, refining wood pulps in a Valley beater required 2,000 kWh/ton for the total refining time of 3 hours (Atic et al. 2005; Spence et al. 2011). In addition, the mechanical pretreatments with a Valley beater and a PFI mill (or wet milling) are performed in water at low pulp consistency of approximately 2% and 10%, respectively. This indicates that these mechanical pretreatment processes produce the cellulose precursors in wet form, which would make difficulties during storage and handling. A shear cutting mill, known as a knife mill (or dry milling) has a potential as a low-energy mechanical pretreatment method, producing the cellulose precursors in dry form, which can be easily handled and stored. Shear cutting process has been used to grind food, feed and biomass, and it was reported that the energy necessary for grinding grasses in a shear cutting mill ranged in 150-200 kwh/ton with a screen size of one mm (Miao et al. 2011). Thus, it can be expected that energy consumption for grinding wood pulps would be comparatively low. In addition, the available screen size is as small as 0.25 mm, and the repeated shear cutting of cellulose pulp with 0.25 mm screen could produce very fine cellulose powder, which can be used as the cellulose precursors for CNF production.

Moreover, chemical pretreatment processes have some drawbacks. These processes consume several organic solvents, leading to increased environmental impacts of cellulose nanofibrils. Specifically, carboxymethylation requires 30 kg of organic solvents to produce one kg of CNF (Arvidsson et al. 2015). It has been also reported that the introduction of functional groups, such as carboxyl and carboxymethyl groups, causes the decrease in thermal stability of cellulose nanofibrils. For example, the onset thermal decomposition of chemically-modified CNF was up to 100 ℃ lower than that of untreated CNF (Fukuzumi et al. 2009; Eyholzer et al.

2010). Alkaline pretreatment process with sodium hydroxide solution could be an alternative chemical pretreatment method, reducing the problems caused by other chemical pretreatments. This process could bring benefits to cellulose nanofibrils in two ways. First, it could improve thermal stability of cellulose nanofibrils by converting cellulose crystalline structure from parallel cellulose I to antiparallel cellulose II, which is considered the most thermally stable among cellulose crystalline forms. Wang et al. (2014) successfully prepared cellulose II nanofibers by processing cellulose fibers in 17.5wt% NaOH solution, and cellulose II nanofibers had a higher onset thermal degradation temperature (326 ℃) than cellulose I nanofibers (302 ℃). Secondly, NaOH treatment is able to help cellulose fibers disintegrated easily since it is capable of swelling the fibers. However, the swelling effect disappears after neutralization. This is because cellulose II chains have opposite polarities each other and are therefore aggregated together when the swelling agents (sodium ions) are rinsed out (Shibazaki et al. 1997; Dinand et al. 2002). It is much more difficult to disintegrate the aggregated cellulose fibers compared with original cellulose fibers, resulting in the increased processing cycles and thus energy input. The use of high concentration of NaOH solution also leads to the considerable water usage during neutralization. Therefore, high-concentration NaOH treatment is unlikely to be applied to a large-scale production. Instead, low-concentration NaOH treatment with a dispersing agent, carboxymethylcellulose (CMC), might be technically feasible. It has been reported that NaOH solutions at 6wt.% or higher concentrations swell and even partially dissolve cellulose fibers when the reaction temperature is below 0 ℃, while causing conversion of the cellulose crystal structure to cellulose II (Sobue et al. 1939; Isogai and Atalla 1998; Cuissinat and Navard 2006; Wang 2008). This is the motivation to propose low-concentration NaOH treatment as an alternative pretreatment technique for cellulose nanofibrils production. We expect that NaOH

solutions at very low concentration (2-6wt.%) are also able to swell cellulose fibers, but without significant dissolution of cellulose. This NaOH treatment also could help improve thermal stability of the resultant cellulose nanofibrils by converting cellulose crystal structure. Wang et al. (2008) demonstrated that cellulose crystal structure was transformed to cellulose II with only 4wt% NaOH. In addition, reduced NaOH concentration would decrease water usage for neutralization.

Moreover, the addition of CMC would minimize the cellulose aggregation during neutralization and facilitate fiber disintegration since it creates the repulsive forces and lubricating effect between cellulose fibers (Yan et al. 2006; Ankerfors 2015). Therefore, the pretreatment process with low-concentration NaOH solutions containing CMC could be a way to make the CNF production easier as well as to improve CNF thermal stability, while causing low environmental impacts compared with other chemical pretreatments.

Finally, a life cycle assessment (LCA) tool can be used to assess the environmental impacts of producing CNF using mechanical and chemical pretreatments. LCA examines every stage of the whole product life cycle from raw material production to final disposal of the product. The impact categories typically include global warming, acidification, eutrophication, ozone depletion, smog, ecotoxicity, and so on. It is very important to perform LCA of a new product at the research and development stage in order to identify which step creates environmental impacts the most and what improvement can be made against the benchmarking product. Cellulose nanofibrils itself is considered sustainable and environmentally-friendly as it can be prepared from forest biomass and energy grasses. However, the CNF production process includes the use of energy and chemicals, which could negatively affect environment and human. Three LCA studies of producing cellulose nanofibrils have been published in the literature

(Hohenthal et al. 2012, Li et al. 2013; Arvidsson et al. 2015). The LCA study by Arvidsson et al. (2015) showed that using chemical pretreatments greatly increased the environmental impacts of CNF production. For instance, CNF production with chemical pretreatments produced CO_2 eq. emission as high as 1,160 kg/kg CNF, which is much higher than from CNF production without any pretreatment (1.2-23 kg/kg CNF). Although these three LCA studies assessed the environmental impacts of producing cellulose nanofibrils with various pretreatment techniques, the environmental impacts of CNF production with a mechanical or an alkaline pretreatment process have been not studied.

Main objectives

The main objective of this study is to develop efficient and cost-effective pretreatment technologies to manufacture cellulose nanofibrils (CNF) for food, biomedical and biomaterials applications. The specific objectives are

- To determine the specific energy consumption and physical characterization of cellulose precursors to produce CNF using a mechanical pretreatment technique (shear cutting method)
- To experimentally investigate the effect of alkaline treatment (NaOH) on the production and properties of CNF.
- To conduct a comparative life cycle assessment of manufacturing CNF from conventional and proposed pretreatment techniques to evaluate energy and environmental impacts.

References

Abe, K., Yano, H., 2009, Comparison of the characteristics of cellulose microfibril aggregates of wood, rice straw and potato tuber, Cellulose, 16:1017–1023.

Ankerfors, M., 2015, Microfibrillated cellulose: Energy-efficient preparation techniques and key properties, PhD. Dissertation, KTH Royal Institute of Technology.

Arvidsson, R., Nguyen, D., Svanstrom M., 2015, Life cycle assessment of cellulose nanofibrils production by mechanical treatment and two different pretreatment processes, Environ. Sci. Technol., 49:6681-6890.

Atic, C., Immamoglu, S., Valchev, I., 2005, Determination of specific beating energy-applied on certain pulps in a valley beater, J. Univ. Chem. Technol. Met., 40(3):199–204.

Besbes, I., Alila, S., Boufi, S., 2011a, Nanofibrillated cellulose from TEMPO-oxidized eucalyptus fibers: Effects of the carboxyl content, Carbohydrate Polymers, 84:975-983.

Besbes, I., Vilar, M.R., Boufi, S., 2011b, Nanofibrillated cellulose from Alfa, Eucalyptus and Pine fibres: Preparation, characteristics and reinforcing potential, Carbohydrate Polymers, 86:1198-1206.

Chakraborty, A., Sain, M., Kortschot, M., 2005, Cellulose microfibrils: A novel method of preparation using high shear refining and cryocrushing, Holzforschung, 59:102-107.

Cuissinat, C., Navard, P., 2006, Swelling and dissolution of cellulose part II: free floating cotton and wood fibres in NaOH–water–additives Systems, Macromolecular Symposia, 244(1):19-30.

Dinand, E., Vignon, M., Chanzy, H., Heux, L., 2002, Mercerization of primary wall cellulose and its implication for the conversion of cellulose I to cellulose II, Cellulose, 9:7-18.

Dufresne, A., 2013, Nanocellulose: From Nature to High Performance Tailored Materials, Walter de Gruyer, Berlin & New York.

Eriksen, Ø., Syverud, K. and Gregersen, Ø., 2008, The use of microfibrillated cellulose produced from kraft pulp as strength enhancer in TMP paper, Nordic Pulp & Paper Research Journal, 23(3):299-304.

Eyholzer, Ch., Bordeanu N., Lopez-Suevos, F., Rentsch D., Zimmermann T., Oksman, K., 2010, Preparation and characterization of water-redispersible nanofibrillated cellulose in powder form, Cellulose 17:19-30.

Fukuzumi, H., Saito, T., Iwata, T., Kumamoto, Y., Isogai, A., 2009, Transparent and high gas barrier films of cellulose nanofibers prepared by TEMPO-mediated oxidation, Biomacromolecules, 10:162-165.

Herrick, F.W., Casebier, R.L., Hamilton, J.K., Sandberg, K.R., 1983, Microfibrillated cellulose: Morphology and accessibility. J. Appl. Polym. Sci.: Appl. Polym. Symp. 37, 797-813.

Hohenthal, C., Ovasakainen, M., Bussini, D., Sadocco, P., Pajula, T., Hannele, L., Kautto, J., Salmenkivi, K., 2012, Final assessment of nanoenhanced new products, VTT Technical Research Centre of Finland.

Li, Q., McGinnis, S., Sydnor, C., Wong, A., Renneckar, S., 2013, Nanocellulose life cycle assessment, ACS Sustainable Chem. Eng., 1:919-928.

Miao, Z., Grift, T.E., Hansen, A.C., Ting, K.C., 2011, Energy requirement for comminution of biomass in relation to particle physical properties, Industrial Crops and Products, 33(2):504-513.

Saito T., Nishiyama Y., Putaux J.L., Vignon M., Isogai A., 2006, Homogeneous suspensions of individualized microfibrils from TEMPO-catalyzed oxidation of native cellulose, Biomacromolecules, 7:1687-1691.

Saito, T., Hirota, M., Tamura, N., Kimura, S., Fukuzumi, H., Heuz, L., Isogai, A., 2009, Individualization of nano-sized plant cellulose fibrils by direct surface carboxylation suing TEMPO catalyst under neutral conditions, Biomacromolecules, 7:1687-1691.

Sharma, S. Nair, S.S., Zhang, Z., Ragauskas, A.J., Deng, Y., 2015, Characterization of micro fibrillation process of cellulose and mercerized cellulose pulp, RSC Advances, 5:63111-63122.

Shibazaki, H., Kuga, S., Okano, T., 1997, Mercerization and acid hydrolysis of bacterial cellulose, Cellulose 4:75-87.

Shibazaki, H., Kuga, S., Okano, T., 1997, Mercerization and acid hydrolysis of bacterial cellulose, Cellulose, 4:75-87.

Sobue, H., Kiessig, H., Hess, K., 1939, The cellulose-sodium hydroxide-water system as a function of the temperature, Z. Physik. Chem. B, 43:309–328.

Spence, K.L., Benditti, R.A., Rojas, O.J., Habibi, Y., Pawlak, J.J., 2011, A comparative study of energy consumption and physical properties of microfibrillated cellulose produced by different processing methods, Cellulose, 18:1097-1111.

Stevens, M.P., 1999, Polymer Chemistry: An introduction, 3rd edition, Oxford University Press, New York.

Syverud, K. and Stenius, P., 2009, Strength and barrier properties of MFC films, Cellulose, 16:75-85.

Turbak, A.F., Snyder, F.W., Sandberg, K.R. 1983a, Microfibrillated cellulose, a new cellulose product: Properties, uses, and commercial potential, J. Appl. Polym. Sci. Appl. Polym. Symp., 37:815-827.

Wågberg, L., Norgren, G.D.M., Lindstrom, T., Ankerfors, M., Axnas, K., 2008, The build-up of polyelectrolyte multilayers of microfibrillated cellulose and cationic polyelectrolytes, Langmuir, 24:784-795.

Wang, H., Li, D., Yano, H., Abe, K., 2014, Preparation of tough cellulose II nanofibers with high thermal stability from wood, Cellulose, 21:1505.

Wang, Y., 2008, Cellulose fiber dissolution in sodium hydroxide solution at low temperature: dissolution kinetics and solubility improvement, PhD dissertation, Georgia Institute of Technology.

Yan, H., Lindstrom, T., Christiernin, M., 2006, Some ways to decrease fibre suspension flocculation and improve sheet formation, Nordic Pulp & Paper Research Journal, 21(1):36-43.

Yano, H., Nakahara, S., 2004, Bio-composites produced from plant microfiber bundles with a nanometer unit web-like network, Journal of Materials Science, 39:1635-1638.

Zhang, J., Song, H., Lin, L., Zhuang, J., Pang, C., 2012, Microfibrillated cellulose from bamboo pulp and its properties, Biomass and Bioenergy, 39:78-83.

CHAPTER 2

REVIEW OF LITERATURE

1. Cellulose

Cellulose is the most abundant natural organic polymer as it is a main component of plant cell walls. Since the total annual biomass production is approximately 1.5×10^{12} tons, cellulose is an almost inexhaustible source. Cellulose is a linear polymer as the repeating units of β-d-glucopyranose are linked by linear β -1, 4 glucosidic linkages (Figure 2.1.). Cellulose has a large number of hydrogen groups at C-2, C-3 and C-6 atoms. Due to its linear structure and multiple hydroxyl groups, cellulose can form extensive intra- and intermolecular hydrogen bonds, which enables cellulose to form a stable three-dimensional structure. Intramolecular hydrogen bonds are also responsible for cellulose stiffness and its insolubility in most solvents (Gavillon 2007; Wang, 2008). Besides, cellulose has a hierarchical morphological structure; elementary fibrils (1.5-3.5 nm in widths), microfibrils (10-30 nm in widths) and microfibrillar bands (larger than 100nm in widths) (Klemm et al. 2005). The elementary fibrils pack to the microfibrils, and the microfibrils form the basic structural units of the plant cell wall. Each microfibril can be considered as a string of cellulose crystals, linked along the chain axis by disordered amorphous regions, merging into fibril bundles.

Cellulose is a skeletal component in plants that have ordered cell wall layers. Figure 2.2. schematically represents the cell walls of cotton and wood fibers. In most plant fibers, cellulose predominately exists in the central layer (S2) of a secondary cell wall, and it is surrounded by the amorphous matrix substances (hemicellulose and lignin, Figure 2.3.). The distribution of

cellulose, hemicellulose and lignin differs depending on the plant type. For instance, softwood typically has 42%, 27% and 28% of cellulose, hemicellulose and lignin content, respectively; while hardwood has 45%, 30% and 20%, respectively (Smook, 2002).

Several crystalline forms of cellulose have been determined: cellulose I, II, III and IV, and cellulose I and II have been widely studied. In nature, cellulose is found in the crystalline form of cellulose I that contains two parallel cellulose chains in a unit cell. In the 1980s, CP/MAS NMR spectroscopic studies showed that native cellulose is composed of two different crystalline cellulose I modifications, Iα and Iβ (Atalla and VanderHart, 1984). The ratio of Iα and Iβ greatly depends on cellulose sources. Iα is the main crystalline form in bacterial and algal celluloses; while, Iβ is dominant in higher plants (cotton, wood and etc.). These two crystalline forms have different patterns of hydrogen bonding. Iα has a triclinic cell with one-chain-per-unit cell; whereas, Iβ has a monoclinic cell with two-chains-per-unit cell (Dufresne, 2013). Native cellulose can be converted into cellulose II by two distinct processes: mercerization (treatment with concentrated sodium hydroxide aqueous solutions) or dissolution followed by regeneration. Cellulose II has a monoclinic unit cell like cellulose Iβ; however, the chain arrangement is transited from parallel to antiparallel (Figure 2.4.). Such antiparallel arrangement allows the formation of a larger number of intermolecular hydrogen bonds than the native form. Since the conversion of cellulose I to cellulose II is irreversible, cellulose II is thermodynamically more stable than cellulose I.

2. Nanocellulose

Nanocellulose refers to a cellulosic material that has at least one dimension at a nano scale. It can be classified into three types, cellulose nanofibrils (CNF), cellulose nanocrystals (CNC) and bacterial nanocellulose (BNC) adapted from Klemm et al. (2011). Each type of nanocellulose is

obtained using a different preparation method, and it has different dimensions that affect its functions. A brief production process for CNF and CNC is shown in Figure 2.5.

First, cellulose nanofibrils, known as microfibrillated cellulose, nanofibrillated cellulose, and cellulose nanofibers, was first developed by Turbak et al. (1983a) and Herrick et al. (1983). They conducted mechanical refining and a high pressure homogenization processes with wood cellulose fibers, and they obtained a gel-like material, naming this new material as microfibrillated cellulose. Since then, a number of studies have been conducted on cellulose nanofibrils. Cellulose nanofibrils generally has a diameter of below 100 nm, and a length of several micrometers (Klemm et al. 2011). Due to high aspect ratio (length/width), it forms rigid network structures that induce remarkable mechanical properties. It has been reported that the CNF films have a tensile strength of up to 310 MPa, which is much higher than commercial polymers, such as polyethylene, polystyrene, and polycarbonate (up to 70 MPa) and high performance polymers, such as polyimide and polyetheretherketon (70-100 MPa). (Stevens 1999; Yano and Nakahara 2004; Abe and Yano, 2009; Fukuzumi et al. 2009; Saito et al. 2009). CNF has been incorporated as a reinforcing agent into various polymer matrices, such as polypropylene, poly(lactic acid) and starch. For instance, Jonoobi et al. (2010) reported that CNF-reinforced poly(lactic acid) had a higher tensile strength and modulus (71 MPa and 3.6 GPa, respectively) than pure poly(lactic acid), which had a tensile strength and modulus of 58 MPa and 2.9 GPa, respectively. In addition, CNF gels have not only high viscosity but also a high degree of shear thinning, which makes CNF injectable (Pääkkö et al. 2007). CNF is also renewable as it can be prepared from forestry and agricultural residues. Due to these outstanding characteristics, cellulose nanofibrils has a wide range of potential application fields, such as food, cosmetics, packaging, electronics, and biomedical applications.

Mechanical disintegration process is required to obtain well-delaminated cellulose nanofibrils from cellulose fibers, which are held by hydrogen bonds. The equipment commonly used to produce CNF includes a high pressure homogenizer, a microfluidizer, and an microgrinder. However, there are several technical problems in the mechanical disintegration process, such as high energy consumption and clogging in a homogenizer (Klemm et al. 2011). More specifically, the energy required by a high pressure homogenizer reaches as high as 70,000 kWh/ton (Eriksen et al. 2008). By comparison, the average U.S. household consumed 11,320 kWh of electricity in 2009 (EIA, 2009). Due to this energy problem, it had been considered that it was almost impossible to commercialize cellulose nanofibrils, and only few studies had been conducted. However, after year 2000, the research on CNF has become a rapidly evolving research area because of the increasing demand for renewable materials and interest of nanotechnology. The development of mechanical, chemical or/and enzymatic pretreatment makes CNF production available at a large scale since the pretreatment facilitates the fibrillation process, reducing energy consumption and clogging. Several pilot and commercial plants for cellulose nanofibrils have opened since 2011.

Cellulose nanocrystals, called nanocrystalline cellulose, cellulose whiskers, and cellulose nanowhiskers, consist of rod-like cellulose particles. Its typical width ranges from 5 to 60 nm, and its length varies on the cellulose sources. For instance, CNC obtained from plants has a length of 100-250 nm, and CNC from tunicate, algae, and bacterial celluloses has a length from 100 nm to several microns. CNC is prepared by strong acid hydrolysis, often followed by sonication. During the acid hydrolysis, amorphous regions of cellulose fibers are removed as the hydronium ions attack weak points of cellulose (glucosidic bonds in amorphous regions); thus, cellulose nanocrystals is highly crystalline (Siqueira et al. 2010). Hydrochloric acid or sulfuric

acid are the two most-used acids for CNC extraction. Sulfuric acid is more commonly used because it reacts with the hydroxyl groups of cellulose, rendering the negatively charged surface sulfate groups. This creates the repulsive forces between cellulose, which allow CNC homogeneously dispersed in water (Dong et al. 1998). CNC acts as a reinforcing agent in polymer composites, but it creates a weak reinforcing effect compared with CNF because of its lower aspect ratio (Xu et al. 2013).

Bacterial nanocellulose (BNC) is generated by *Gluconacetobacter* bacteria strains. BNC is produced by using a biotechnological bottom-up method unlike CNF and CNC, which are produced by breaking macro-scale materials to nano-scale materials. Cellulose is synthesized from biochemically activated dextrose between the outer and plasma membranes of the bacterial cell by a cellulose-synthesizing complex. This complex is associated with pores at the surfaces of the bacterial cell, having a diameter of around 3 nm (Gatenholm and Klemm, 2010). BNC has a width ranging from 20 to 100 nm (Klemm et al. 2011). It has extensive networks due to the random motion of bacteria. Moreover, BNC is pure cellulose that does not include functional groups, such as carbonyl and carboxyl groups, and other polymers, such as hemicellulose and lignin; therefore, it is the most-used nanocellulose in the biomedical application (Gatenholm and Klemm, 2010).

3. Production of cellulose nanofibrils

Cellulose nanofibrils is typically prepared by mechanical disintegration process using three common methods: high pressure homogenization (Turbak et al. 1983a and 1983b; Herrick et al. 1983; Dufresne et al. 2000; Iwamoto et al. 2005; Malainine et al. 2005; Besbes at et al. 2011a and 2011b; Li et al. 2012; Alila et al. 2013; Chaker et al. 2013), microfluidization (Pääkkö et al. 2007; Zimmermann et al. 2010; Spence et al. 2011; Zhu et al. 2011; Zhang et al. 2012) and

micro-grinding (Iwamoto et al. 2005, 2007 and 2008; Jonoobi et al. 2012; Josset et al. 2014). Each method has its own advantages and disadvantages.

High pressure homogenization is the first method used to produce cellulose nanofibrils from woody cellulose fibers (Turbak et al., 1983a; Herrick et al. 1983). Cellulose aqueous suspension is pumped at a high pressure through a spring-loaded valve assembly. The valve is opened and closed repetitively, so the fibers are subjected to a large pressure drop with high shear and impact forces generated in the narrow silt of the valve (Figure 2.6.). This combination of forces facilitates the disintegration of the cellulose fibers into cellulose nanofibrils. This process can be easily scaled up and operated continually. On the other hand, it consumes a substantial amount of energy over 25,000 kWh/ton. By comparison, the average annual electricity usage in a single US home was 11,320 kWh in 2009 (EIA, 2009). Another disadvantage is clogging in the homogenizer, particularly at the in-line valves, which must be dissembled and cleaned. A microfluidizer is as an alternative to the high pressure homogenizer. In this equipment, cellulose/water slurry is passed through thin z-shape chambers with different channel dimensions (commonly 100-400 um) under high pressure (Figure 2.7.). Then, it is converted into a gel-like material by the application of shear and impact forces. This process does not use in-line moving parts, thus reduces the likelihood of clog. If the clogging occurs, the microfluidizer has to be cleaned by reverse flow through the chamber.

When processing with a micro-grinder, cellulose/water suspension is passed between a static grind stone and a rotating grind stone generally at 1,500 rpm. Cell wall structures and hydrogen bonds are broken down by the shearing forces generated by the grinding stones, and nanofibers in a multi-layer structure are liberated. This method is considered less energy-demanding than other two methods, and it does not have issues related to clogging. However, the main

disadvantage of micro-grinding is disk maintenance and replacement because disks are worn down.

Other than these three methods, French pressure cell press (Figure 2.8.) is a potential method to produce cellulose nanofibrils. It is a high-pressure extrusion press commonly used to disrupt cell under high pressure. It consists of a piston, a cell body and a closure plug with a needle valve and an outlet tube. A compression force is exerted on the piston to drive it within the cell body that contains a liquid sample. As the compressed fluid is dispensed through the outlet tube (1/16 inch in diameter), the external pressure on the cell walls drops rapidly toward atmospheric pressure. This large pressure drop leads to the disruption of cell wall membrane and the release of the intra-cellular contents. The operating pressure can be as high as 40,000 psi and carefully manipulated. However, the sample capacity of this method is limited up to 40 ml, and clogging the valve may occur with certain types of samples.

4. Pretreatment methods

4.1. Mechanical pretreatments for CNF production

Mechanical pretreatment aims to pre-fibrillate cellulose fibers and reduce fiber size in order to facilitate the fiber disintegration easily. This process can damage the cellulose fibrillary structure, causing external fibrillation that exposes secondary cell wall, where individual cellulose fibrils are organized. Such process can also produce internal fibrillation that loosens the fiber wall (Hamad 1997; Nakagaito and Yano 2004). Alternatives for mechanical pretreatment include manual cutting, disk refiners, PFI mills, Valley beaters, and blenders (Turbak et al. 1983a; Herrick et al. 1983; Iwamoto et al. 2005; Chakraborty et al. 2005; Zhang et al. 2012; Spence et al. 2011; Dinand et al. 1999, Dufresne et al. 2000; Malainine et al. 2005). The PFI mill and the Valley beater are commonly used for refining pulps in the laboratory scale (Figure 2.9.).

Firstly, the PFI mill is a high-energy and low intensity refiner (Gharehkhani et al. 2015). This device refines pulps between the inner roll and outer bedplate that rotate in the same direction but with different peripheral speeds; thus, the pulps are exposed to mechanical shearing action (TAPPI T 248 sp-00). Compared to the PFI mill, the Valley beater needs the bigger amount of pulp samples and longer operating time (Gharehkhani et al. 2015). In the beating process, the pulps are looped around a well and forced between a rotor and loaded bedplate (TAPPI T 200 sp-01). These mechanical pretreatments have some drawbacks. One of the drawbacks is its energy use, leading to the increase in cost for manufacturing cellulose nanofibrils. The energy necessary for beating pulps in a Valley beater was estimated in an empirical relation with water retention value (WRV) as equal to $1.132 \times \ln(WRV[g/g]) - 0.9$ (Jones et al. 2013). It was reported that the effective beating energy in a Valley beater was about 482 kWh/ton and 578 kWh/ton for bleached eucalyptus and bleached pine, respectively, for a total beating time of one hour. When no-load power was included, the total beating energy was approximately 3,000 kWh/ton (Atic et al. 2005). It was also reported that the three-hour beating process consumed about 2,000 kWh/ton, while producing cellulose microfiber 0.24 μm in diameter from cellulose fibers 30 μm in diameter (Spence et al. 2011). With respect to the PFI mill, Welch and Kerekes (1994) estimated the refining energy for PFI milling as 0.18 kWh/ton-rev. If the pulps are refined in a PFI mill for 20,000 revolutions prior to the mechanical disintegration process as described by Sharma et al. (2015), the PFI mill would consume approximately 3,600 kWh/ton. In addition, the refining energy required by a PFI mill was estimated as high as 21,700 kWh/ton to generate cellulose microfiber 1.3 μm in diameter from bleached softwood kraft pulp 13 μm in diameter (Chakraborty et al. 2007). Therefore, the development of low-energy mechanical pretreatment technique can contribute to the reduction in the overall energy use for CNF production.

Moreover, the standard mechanical refining process is a wet processing. The mechanical pretreatment process using a PFI mill is performed at the initial pulp consistency of 10%. Specifically, 300g of cellulose slurry containing 30g of cellulose (dry basis) can be refined per run (TAPPI T 248 sp-00). The process with a Valley beater is carried out at the pulp consistency of 1.57%, having 360g of cellulose (dry basis) in 23 L (TAPPI T 200 sp-01). This indicates that both mechanical pretreatment processes produce wet cellulose precursors, and their bulk volume would make it difficult to store and handle these cellulose precursors.

A shear cutting mill, known as a knife mill, has a potential as a mechanical pretreatment method. It has been widely used for size reduction of biomass, such as wood and agricultural crops. The literature reported that the effective energy for grinding biomass in a shear cutting mill ranged from several tens kWh/ton to 200 kWh/ton (Cadoche and López 1989; Bitra et al. 2009; Miao et al. 2011). The energy requirement for grinding depends on many factors, such as machine parameters, initial particle size, moisture content, and material properties (Mani et al. 2004). Cadoche and López (1989) demonstrated that the effective energy necessary for the shear-cutting mill to grind hardwood chips was 130 kWh/ton and 50 kWh/ton for 1.6 mm and 3.2 mm particle size, respectively. Energy consumption for grinding miscanthus and switchgrass in the shear cutting mill equipped with 1 mm screen was 200 kWh/ton and 150 kWh/ton, respectively. When the screen size increased to 2 mm, the grinding energy decreased to 100 kWh/ton for both grasses (Miao et al. 2011). Unfortunately, there is no study that has tested the shear cutting mill either on cellulose pulps or for fine grinding even though the screen size is available as small as 0.25 mm. Shear cutting process with 0.25 mm screen would produce very fine particles. It is expected that shear cutting of cellulose pulp with 0.25 mm screen would produce cellulose precursors for manufacturing cellulose nanofibrils, while requiring a relatively low compared

with other mechanical pretreatment processes. Moreover, this process is performed without water. Consequently, a shear cutting mill could be an alternative mechanical pretreatment method which produces dry cellulose precursors and reduces overall energy consumption for producing cellulose nanofibrils.

4.2. Chemical pretreatments for CNF production

4.2.1. Conventional chemical pretreatments for CNF production

Several chemical pretreatments have been developed in order to facilitate the mechanical disintegration of cellulose. 2,2,6,6,-tetramethylpiperidine-1-oxyl radial (TEMPO)-mediated oxidation has been widely studied as a chemical pretreatment for cellulose nanofibrils production. (Saito et al. 2006 and 2007; Besbes et al. 2011a and 2011b; Zhang et al. 2012; Alila et al. 2013; Chaker et al. 2013). This process converts half of C6 primary hydroxyl groups on cellulose surface into C6 carboxyl groups (Figure 2.10.). TEMPO oxidation helps cellulose fibers to be delaminated in several ways; 1) repulsive forces between cellulose fibers from the introduction of the carboxyl groups, 2) TEMPO oxidation favors the hydration and swelling of cellulose fibers, making the fibers more flexible and also increasing the accessibility of their crystalline regions, 3) the oxidation also makes the S2 layer more accessible and more prone to be fibrillated by loosening the primary S1 cell wall, and 4) the oxidation leads to chain scission in the amorphous region, which creates weak points within the cell wall (Besbes et al. 2011a).

Carboxymethylation process is another common chemical pretreatment method. Cellulose fibers are first reacted with sodium hydroxide to become more accessible to chemicals, and then with monochloroacetic acid to introduce carboxymethyl groups as shown in Figure 2.11. The introduction of such charged groups is expected to enhance delamination of cellulose fibers by giving electrostatic repulsive forces between fibers. In addition, carboxymethylation

leads to fiber swelling, and carboxymethyl groups should be in the form of their sodium salts in order to cause as much swelling of cellulose fibers as possible. Swollen fibers are more susceptible to be delaminated as they have lower cell-wall cohesion than less swollen fibers (Klemm et al. 2011). It was reported that with the carboxymethylation process, cellulose nanofibrils was successfully obtained only after one pass through a high pressure fluidizer and had a diameter of 5-10 nm (Wågberg et al. 2008; Aulin et al. 2010).

There are several disadvantages of chemical pretreatment methods. First, these processes require various chemicals and organic solvents, which is far from environmentally benign technology. TEMPO oxidation uses sodium hypochlorite or/and sodium chlorite, sodium bromide, TEMPO and ethanol. Carboxymethylation is based on the reaction in organic solvents, such as ethanol, methanol and isopropanol. More specifically, a total of 30 kg of organic solvents are consumed to manufacture one kg of cellulose nanofibrils (Arvidsson et al. 2015). In addition, the introduction of functional groups, such as carboxyl and carboxymethyl groups, decreases thermal stability of cellulose due to decarbonation (Britto and Assis 2009). Fukuzumi et al. (2009) demonstrated that TEMPO-oxidized cellulose nanofibrils had an onset thermal degradation temperature (T_o) of approximately 200 ℃, while original cellulose had a T_o of approximately 300 ℃. Other studies also confirm that the thermal degradation of cellulose nanofibrils containing functional groups takes place at lower temperature than pure cellulose nanofibrils (Fukuzumi et al. 2010; Eyholzer et al. 2010).

4.2.2. Alkaline pretreatment for CNF production

Alkaline treatment with high concentrated sodium hydroxide solution has been used to activate cellulose. When cellulose fibers are soaked in 17-20 wt.% NaOH solution at room temperature, native cellulose is converted into alkali-cellulose (Na-cellulose) as below:

$$\text{Cell-OH} + \text{NaOH} \longrightarrow \text{Cell-O-, Na+} + H_2O$$

In this stage, cellulose fibers are swollen and activated for further modification or/and dissolution (Wang 2008). For instance, this treatment is a prerequisite in the production of cellulose derivatives, such as carboxymethyl cellulose, and in the manufacturing of cellulose-based sponges (Porro et al., 2007). NaOH treatment also enhances cellulose mobility, causing the rearrangement of cellulose chains from cellulose I to Na-cellulose and after washing to cellulose II as seen in Figure 2.12. (Simon et al. 1988; Shibazaki et al. 1997). This transformation is called as mercerization. Cellulose II is considered more thermally stable than cellulose I as mentioned earlier.

Few studies have been conducted on cellulose nanofibrils with a cellulose II crystal structure (Shibazaki et al. 1997; Dinand et al. 1999, 2002; Abe and Yano 2012; Wang et al. 2014). Dinand et al. (2002) reported that fibrillated cellulose fibers became swollen and mercerized when treated with 10% or higher NaOH. They found that the mercerization induced a drastic modification of cellulose morphology. All individual microfibrils were destroyed and irregularly aggregated. During subsequent washing, the entire sample was converted into a precipitate. This morphological change can be explained by an interdigitation mechanism suggested by Okano and Sarko (1985). A cell wall of native cellulose consists of microfibrils with different polarities: “up” and “down”, and a single microfibril contains cellulose chains of the same polarity. During the mercerization process, microfibrils are swollen and therefore liberate cellulose chains. The cellulose chains of opposite polarity could coalesce and interdigitate to form antiparallel cellulose II as shown in Figure 2.13. (Kim et al. 2006). Abe and Yano (2012) produced cellulose II hydrogel by processing cellulose nanofiber suspension in 15 wt.% NaOH solution and suggested that the resultant hydrogels had a continuous and strong

network formed via the firm interdigitation between the nanofibers. Recently, well-dispersed cellulose II nanofibrils was successfully prepared by delaminating cellulose II fibers (Wang et al. 2014; Sharma et al. 2015). Cellulose II nanofibers would have better thermal stability than cellulose I nanofibers due to the stronger hydrogen bonding in cellulose II crystal structure if both cellulose I and II nanofibers have a similar degree of fibrillation and therefore have a similar surface area. Wang et al. (2014) found that cellulose II nanofibers had a higher onset and maximum thermal decomposition temperature at 326 ℃ and 353 ℃, respectively, compared with those for cellulose I nanofibers at 302 ℃ and 348 ℃, respectively. On the other hand, Sharma et al. (2015) reported that cellulose I and II nanofibers had a different thermal behavior. In case of cellulose I nanofibers, a significant drop in maximum thermal degradation temperature was observed after microgrinding for 20 passes; while cellulose II nanofibers showed a large decrease in thermal stability after microgrinding for 60 passes. This is because a significant decrease in size of cellulose I and II nanofibers occurred at different stages of microgrinding (after 20 and 60 passes, respectively). However, this NaOH treatment is unlikely to be applied to the large-scale CNF production for the following reasons: difficulty in fibrillation of cellulose II fibers and high water consumption for neutralization. Firstly, it is difficult to produce well-delaminated cellulose II nanofibers due to the interdigitation and aggregation of cellulose II fibers as described above. Wang et al. (2014) obtained well-delaminated cellulose II nanofibers by a single grinder treatment followed by 50 homogenization treatments and centrifugation. Sharma et al. (2015) also reported that the higher number of passes through a microgrinder was required to produce cellulose II nanofibers compared to cellulose I nanofibers. They found that cellulose II fibers at the submicron level could be obtained after microgrinding for 60 passes, while cellulose I fibers had diameters of the order of hundreds of nanometers after 20 passes and

diameters of few nanometers after 60 passes. Moreover, cellulose II fibers are obtained by processing cellulose I fibers in high concentration of NaOH solution. This results in the considerable water usage during neutralization.

Instead of using high-concentration NaOH solution, Sobue et al. (1939) found that low-concentration NaOH solution (6-10 wt.%) highly swelled and even partly dissolved cellulose when temperature ranged from -10 ℃ to 4 ℃. Since then, extensive studies on NaOH treatment of cellulose at low temperatures have been conducted (Isogai et al. 1998; Roy et al. 2001; Cuissinat and Navard, 2006; Egal et al. 2007; Wang, 2008). Cuissinat and Navard (2006) identified five modes of cellulose swelling and dissolution by the NaOH treatment; (a) Fast dissolution by disintegration into rod-like fragments (Mode 1); (b) Large swelling by ballooning and then dissolution of the whole fiber (Mode 2); (c) Large swelling by ballooning and partial dissolution of the fiber, still keeping fibrous shape (Mode 3); (d) Homogeneous swelling and no dissolution of any part of the fiber (Mode 4); and (e) No swelling and no dissolution (Mode 5, case of a non-solvent). Cellulose with low degree of polymerization (DP < 200) could be fully dissolved in 9wt% NaOH solution at low temperature, indicating mode 1. However, most commercial wood pulps have DP value of about 800, which cannot be fully dissolved in NaOH solution even at low temperature, and such high DP cellulose appears to be in mode 3. Particularly, Wang (2008) reported that cotton fiber with DP value of 800 had a limited solubility of up to 30% in 6% NaOH solution when the reaction temperature was below -10 ℃. In addition, the low-concentration NaOH treatment converts cellulose crystalline structure to cellulose II as the high-concentration NaOH treatment does. Even with 4wt% NaOH, cellulose crystal structure was transformed from cellulose I to cellulose II at low temperature (Wang 2008).

4.2.3. Carboxymethylcellulose (CMC) addition for CNF production

Carboxymethylcellulose (CMC) is a cellulose derivative achieved by introducing carboxymethyl groups on cellulose backbone. Several researchers used CMC for the production of cellulose nanofibrils with redispersibility. Herrick (1984) reported that the addition of CMC inhibited hydrogen bonds between cellulose fibers; thus, the resultant cellulose nanofibrils was able to be redispersed after drying. However, a large amount of CMC was required, at least one half the weight of cellulose on dry basis. Cantiani et al. (2002) used CMC with a high degree of substitution (higher than 0.95) to prepare redispersible cellulose nanofibrils from cells with primary walls. They reported that the required amount of CMC was relatively small, less than or equal to 30% by weight relative to the weight of cellulose. Besides, it was found that CMC could be irreversibly attached to cellulose fibers, and a small amount of the attached CMC was sufficient to produce paper with high wet strength (Laine et al. 2000 and. 2002, Lindström, 2006; Duker et al. 2008). Recently, CMC attachment was applied in cellulose nanofibrils production (Ankerfors 2015). CMC attachment facilitates disintegration of cellulose fibers in two ways. First, CMC basically introduces charges into cellulose fibers, preventing the formation of hydrogen bonds between cellulose fibers. CMC also serves as a lubricant, creating the lubricating effect between fibers and possibly between fibrils in the fiber wall (Yan et al. 2006 and Ankerfors 2015). CMC can be attached on the cellulose surface or in the fiber wall, and whether CMC is attached on the surface or in the fiber wall depends on the molecular weight of CMC (Laine et al. 2000). The attachment of high-molecular-weight CMC is limited on the fiber surface, while low-molecular-weight CMC can penetrate the fiber wall; thus can be attached either on the surface or in the fiber wall. Types of CMC play an important role in the production of CNF. Ankerfors (2015) prepared cellulose nanofibrils using three different types of CMC:

amphoteric CMC, anionic CMC with high molecular weight, and anionic CMC with low molecular weight. Cellulose nanofibrils gel was prepared with 20 mg or more of amphoteric CMC per gram of cellulose. It was also able to obtain cellulose nanofibrils gel with high-molecular-weight anionic CMC; however, the added amount of the CMC was 3-4 times higher than that of the amphoteric CMC. In contrast, the addition of low-molecular-weight anionic CMC could neither avoid clogging in a homogenizer, nor produce cellulose nanofibrils gel.

5. Life cycle assessment (LCA)

Life cycle assessment (LCA) is a reliable tool to evaluate the environmental impacts of a process or a product throughout its life cycle. LCA is used to quantify material usage, energy consumption and emissions in a life cycle context. A LCA study includes several impact categories, such as global warming potential, acidification, eutrophication, ozone depletion, and ecotoxicity. The LCA process consists of four main phases: goal and scope definition, inventory analysis, impact assessment, and interpretation. Goal and scope definition aims to clarify the purpose and extent of the LCA study. At this phase, the functional unit or basis for assessment should be determined, and a clear description of the system boundary should be provided. Life cycle inventory analysis is a process of quantifying energy, water, raw material, and environmental release. It begins with the construction of a process flowchart that shows the inputs and outputs required for the life cycle of the product or the process. It also includes data collection and data calculation in relation to the functional unit. Impact assessment uses the inventory results to evaluate the potential impact on environment and human. Interpretation is needed to analyze the results of the inventory analysis and impact assessment, reach conclusions, explain limitations and provide recommendations.

5.1. LCA of CNF production

Three LCA studies related to cellulose nanofibrils have been conducted (Hohenthal et al. 2012, Li et al. 2013; Arvidsson et al. 2015). Hohenthal et al. (2012) assessed environmental impacts of CNF production from three different processing routes, including TEMPO-oxidation or enzymatic pretreatment with homogenization, and TEMPO-oxidation with Cavitron dispersion. This LCA report unfortunately did not clearly describe the source for quantitative inventory data. The LCA study conducted by Li et al. (2013) is the only one that studied CNF production in the United States. They reported environmental impacts of CNF production from four different processing routes in combination of two chemical pretreatments (TEMPO-oxidation and chloroacetic acid etherification) and two mechanical disintegration processes (high pressure homogenization and sonication). The results showed that the production route using TEMPO oxidation and homogenization was the best process with the lowest energy demand of 3,470 MJ for producing one kg cellulose nanofibrils, while the production route with etherification and sonication required the highest energy demand of 17,610 MJ for producing one kg of CNF. Comparing the two chemical pretreatment techniques, TEMPO oxidation was less energy-intensive than chloroacetic acid etherification since TEMPO oxidation needed a small amount of organic solvents compared with chloroacetic acid etherification. With respect to the mechanical disintegration process, the energy demand for sonication was around 3,000 MJ/kg CNF higher than for homogenization. This was because sonication required an additional step of centrifugation. However, this report has limitations since the data was obtained from lab-scale measurements. Arvidsson et al. (2015) assessed the life cycle environmental impacts of CNF produced from three different production routes; (1) enzymatic pretreatment with microfluidization, (2) carboxymethylation with microfluidization, and (3) high pressure

homogenization with no pretreatment. In this report, four impact categories were selected: energy use, global warming potential, acidification and water use. Carboxymethylation route had the higher impact for all impact categories due to the high chemical consumption. In particular, total chemical input for carboxymethylation was 30 kg for producing one kg of cellulose nanofibrils. The carboxymethylation route required approximately 1,800 MJ of energy to manufacture one kg CNF, which is 7-fold and 10-fold higher energy demand compared to the no pretreatment route and enzymatic route, respectively. The global warming potential of the carboxymethylation route was around 100 kg CO_2 eq./kg CNF. In contrast, other routes generated less than 5 kg CO_2 eq. of emissions to produce one kg of CNF. With respect to terrestrial acidification, the carboxymethylation route had the highest impacts, around 0.2 kg SO_2 eq./kg CNF; whereas, the acidification impact of the enzymatic route and no treatment route was 20 times lower (around 0.01 kg SO_2 eq./kg CNF). Finally, considering water use, the carboxymethylation required the highest water intake of 1.2 m^3 for producing one kg of cellulose nanofibrils, followed by the enzymatic route (0.25 m^3) and the no pretreatment route (0.1 m^3). Although these three LCA study thoroughly assessed the environmental impacts of producing cellulose nanofibrils with various pretreatment techniques, the environmental impacts of CNF production with mechanical and alkaline pretreatment techniques have been not investigated. The environmental impacts of the mechanical and alkaline pretreatment and its contribution of total environmental impacts of CNF production need to be verified.

6. Summary

Cellulose nanofibrils (CNF) refers to the cellulosic material with a diameter of 5-100 nm and a length of several microns. Cellulose nanofibrils was first obtained from wood pulps by high pressure homogenization in early 1980s, but the commercialization of CNF is still challenging.

This is mainly due to high energy consumption for homogenization (over 25,000 kWh/ton) and standardizing CNF production process and its characteristics for specific applications. In addition, development of large volume use of CNF for specific field of application is critical for accelerating commercialization of this technology. Although less energy-demanding disintegration methods have been developed, such as microfluidization and microgrinding, pretreatment processes are required to further reduce energy required for the mechanical disintegration process, thus making CNF production economically favorable. Several pretreatment processes have been developed using mechanical, chemical or/and enzymatic methods. Each process has its own advantages and disadvantages. Firstly, mechanical pretreatment by a wet milling method, such as a Valley beater and a PFI mill, has been used to reduce fiber size and pre-fibrillate fibers, facilitating the delamination of cellulose fibers into CNF. This pretreatment produces wet cellulose precursors, which make difficulties during storage and handling. It would also contribute to the increase in the total energy demand for CNF. A shear cutting mill known as a knife mill could be used as a mechanical pretreatment method, producing dry cellulose precursors and potentially reducing overall energy consumption for manufacturing cellulose nanofibrils since the shear cutting process is performed without water and requires up to 200 kWh/ton to grind wood and grasses. In addition, chemical pretreatment has been used to reduce interaction between cellulose fibers, making them more accessible during fibrillation by introducing charged groups on the cellulose surface. However, it leads to the increase in CNF environmental impacts as it uses chemicals and organic solvents. The introduction of charged groups reduces the thermal stability of the resultant cellulose nanofibrils. Alkaline treatment with low-concentration NaOH solutions in the presence of carboxymethylcellulose (CMC) could be an alternative chemical pretreatment method over other

chemical pretreatment methods. This treatment could facilitate the fibrillation of cellulose fibers due to the swelling effect of NaOH. It is environmentally friendly as well as simple because it is a water-based process. NaOH-treated cellulose nanofibrils could present improved thermal stability over original cellulose nanofibrils since it could have thermally stable crystal structure, cellulose II. Finally, life cycle assessment (LCA) of producing cellulose nanofibrils has been conducted to assess environmental impacts of CNF on its entire life cycle. Overall, the environmental impacts of CNF depend on the pretreatment method and mechanical disintegration method. The use of chemical pretreatment significantly increased the environmental impacts of CNF, and high pressure homogenization generally creates high environmental impacts compared with other mechanical disintegration methods (microfluidization and microgrinding) because it requires a high amount of energy. None of the published LCA studies investigated mechanical and alkaline pretreatment techniques and their impacts on the environment. Thus, additional LCA study is needed to verify the effects of these pretreatment technologies on the environmental impacts of CNF production.

References

Abe, K., Yano, H., 2009, Comparison of the characteristics of cellulose microfibril aggregates of wood, rice straw and potato tuber, Cellulose, 16:1017–1023.

Abe, K., Yano, H., 2012, Cellulose nanofiber-based hydrogels with high mechanical strength, Cellulose, 19:1907–1912.

Alila, S., Besbes, I., Vilar, M.R., Mutje, P., Boufi, S., 2013, Non-woody plants as raw materials for production of microfibrillated cellulose (MFC): A comparative study, Industrial crops and products, 41:250-259.

Ankerfors, M., 2015, Microfibrillated cellulose: Energy-efficient preparation techniques and key properties, PhD. Dissertation, KTH Royal Institute of Technology.

Arvidsson, R., Nguyen, D., Svanstrom M., 2015, Life cycle assessment of cellulose nanofibrils production by mechanical treatment and two different pretreatment processes, Environ. Sci. Technol., 49:6681-6890.

Atalla, R.H., VanderHart, D.L., 1984, Native cellulose: a composite of two distinct crystalline forms, Science, 223:283-285.

Atic, C., Immamoglu, S., Valchev, I., 2005, Determination of specific beating energy-applied on certain pulps in a valley beater, J. Univ. Chem. Technol. Met., 40(3):199–204.

Aulin, C., Gällstedt, M., Lindström, T., 2010, Oxygen and oil barrier properties of microfibrillated cellulose films and coatings, Cellulose, 17:559-574.

Besbes, I., Alila, S., Boufi, S., 2011a, Nanofibrillated cellulose from TEMPO-oxidized eucalyptus fibers: Effects of the carboxyl content, Carbohydrate Polymers, 84:975-983.

Besbes, I., Vilar, M.R., Boufi, S., 2011b, Nanofibrillated cellulose from Alfa, Eucalyptus and Pine fibres: Preparation, characteristics and reinforcing potential, Carbohydrate Polymers, 86:1198-1206.

Bitra, V.S.P., Womac, A.R., Igathinathane, C., Miu, P.I., Yang, Y.T., Smith, D.R., Chevanan, N., Sokhansanj, S., 2009, Direct measures of mechanical energy for knife mill size reduction of switchgrass, wheat straw, and corn stover, Bioresource Technology 100:6578–6585.

Britto, D., and Assis, O.B.G., 2009, Thermal degradation of carboxymethylcellulose in different salty forms, Thermochimica Acta, 494:115-122.

Cadoche, L., López, G.D., 1989, Assessment of size reduction as a preliminary step in the production of ethanol for lignocellulosic wastes, Biological Wastes, 30:153–157.

Cantiani, R., Knipper, M., Vaslin, S., 2002, Use of cellulose microfibrils in dry form in food formulations, US Patent 6,485,767 B1.

Chaker, A., Alila, S., Mutje, P., Vilar, M.R., Boufi, S., 2013, Key role of the hemicellulose content and the cell morphology on the nanofibrillation effectiveness of cellulose pulps, Cellulose, 20:2860-2875.

Chakraborty, A., Sain, M., Kortschot, M., 2005, Cellulose microfibrils: A novel method of preparation using high shear refining and cryocrushing, Holzforschung, 59:102-107.

Chakraborty, A., Sain, M.M., Kortschot, M.T., Ghosh, S.B., 2007, Modeling energy consumption for the generation of microfibres from bleached kraft pulp fibres in a PFI mill, BioResources, 2(2):210-222.

Cuissinat, C., Navard, P., 2006, Swelling and dissolution of cellulose part II: free floating cotton and wood fibres in NaOH–water–additives Systems, Macromolecular Symposia, 244(1):19-30.

Dinand, E., Chanzy, H., Vignon, M.R., 1999, Suspensions of cellulose microfibrils from sugar beet pulp, Food hydrocolloids, 13:275-283.

Dinand, E., Vignon, M., Chanzy, H., Heux, L., 2002, Mercerization of primary wall cellulose and its implication for the conversion of cellulose I to cellulose II, Cellulose, 9:7-18.

Doherty, W.O.S., Mousavioun, P., Fellows, C.M., 2011, Value-adding to cellulosic ethanol: lignin polymers, Industrial Crops and Products, 33:259–276.

Dong, X.M., Revol. J., Gray. D.G., 1998, Effect of microcrystalline preparation conditions on the formation of colloid crystals of cellulose, Cellulose, 5:19-32.

Dufresne, A., Dupeyre, D., Vignon, M.R., 2000, Cellulose Microfibrils from Potato Tuber Cells: Processing and Characterization of Starch–Cellulose Microfibril Composites, Journal of Applied Polymer Science, 76:2080-2092.

Dufresne, A., 2013, Nanocellulose: From Nature to High Performance Tailored Materials, Walter de Gruyer, Berlin & New York.

Duker, E., Ankerfors, M., Lindström, T., Nordmark, G.G., 2008, The use of CMC as a dry strength agent – the interplay between CMC attachment and drying, Nordic pulp & paper research journal, 23(1):65-71.

Egal, M., Budtova, T., Navard, P., 2007, Structure of aqueous solutions of microcrystalline cellulose/sodium hydroxide below 0 C and the limit of cellulose limitation, Biomacromolecules, 8(7):2282-2287.

EIA, 2009, Residential Energy Consumption Survey, U.S. Energy Information Administration.

Eriksen, Ø., Syverud, K., Gregersen, Ø., 2008, The use of microfibrillated cellulose produced from kraft pulp as strength enhancer in TMP paper, Nordic Pulp & Paper Research Journal. 23(3):299-304.

Eyholzer, Ch., Bordeanu, N., Lopez-Suevos, F., Rentsch, D., Zimmermann, T., Oksman, K., 2010, Preparation and characterization of water-redispersible nanofibrillated cellulose in powder form, Cellulose 17:19-30.

Fukuzumi, H., Saito, T., Iwata, T., Kumamoto, Y., Isogai, A., 2009, Transparent and high gas barrier films of cellulose nanofibers prepared by TEMPO-mediated oxidation, Biomacromolecules, 10:162-165.

Fukuzumi, H., Saito, T., Okita, Y., Isogai, A., 2010, Thermal stabilization of TEMPO-oxidized cellulose, Polymer Degradation and Stability, 95:1502-1508.

Gatenholm, P., Klemm, D., 2010, Bacterial nanocellulose as a renewable material for biomedical applications, MRS Bulletin, 35:208-213.

Gavillon, R., 2007, Preparation and characterization of ultra porous cellulosic materials, Master's thesis, Mechanics. Ecole Nationale Superieure des Mines de Paris.

Gharehkhani, S., Sadeghinezhad, E., Kazi, S.N., Yarmand, H., Badarudin, A., Safaei, M.R., Zubir, M.N., 2015, Basic effects of pulp refining on fiber properties-a review, Carbohydrate Polymer, 115:785-803.

Hamad, W.Y., 1997, Some microrheological aspects of wood-pulp fibres subjected to fatigue loading, Cellulose 4:51-56.

Herrick, F.W., 1984, Redispersible microfibrillated cellulose, US patent 4,481,076.

Herrick, F.W., Casebier, R.L., Hamilton, J.K., Sandberg, K.R., 1983, Microfibrillated cellulose: Morphology and accessibility, J. Appl. Polym. Sci. Appl. Polym. Symp., 37:797-813.

Hohenthal, C., Ovasakainen, M., Bussini, D., Sadocco, P., Pajula, T., Hannele, L., Kautto, J., Salmenkivi, K., 2012, Final assessment of nanoenhanced new products, VTT Technical Research Centre of Finland.

Isogai A., Saito, T., Fukuzumi, H., 2011, TEMPO-oxidized cellulose nanofibers, Nanoscale, 3:71-85.

Isogai, A., Atalla, R.H., 1998, Dissolution of cellulose in aqueous NaOH solutions, Cellulose, 5:309-319.

Iwamoto, S., K. Abe, Yano, H., 2008, The effect of hemicellulose on wood pulp nanofibrillation and nanofiber network characteristics, Biomacromolecules, 9:1022-1026.

Iwamoto, S., Nakagaito, A.N., Yano, H., 2007, Nano-fibrillation of pulp fibers for the processing of transparent nanocomposites, Appl. Phys.A-Mater.Sci.Process, 89:461-466.

Iwamoto, S., Nakagaito, A.N., Yano, H., Nogi, M., 2005, Optically transparent composites reinforced with plant fiber-based nanofibers, Appl. Phys. A, 81:1109-1112.

Jones, B.W., Venditti, R., Park, S., Jameel, H., Koo, B., 2013, Enhancement in enzymatic hydrolysis by mechanical refining for pretreated hardwood lignocellulosics, Bioresource Technology, 147:353-360.

Jonoobi, M., Harun, J., Mathew, A.P., Oksman, K., 2010, Mechanical properties of cellulose nanofiber (CNF) reinforced polylactic acid (PLA) prepared by twin screw extrusion, Composites Science and Technology, 70(12):1742-1747.

Jonoobi, M., Mathew, A.P., Oksman, K., 2012, Producing low-cost cellulose nanofiber from sludge as new source of raw materials, Industrial Crops and Products, 40:232–238.

Josset, S., Orsolini, P., Siqueira, G., Tejado, A., Tingaut, P., Zimmermann, T., 2014, Energy consumption of the nanofibrillation of bleached pulp, wheat straw and recycled newspaper through a grinding process, Nordic Pulp & Paper Research Journal, 29(1):167-175.

Kim, N., Imai, T., Wada, M., Sugiyama, J., 2006, Molecular Directionality in Cellulose Polymorphs, Biomacromolecules, 7:274-280.

Klemm, D., Heublein, B., Fink, H-P., Bohn, A., 2005, Cellulose: Fascinating biopolymer and sustainable raw material, Angew. Chem. Int. Ed., 44:3358-3393.

Klemm, D., Kramer, F., Mortiz, S., Lindstrom, T., Ankerfors, M., Gray, D., Dorris, A., 2011, Nanocelluloses: a new family of nature-based materials, Angew. Chem. Int. Ed., 50(24):5438-5466.

Laine, J., Lindstrom, T., Nordmark, G.G., Risinger, G., 2000, Studies on topochemical modification of cellulosic fibres Part1., Chemical conditions for the attachment of carboxymethyl cellulose onto fibres, Nordic Pulp & Paper Research Journal, 15(5):520-526.

Laine, J., Lindstrom, T., Nordmark, G.G., Risinger, G., 2002, Studies on topo chemical modification of cellulosic fibres Part2., The effect of carboxymethyl cellulose attachment on fibre swelling and paper strength, Nordic Pulp & Paper Research Journal, 17(1):50-56.

Li, J., Wei, X., Wanga, Q., Chena, J., Changa, G., Kongc, L., Sud, J., Liue, Y., 2012, Homogeneous isolation of nanocellulose from sugarcane bagasse by high pressure homogenization, Carbohydrate polymer, 90:1609-1613.

Li, Q., McGinnis, S., Sydnor, C., Wong, A., Renneckar, S., 2013, Nanocellulose life cycle assessment, ACS Sustainable Chem. Eng., 1:919-928.

Lindström, T., 2006, Modifying cellulose fibres by using amphoteric cellulose derivative Patent WO2005080678A1.

Malainine, M.E., Mahrouz, M., Dufresne, A., 2005, Thermoplastic nanocomposites based on cellulose microfibrils from Opuntia ficus-indica parenchyma cell, Composites Sci. and Tech., 65:1520-1526.

Mani, S., Tabil, L.G., Sokhansanj, S., 2004, Grinding performance and physical properties of wheat and barley straws, corn stover and switchgrass, Biomass and Bioenergy, 27(4):339-352.

Miao, Z., Grift, T.E., Hansen, A.C., Ting, K.C., 2011 Energy requirement for comminution of biomass in relation to particle physical properties, Industrial Crops and Products, 33(2):504-513.

Missoum, K, Belgacem, M.N., Bras, J., 2013, Nanofibrillated cellulose surface modification: A review, Material, 6:1745-1766.

Nakagaito A.N. Yano H., 2004, The effect of morphological changes from pulp fiber towards nano-scale fibrillated cellulose on the mechanical properties of high-strength plant fiber based composites, Appl. Phys. A, 78:547-552.

Okano, T., Sarko, A., 1985, Mercerization of cellulose. II. Alkali-cellulose intermediates and a possible mercerization mechanism, J. Appl. Polym. Sci., 30:325–332.

Pääkkö, M., Ankerfors. M., Kosonen, H., Nykänen, A., Ahola, S., Osterberg, M., Ruokolainen, J., Laine, J., Larsson, P.T., Ikkala, O., Lindström, T., 2007, Enzymatic hydrolysis combined with mechanical shearing and high-pressure homogenization for nanoscale cellulose fibrils and strong gels, Biomacromolecules, 8:1934-1941.

Porro, F., Bedue, O., Chanzy, H., Heux, L., 2007, Solid-state C-13 NMR study of Nacellulose complexes. Biomacromolecules, 8(8):2586-2593.

Repellin, V., Govin, A., Rolland, M., Guyonnet, R., 2010, Energy requirement for fine grinding of torrefied wood, Biomass & Bioenergy, 34(7):923-930.

Roy, C., Budtova, T., Navard, P., Bedue, O., 2001, Structure of cellulose-soda solutions at low temperatures, Biomacromolecules, 2(3):687-693.

Saito, T., Nishiyama, Y., Putaux, J.L., Vignon, M., Isogai, A., 2006, Homogeneous suspensions of individualized microfibrils from TEMPO-catalyzed oxidation of native cellulose, Biomacromolecules, 7:1687-1691.

Saito, T., Hirota, M., Tamura, N., Kimura, S., Fukuzumi, H., Heuz, L., Isogai, A., 2009, Individualization of nano-sized plant cellulose fibrils by direct surface carboxylation suing TEMPO catalyst under neutral conditions, Biomacromolecules, 7:1687-1691.

Saito, T., Kimura, S., Nishiyama, Y., Isogai, A., 2007, Cellulose nanofibers prepared by TEMPO-mediated oxidation of native cellulose, Biomacromolecules, 8:2485-2491.

Sharma, S. Nair, S.S., Zhang, Z., Ragauskas, A.J., Deng, Y., 2015, Characterization of micro fibrillation process of cellulose and mercerized cellulose pulp, RSC Advances, 5:63111-63122.

Shibazaki, H., Kuga, S., Okano, T., 1997, Mercerization and acid hydrolysis of bacterial cellulose, Cellulose 4:75-87.

Simon, I., Glasser, L., Scheraga, H. A., Manley, R. S. J., 1988, Structure of cellulose. 2. low-energy crystalline arrangements, Macromolecules, 21:990–998.

Siqueira G., Tapin-Lingua S., Bras J., da Silva Perez D., Dufresne A., 2010, Morphological investigation of nanoparticles obtained from enzymatic and acid hydrolysis of sisal fibers, Cellulose, 17:1147-1158.

Smook, G.A., 2002, Handbook for Pulp & Paper Technologists, 3rd edition, Angus Wilde Publications Inc., Vancouver, Canada.

Sobue, H., Kiessig, H., Hess, K., 1939, The cellulose-sodium hydroxide-water system as a function of the temperature, Z. Physik. Chem. B, 43:309–328.

Spence, K.L., Benditti, R.A., Rojas, O.J., Habibi, Y., Pawlak, J.J., 2011, A comparative study of energy consumption and physical properties of microfibrillated cellulose produced by different processing methods, Cellulose, 18:1097-1111.

Stevens, M.P., 1999, Polymer Chemistry: An introduction, 3rd edition, Oxford University Press, New York.

Syverud, K. and Stenius, P., 2009, Strength and barrier properties of MFC films, Cellulose, 16:75-85.

TAPPI, 2000, T248 sp-00, Laboratory beating of pulp (PFI mill method), Technical Association of the Pulp and Paper Industry, Norcross, GA.

TAPPI, 2001, T200 sp-01, Laboratory beating of pulp (Valley beater method), Technical Association of the Pulp and Paper Industry, Norcross, GA.

Tingaut, P., Eyholzer, C., Zimmermann, T., 2012, Functional Polymer Nanocomposite Materials from Microfibrillated Cellulose, Advances in Nanocomposite Technology, Dr. Abbass Hashim (Ed.), InTech, DOI: 10.5772/20817, Available from: http://www.intechopen.com/books/advances-in-nanocomposite-technology/functional-polymer-nanocomposite-materials-from-microfibrillated-cellulose, Last accessed on 07/02/16.

Turbak, A.F., Snyder, F.W., Sandberg, K.R. 1983a, Microfibrillated cellulose, a new cellulose product: Properties, uses, and commercial potential, J. Appl. Polym. Sci. Appl. Polym. Symp., 37:815-827.

Turbak, A.F., Snyder, F.W., Sandberg K.R., 1983b, Suspensions containing microfibrillated cellulose, US Pat. 4378381 A.

Wågberg, L., Norgren, G.D.M., Lindstrom, T., Ankerfors, M., Axnas, K., 2008, The build-up of polyelectrolyte multilayers of microfibrillated cellulose and cationic polyelectrolytes, Langmuir, 24:784-795.

Wang, H., Li, D., Yano, H., Abe, K., 2014, Preparation of tough cellulose II nanofibers with high thermal stability from wood, Cellulose, 21:1505-1515.

Wang, Y., 2008, Cellulose fiber dissolution in sodium hydroxide solution at low temperature: dissolution kinetics and solubility improvement, PhD dissertation, Georgia Institute of Technology.

Welch, L.V., Kerekes, R.J., 1994, Characterization of the PFI mill by the C-factor, APPITA, 47(5):387-390.

Xu, X., Liu, F., Jiang, L., Zhu, J.Y., Haagenson, D., Wiesenborn, D.P., 2013, Cellulose Nanocrystals vs. Cellulose Nanofibrils: A Comparative Study on Their Microstructures and Effects as Polymer Reinforcing Agents, Appl. Mater. Interfaces, 5:2999-3009.

Yan, H., Lindstrom, T., Christiernin, M., 2006, Some ways to decrease fibre suspension flocculation and improve sheet formation, Nordic Pulp & Paper Research Journal, 21(1):36-43.

Yano, H., Nakahara, S., 2004, Bio-composites produced from plant microfiber bundles with a nanometer unit web-like network, Journal of Materials Science, 39:1635-1638.

Zhang, J., Song, H., Lin, L., Zhuang, J., Pang, C., 2012, Microfibrillated cellulose from bamboo pulp and its properties, Biomass and Bioenergy, 39:78-83.

Zhu, J.Y., Sabo, R., Luo, X., 2011, Integrated production of nano-fibrillated cellulose and cellulosic biofuel (ethanol) by enzymatic fractionation of wood fibers, Green Chem., 13:1339-1344.

Zimmermann, T., Bordeanu, N., Strub, E., 2010, Properties of nanofibrillated cellulose from different raw materials and its reinforcement potential, Carbohydrate polymers, 79:1086-1093.

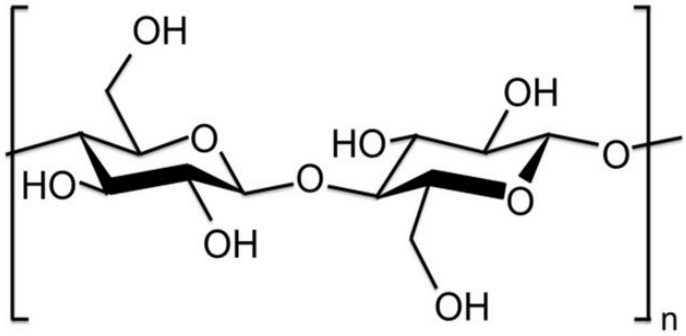

Figure 2.1. Chemical strucutre of cellulose.

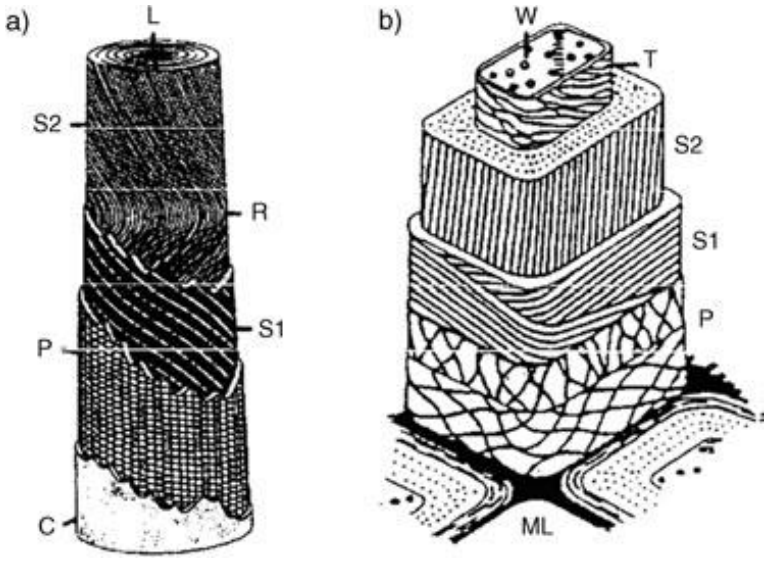

Figure 2.2. Schematic structure of (a) cotton fiber and (b) wood fiber: C=cuticle layer, L=lumen, ML=middle lamella, P=primary cell wall layer, R=reversing point, S1=secondary cell wall layer 1, S2=secondary cell wall layer 2, T=tertiary cell wall, W=wart layer (Klemm et al. 2005).

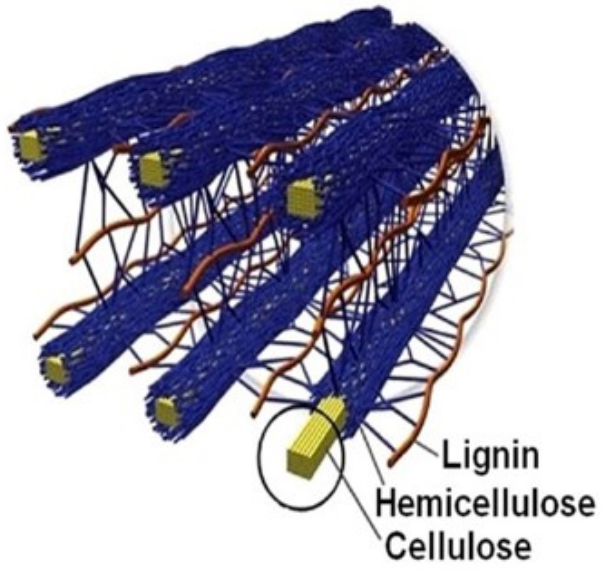

Figure 2.3. Cellulose fibrils surrounded by hemicellulose and lignin (Doherty et al. 2011).

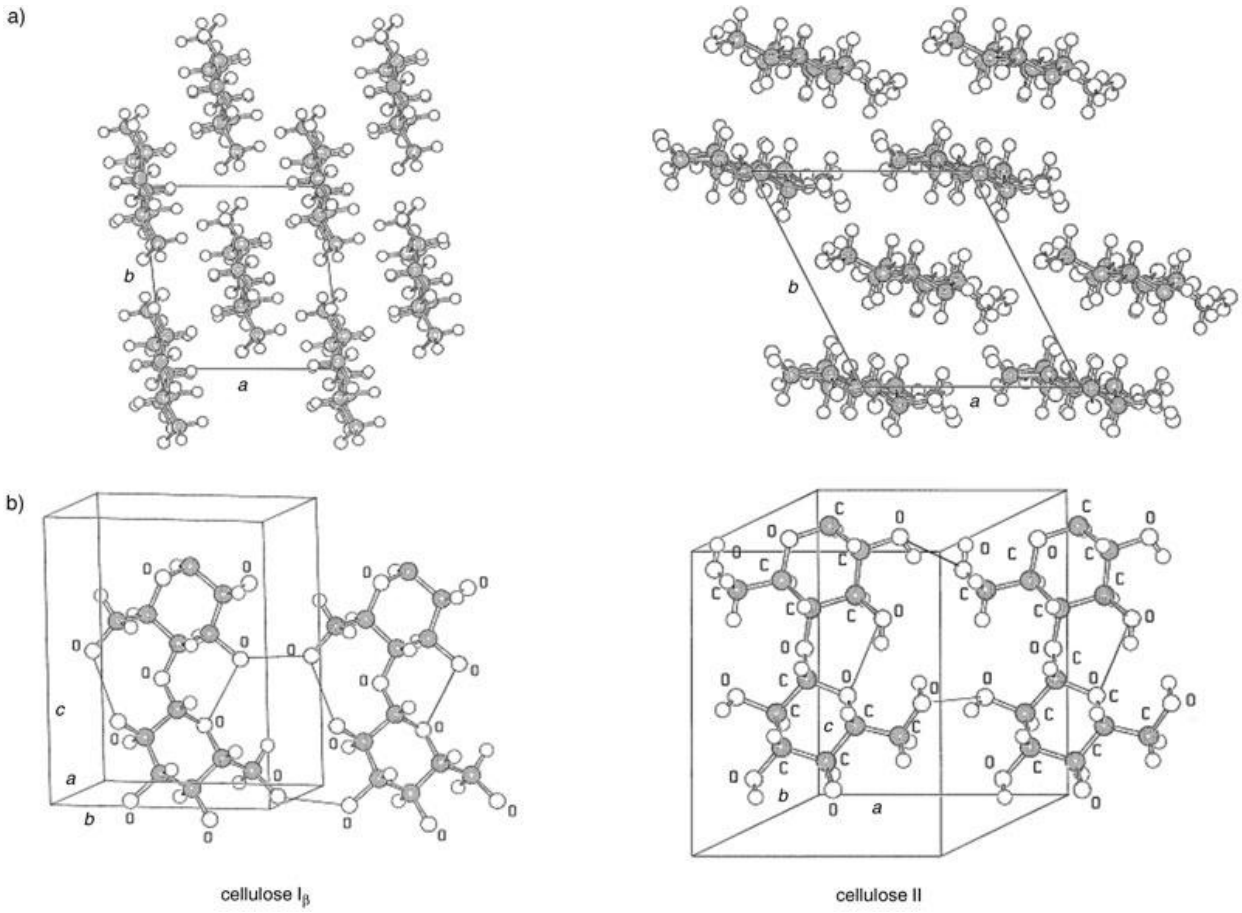

Figure 2.4. Crystal structure of cellulose Iβ and cellulose II: (a) projection of the unit cell (UC) along the a-b plane; (b) projection of the UC parallel to the (100) lattice plane (celluose I) and the (010) lattice plane (cellulose II) (Klemm et al. 2005).

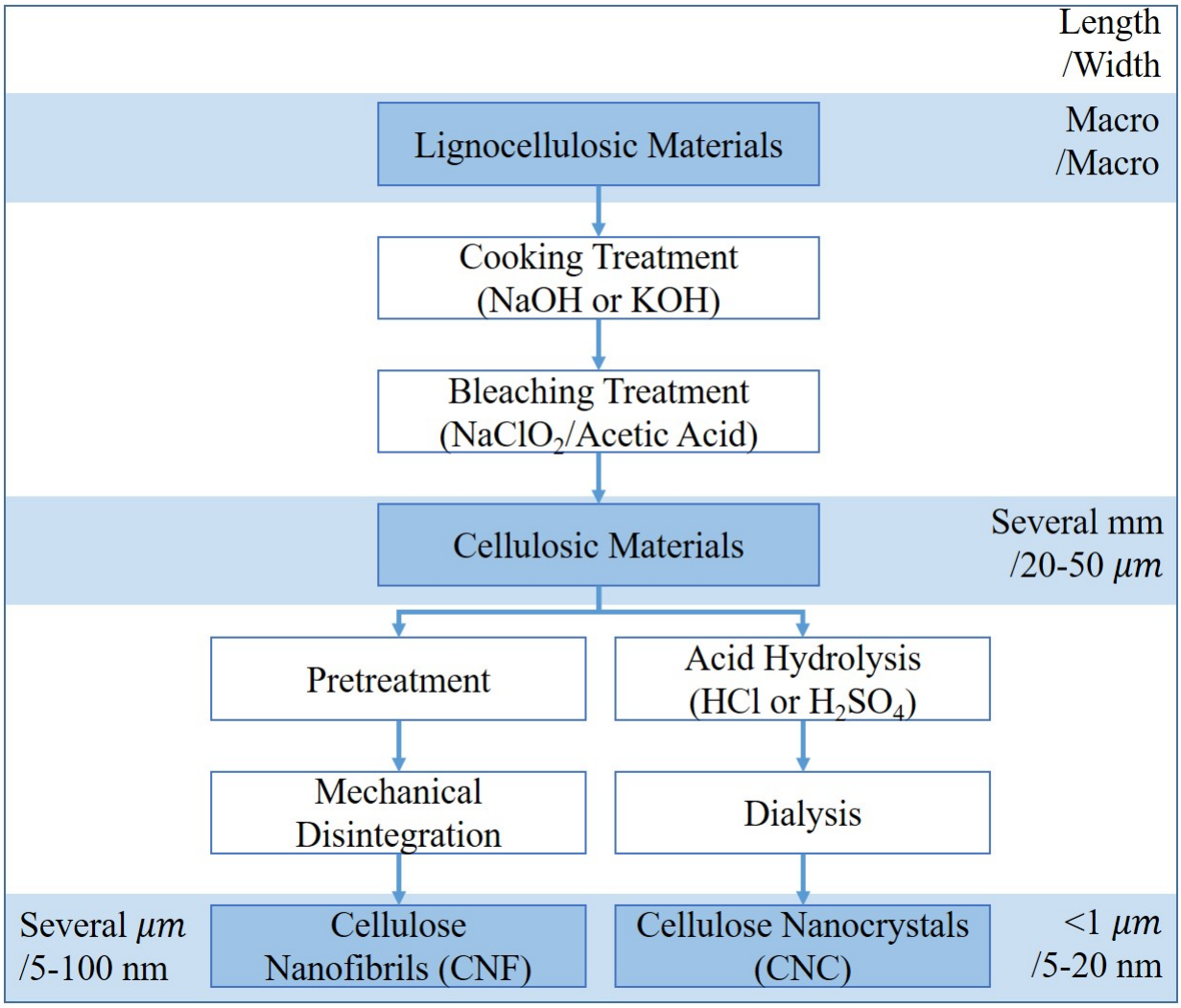

Figure 2.5. A brief production process of cellulose nanofibrils (CNF) and cellulose nanocrystals (CNC) from lignocellulosic materials

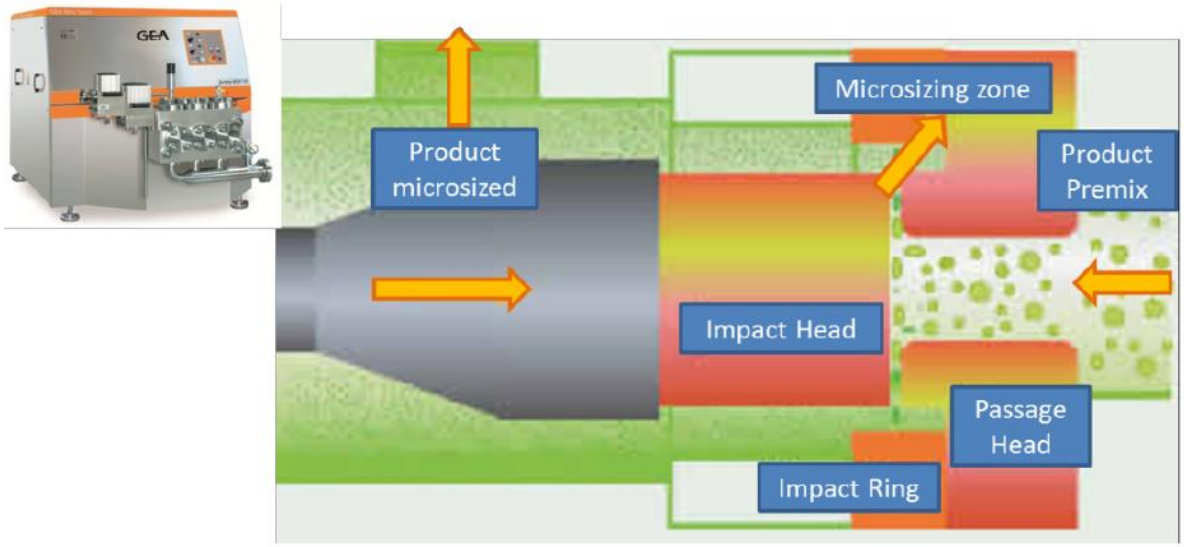

Figure 2.6. Description of homogenizer systems (Missoum et al. 2013).

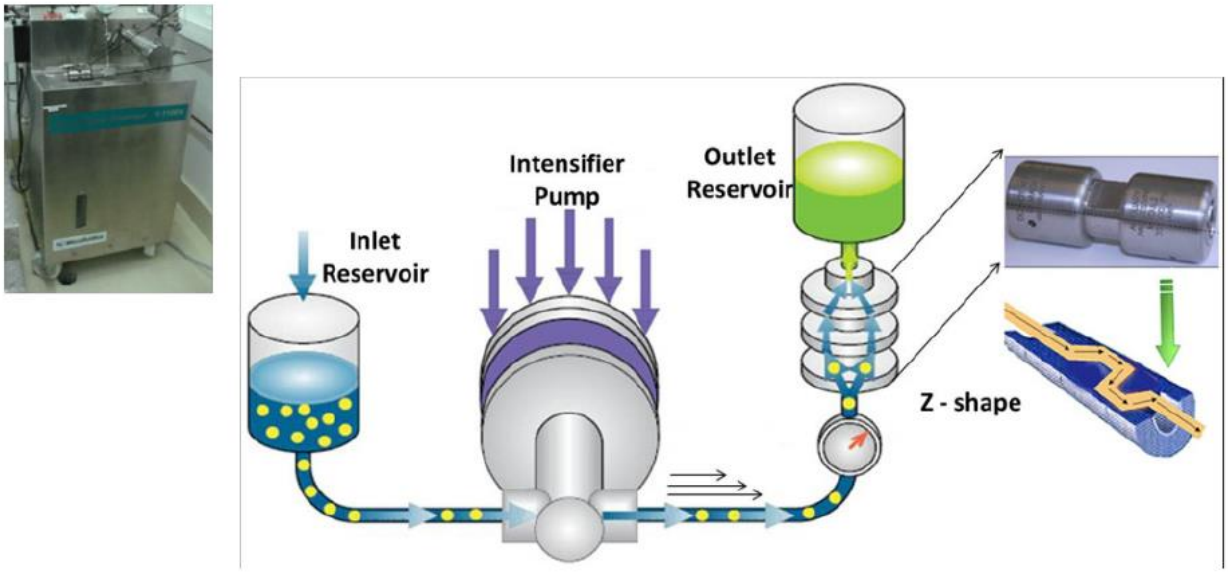

Figure 2.7. Description of microfluidizer systems (Missoum et al. 2013).

Figure 2.8. French pressure cell press.

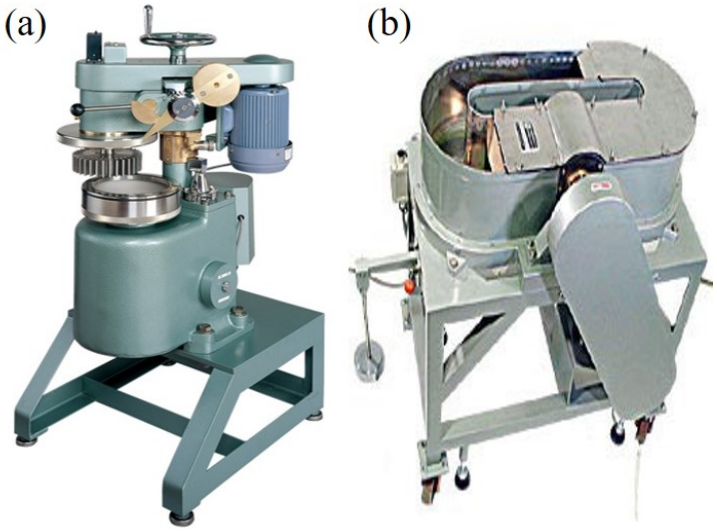

Figure 2.9. PFI Mill (KRK Kumagai) and Valley beater (Testing Machines, Inc.).

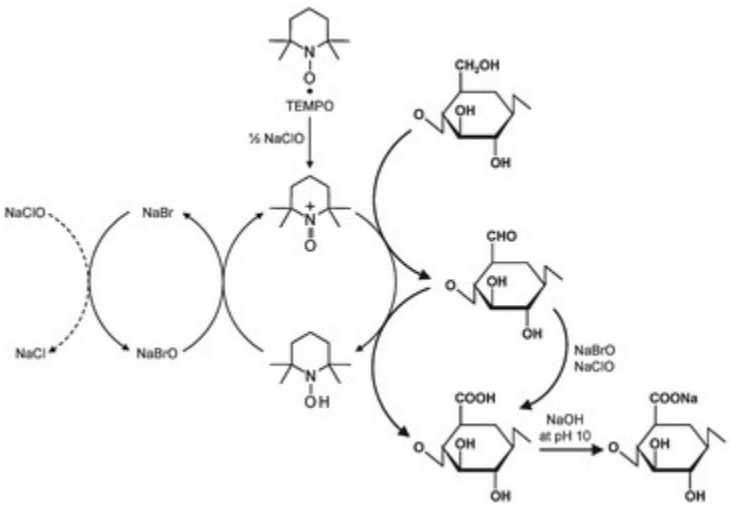

Figure 2.10. TEMPO-mediated oxidation of cellulose at pH 10-11 (Isogai et al. 2011).

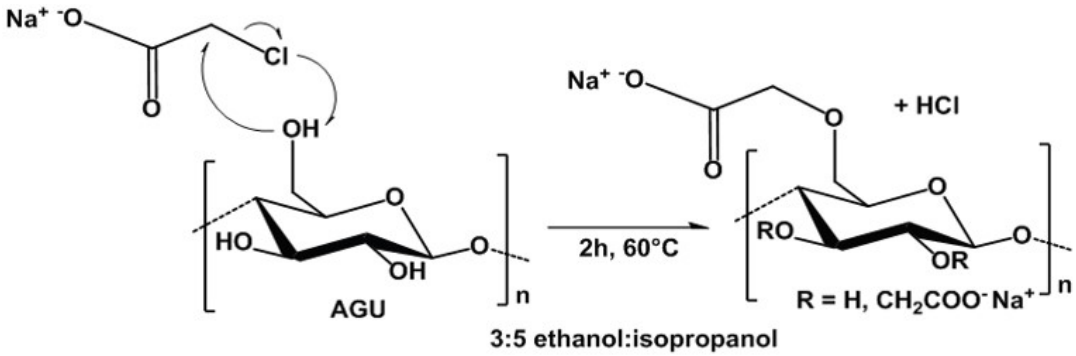

Figure 2.11. Carboxymethylation of cellulose (Tingaut et al. 2011).

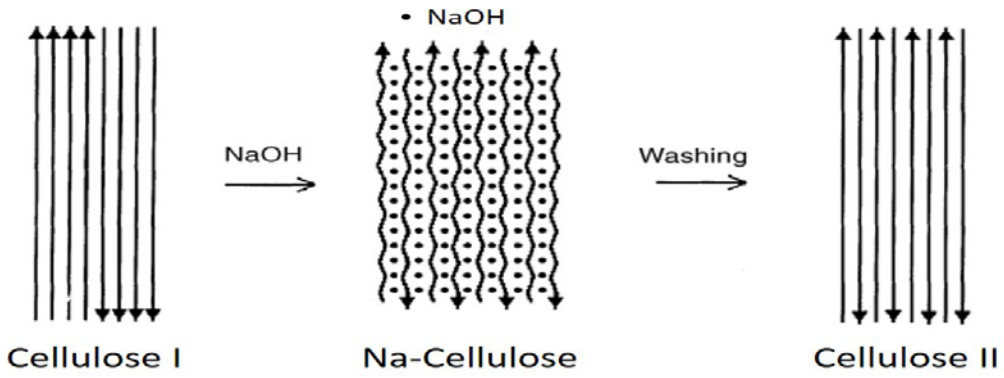

Figure 2.12. Molecular rearrangement of cellulose chains in mercerization (Shibazaki et al. 1997).

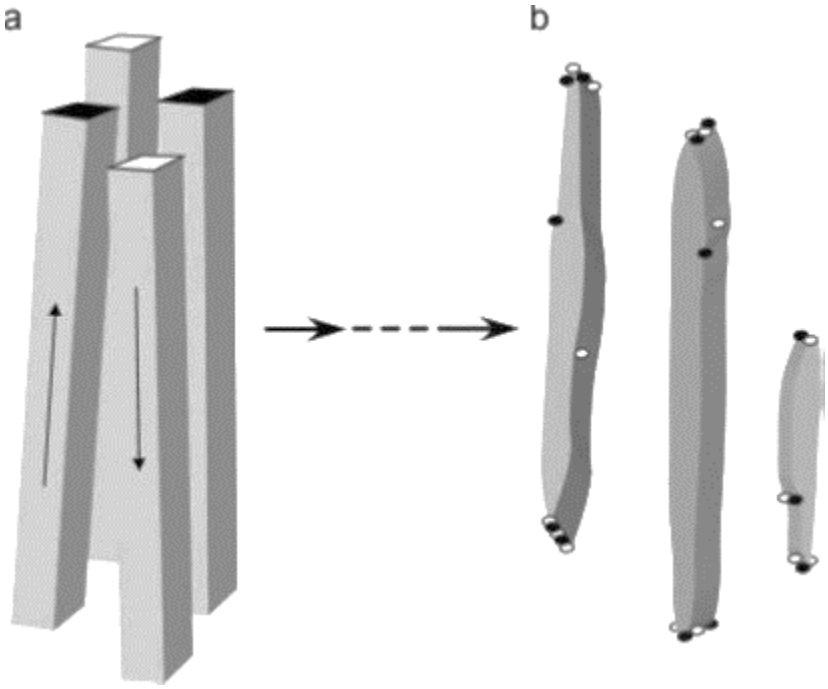

Figure 2.13. Schematic conversion of cellulose I (a) into cellulose II (b) in a ramie fiber. In (b) the dark dots correspond to chain ends of “up” polarity whereas the white dots correspond to chain end of “down” polarity (Kim et al. 2006).

CHAPTER 3

MECHANICAL PRETREATMENT OF FLUFF PULP TO PRODUCE CELLULOSE NANOFIBRILS (CNF) PRECURSORS

Lee, Hansol and Mani, Sudhagar

To be submitted to the Journal of Industrial Crops and Products

Abstract

Cellulose nanofibrils (CNF) is commonly produced by mechanical pretreatment using wet milling methods to facilitate easy disintegration of cellulose fibers by pre-fibrillation and fiber size reduction. However, the use of high energy and water during wet milling methods leads to the increase in overall energy consumption during CNF production and poses challenges during storage and handling. The objectives of this study were to determine the specific energy required for shear cutting of fluff pulp as CNF precursors and to determine the characteristics of the precursors for manufacturing CNF. Specific energy required for shear cutting of fluff cellulose pulp for up to three cycles with a screen size of 0.25 mm was measured. The ground sample received after each cycle was sampled to characterize its properties and its potential to produce CNF hydrogels. As the number of grinding cycle increased, the specific energy required per cycle decreased. The first grinding cycle consumed the highest specific energy of 630 kWh/ton, followed by 186 kWh/ton for the second cycle and 78 kWh/ton for the third cycle. Among three cycles, the third cycle cellulose powder was successfully disintegrated into cellulose nanofibrils with an average diameter of 119 nm without any clogging. In conclusion, the three-cycle shear cutting cellulose powder was sufficient to produce CNF, while reducing the overall energy consumption during CNF production.

Keywords: Shear cutting mill, Cellulose nanofibrils, Mechanical pretreatment, Cellulose, Fluff pulp, Specific grinding energy.

1. Introduction

Cellulose nanofibrils (CNF) is one type of nano-structured cellulose. It typically has a width of below 100 nm and a length of several micrometers. CNF exhibits a number of desirable properties, such as high specific surface area (at least ten times larger than that of raw cellulose fibers), extensive hydrogen-bonding ability, and high tensile strength up to 310 MPa (Abe and Yano, 2009; Fukuzumi et al., 2009; Saito et al. 2009; Yano and Nakahara, 2004). Due to these properties, CNF shows a wide range of applications, such as paper and pulp, biomedical, electronic, automotive, and food applications (Lavoine et al., 2012). To produce cellulose nanofibrils, cellulose fibers are subjected to the mechanical disintegration process where high impact and shear forces are applied. Conventional disintegration methods include high pressure homogenizers, microfluidizers and microgrinders. However, this process has two main challenges; 1) high energy consumption, and 2) clogging problems in a homogenizer.

To address these problems, cellulose fibers are mechanically treated prior to the disintegration process. The mechanical pretreatment process pre-fibrillates cellulose fibers, reduces cellulose fiber size and produces fines (particles that will pass a round hole 76 μm or a nominally 200 mesh screen). Therefore, it makes the disintegration process an easier task, potentially reducing the energy use and clogging issues. Alternatives for mechanical pretreatment include manual cutting, disk refiners, PFI mills, Valley beaters, and blenders (Chakraborty et al., 2005; Dinand et al., 1999; Dufresne et al., 2000; Fukuzumi et al., 2009; Herrick et al., 1983; Iwamoto et al., 2005; Malainine et al., 2005; Spence et al., 2011; Stelte and Sanadi, 2009; Turbak et al., 1983; Zhang et al., 2012). The PFI mill and the Valley beater are commonly used for producing cellulose precursors of cellulose nanofibrils in the laboratory scale. These methods require energy input, leading to the increase in total manufacturing cost for

cellulose nanofibrils. It was reported that a Valley beater needed the effective and total energy of approximately 500 kWh/ton and 3,000 kWh/ton, respectively, for beating bleached eucalyptus and pine pulp for one hour (Atic et al., 2005). Spence et al. (2011) described that the required energy for beating pulp in the Valley beater was 2,000 kWh/ton when a total refining time was three hours. In case of the PFI mill, Welch and Kerekes (1994) estimated the refining energy for PFI milling as 0.18 kWh/ton-rev. If the pulps are refined in a PFI mill for 20,000 revolutions prior to the mechanical disintegration process as described by Sharma et al. (2015), the PFI mill would consume approximately 3,600 kWh/ton. Moreover, theses mechanical pretreatment processes are performed with water at low pulp consistency. The initial pulp consistency for refining in a PFI mill is 10%. 300 g of cellulose slurry containing 30g of cellulose (dry basis) is loaded per run (TAPPI T 248 sp-00). Valley beating is carried out at pulp consistency of 1.57%, having 360g of cellulose (on dry basis) in 23 L (TAPPI T 200 sp-01). The cellulose precursors produced from a PFI mill and a Valley beater are wet, which makes difficulties during storage and handling due to the bulk volume and contamination issues.

A shear cutting mill known as a knife mill has been widely used to grind food and feed. It also has been used for size reduction of biomass. The shear cutting mill could be used to produce cellulose powders, which is can be used as cellulose precursors for cellulose nanofibrils. Energy requirement for pretreating pulps in a shear cutting mill might be lower than that from a Valley beater or a PFI mill. It has been reported that the effective energy for grinding biomass in a shear cutting mill ranged from several tens kWh/ton to 200 kWh/ton although none of studies has tested the shear cutting mill either on cellulose pulp or for fine grinding (Bitra et al., 2009; Cadoche and López, 1989; Miao et al., 2011). In addition, the shear cutting process is a dry processing, thus the cellulose precursors from the shear cutting mill would be easier to handle

and maintain their quality during storage. Consequently, the shear cutting mill can be an alternative mechanical pretreatment method to produce CNF precursors in the form of dry powder, while reducing overall manufacturing energy use.

The main objective of this study is to determine the specific energy consumption and physical characterization of cellulose precursors to produce CNF using a mechanical pretreatment technique (shear cutting method). The investigated physical properties include morphology, moisture content, geometric mean diameter, particle size distribution, bulk and tapped densities, and crystallinity. This study also aims to explore the production of cellulose nanofibrils from cellulose powder obtained by shear cutting process and characterize the resultant CNF.

2. Materials and Method

2.1. Material and shear cutting process

Fluff cellulose pulp (dissolving pulp) was obtained from the commercial paper mill in Georgia, USA. It was oven-dried overnight before grinding. A known quantity of the dried fluff pulp was taken and ground one to three times through a laboratory heavy-duty knife mill (Retsch SM 2000, Germany, Figure 3.1.) with a 0.25 mm screen. The knife mill consisted of a cutting blade rotor (1690 rpm, 60 Hz) which was powered by a 1.5 kW electric motor. The sample was continually fed without exceeding the maximum capacity of the knife mill.

2.2. Shear cutting energy consumption study

To calculate energy requirement for shear cutting of fluff pulp, a multi-function transducer (CR Manetics Inc., MO) was assembled with a computer's data logger and connected to the shear cutting mill (the knife mill) to measure instantaneous power as shown in Figure 3.2. The power data was recorded every 2 seconds. The power required to run the shear cutting mill

empty was measured before the material was fed into the mill in order to determine the net power required to grind the material. Total specific energy consumption for grinding was determined by integrating the area under the instantaneous power consumption curve over grinding duration, and effective specific energy was calculated by subtracting the power consumption under no-load condition from total specific energy (Mani et al., 2004). Each test was repeated three times.

2.3. Characterization of knife-milled powders

2.3.1. Morphology

The morphology of raw fluff pulp and knife-milled powders was determined using an optical microscope (DMI 3000B, Leica). Fluff pulp and knife-milled powder were observed at 5 times and 20 times magnification, respectively. The images presented were regarded to be representative of the fiber surfaces of fluff pulp and knife-milled powder. To determine the change in the morphology by shear cutting, the widths and lengths of fluff pulp and knife-milled powder were measured (widths were measured at the thickest point). In case of fluff pulp, 30 measurements were made to obtain an average value. For the knife-milled powders, the powders were divided into three groups by sieving; smaller than 45 μm, 45-100 μm and larger than 100 μm. 30 measurements were made for each group, and the weight averaged width and length were calculated as follows:

$$\text{Weight averaged width } (\mu m) = (W_1 \times Wt_1 + W_2 \times Wt_2 + W_3 \times Wt_3)/30 \quad (1)$$

$$\text{Weight averaged length } (\mu m) = (L_1 \times Wt_1 + L_2 \times Wt_2 + L_3 \times Wt_3)/30 \quad (2)$$

where W_1, W_2 and W_3 are the sum of widths of knife-milled powder from each group, and L_1, L_2 and L_3 are the sum of lengths of knife-milled powder from each group. Wt_1, Wt_2, and Wt_3 are the

weight percent of knife-milled powder smaller than 45 μm, in size of 45-100 μm and larger than 100 μm, respectively.

Average aspect ratio was calculated as:

Average aspect ratio = Weight averaged length/Weight averaged width (3)

2.3.2. Size distribution

A sample of 15 g cellulose powder was placed in a set of sieves. The sieve sizes used were 250, 200, 160, 125, 100, 63, and 45 μm. Since the powder was very light and fluffy, two glass beads (diameter: 1.5 cm) were placed on each sieve to make sure that the sieving was complete. The set of sieves was placed on the analytical sieve shaker (Retsch AS 2000, Germany), and sieving was performed for 15 minutes. After sieving, the mass of powder remained on each sieve was measured and recorded as a percentage of the original sample mass. Each test was repeated three times. The geometric mean diameter and geometric standard deviation were calculated according to standard ANSI/ASAE-S319.4.

2.3.3. Determination of fines percentage

15 g of raw fluff pulp and knife-milled powders were placed in a sieve of 76 μm. For fluff pulp, ten glass beads were placed on the sieve to facilitate sieving; otherwise, two glass beads were placed on the sieve. Sieving was performed for 15 minutes. After sieving, the mass of powder remained on the sieve was measured to calculate the fines percentage. Each test was repeated three times.

2.3.4. Moisture content

The moisture contents of fluff pulp and knife-milled powders were determined by oven drying and reported in wet basis (equation 4). 10g of the sample was placed on a weight dish and

dried in an oven at 105 ℃ until the weight becomes constant (ASTM D4442-15). Each test was repeated three times.

$$\text{Moisture content (\%)} = (w_o - w_d)/w_o \times 100 \quad (4)$$

where w_o and w_d are the weight of original and dried sample, respectively.

2.3.5. Bulk density and tapped density

Bulk and tapped densities of knife-milled powders were measured. A known amount (m) of the sample was gently poured into a dry graduated cylinder of 250 ml (readable to 2 ml) without compacting. The volume of sample (Vo) was measured, and the bulk density was determined as:

$$\text{Bulk density (kg/m}^3) = m/V_o \quad (5)$$

The cylinder with knife-milled powder was tapped 300 ± 10 times on a wooden platform. The final tapped volume (Vt) was measured, and tapped density was determined as:

$$\text{Tapped density (kg/m}^3) = m/V_t \quad (6)$$

2.3.6. X-ray diffraction analysis (XRD)

The X-ray diffraction analysis was performed to determine the effect of shear cutting on the cellulose crystal structure and crystallinity. One gram of the sample was prepared for XRD in the form of a film. XRD was carried out with the scanning region from 10° to 35° at scan rate of 1°/min, and crystallinity degree (CrD) was calculated using the Segal method as follows:

$$\text{CrD (\%)} = (I_{200} - I_{am})/I_{200} \times 100 \quad (7)$$

where I_{200} and I_{am} are the intensity value for the crystalline cellulose ($2\theta = 22.5°$) and the amorphous cellulose ($2\theta = 18.5°$), respectively.

2.4. Cellulose nanofibrils preparation

Cellulose nanofibrils was prepared using a French pressure cell press. 2wt% cellulose aqueous suspension was prepared by mixing 0.7 g of knife-milled cellulose powder and 35 ml of hot water containing carboxymethylcellulose (CMC, 0.6 wt.%, average molecular weight ~250kD). The suspension was loaded and passed through the French press 15 times at the operating pressure of 1,000-1,200 bar.

2.5. Characterization of cellulose nanofibrils

The properties of cellulose nanofibrils obtained through a French cell press were investigated, such as morphology, light transmittance and suspension stability. Commercially available cellulose nanofibrils from the University of Maine was used as a standard for all the properties.

2.5.1. Morphology of cellulose nanofibrils

2.5.1.1. Optical microscopy

The obtained cellulose nanofibrils was observed using an optical microscope (DMI 3000B, Leica) at 20 times magnification as described in section 2.3.1. A drop of cellulose nanofibrils suspension was placed on a glass side covered with a coverslip. The images presented were considered to be representative of the fiber surfaces of cellulose nanofibrils

2.5.1.2. Field-emission scanning electron microscopy (FE-SEM)

The obtained CNF and standard CNF were observed using a scanning electron microscopy (FEI Inspect F FEG-SEM). The CNF gel was diluted to 0.1wt%. A drop of the diluted suspension was deposited on a silicon wafer and dried for 24 hours at room temperature. The samples were coated with a thin gold-palladium layer applied by ion sputtering with a thickness limited to 5 nm. To prevent damage on the samples, the relatively low acceleration

voltage was used at 4-5 kV. The fiber width was measured with 80 measurements to get an average value. The images presented were considered to be representative of the fiber surfaces of cellulose nanofibrils

2.5.2. Specific surface area study

Specific surface area (SSA) was measured using the Congo red adsorption method (Ougiya et al. 1998; Goodrich and Winter 2007; and Spence et al. 2010b). SSA measurement was made with the third cycle cellulose powder, cellulose nanofibrils prepared from the French cell press, and the standard CNF. Samples were placed into a 0.1 M phosphate butter at pH 6 and treated with various concentrations of Congo red at a final solid content of 0.5%. The samples were incubated at 60 ℃ for 24 h. A small amount of NaCl (10wt% of cellulose weight on dry basis) was added to the samples at the beginning of the experiment in order to neutralize charged surface sites. After 24 hours, the samples were centrifuged at 12,000 rpm (14,000 rcf) for 5 min and 15 min for cellulose powder and the CNF samples, respectively. The supernatant was put into a quartz cuvette, and its absorbance was measured at 500 nm using an ultraviolet (UV)-visible spectrometer (Genesys 10S, Thermo Fisher Scientific). All runs were duplicated with the reported values being the averages. The maximum amount of Congo red absorbed was calculated from the equation (8) derived from Langmuir's absorption theory.

$$[E]/[A] = 1/K_{ad}[A]_{max} + [E]/[A]_{max} \quad (8)$$

where $[E]$ is the solution concentration of Congo red at adsorption equilibrium in mg/ml, $[A]$ is the amount of Congo red adsorbed onto the cellulose surface in mg/g, $[A]_{max}$ is the maximum amount of Congo red adsorbed onto the cellulose surface in mg/g, and K_{ad} is the equilibrium constant. The specific surface area was determined as follows:

$$SSA = ([A]_{max} \times N \times SA)/(M_w \times 10^{21}) \quad (9)$$

where N is Avogadro's constant, SA is the surface area occupied by a single dye molecule (1.73 nm^2), and M_w is the molecular weight of Congo red (696 g/mole)

2.5.3. Visual examination

The stability of cellulose nanofibrils suspensions was investigated through visual examination as described by other authors (Besbes et al., 2011; Chen et al., 2011), but at a lower solid content. The cellulose nanofibrils gel was diluted with deionized water to 0.1 wt.% solid content. The samples were placed motionlessly for 90 minutes, and the photos were taken at 0, 10 and 90 minutes.

2.6. Statistical analysis

Statistical analyses were performed using a scientific software (SAS, University Edition). The effects of grinding amount on grinding energy and rate, and the physical properties of cellulose powders (fines percentage, bulk density and tapped density) were evaluated using one-way ANOVA. Multiple comparisons were also conducted using Tukey method. All differences were considered significant at $p<0.05$. Detailed results are provided in Appendix A.

3. Results and discussion

3.1. Energy consumption for shear cutting process

Specific energy consumption for grinding fluff pulp in a shear cutting mill is given in Table 3.1. A required energy for shear cutting per cycle was reduced as the number of grinding cycles increased. Effective specific energy for the first, second and third cycles were 630.40, 186.29 and 77.51 kWh/ton, respectively. The total effective energy for shear cutting process with three cycles was estimated to be 894.20 kWh/ton. One-way ANOVA test also showed that the specific energy depended on the grinding cycle ($p <0.0001$), but the multiple comparisons by

Turkey test indicated that the specific energy required for the second and third cycles was not significantly different ($p=0.1464$).

The shear cutting mill required 100-200 W of power to be run without sample loaded. When the energy required to run the shear cutting mill empty was included, the total energy for three-cycle shear cutting process was increased to 1,458.54 kWh/ton, which could be lower than the required energy for conventional mechanical pretreatment processes. For instance, Atic et al. (2005) reported that refining bleached pine fibers in a Valley beater required a total beating energy of 2,995 kWh/ton which included a net beating energy of 578 kWh/ton for a total refining time of one hour. Spence et al. (2011) performed three-hour refining process using a Valley beater prior to the mechanical disintegration process, and they reported that the required beating energy was 2,000 kWh/ton. However, it is not clear whether this value included no-load power or not. With respect to a PFI mill, Welch and Kerekes (1994) estimated the energy requirement for pulp refining in the PFI mill as a function of revolutions (0.18 kWh/ton-rev.). If the pulp fibers are refined in a PFI mill for 20,000 revolutions prior to the mechanical disintegration process as described by Sharma et al. (2015), the required energy would be 3,600 kWh/ton based on the estimation by Welch and Kerekes. The mechanical pretreatment process with the PFI mill could be performed at very high revolutions. As an example, Chakraborty et al. (2005) refined bleached kraft pulp in a PFI mill at 125,000 revolutions to produce submicron sized cellulose precursors before the mechanical disintegration process. The energy consumption for this PFI milling process was estimated to be 21,700 kWh/ton (Chakraborty et al., 2007). Consequently, three-cycle shear cutting of fluff pulp has a potential to reduce energy consumption for the mechanical pretreatment process up to 15 folds.

Besides, grinding rate was measured for every cycle of shear cutting process. It increased with increasing grinding cycle from 7.42 to 34.73 g/min. One-way ANOVA results also showed that there was a significant difference in the grinding rate across the number of the grinding cycles ($p = 0.0003$). This increase in grinding rate indicates that the finer particles were obtained with the increased grinding amount since fine particles can pass through the screen more easily than coarse particles.

3.2. Morphology of cellulose precursor/powders

Fluff pulp consisting of long cellulose fibers was ground into powders by passing through a shear cutting mill as shown in Figure 3.3. The number of grinding cycle did not affect visual appearance of knife-milled powders. Optical microscopic images also show that during the first grinding cycle, the major morphological change occurred; whereas, during the second and third cycles, there was no significant change in morphology of knife-milled powders (Figure 3.4).

With respect to pulp dimensions, fluff pulp had an average length and width of 3.63 mm and 41.69 μm, respectively, and its average aspect ratio was calculated at 88.76. After the first grinding cycle, the average length and width of cellulose fibers greatly decreased from 3.63 mm to 302.67 μm and from 41.69 μm to 32.12 μm, respectively. There was no further noticeable decrease in the fiber width after the second and third cycles. The average width was 30.44 μm and 31.73 μm for two-cycle and three-cycle knife-milled pulp, respectively. In contrast, the average length continuously decreased with increasing grinding cycles. Two-cycle and three-cycle knife-milled powders had an average length of 290.71 μm and 271.78 μm, respectively. This indicates that the major size reduction was achieved during the first grinding cycle as described earlier. In addition, the gradual decrease in length, but not in width suggests that cellulose pulp was cut in longitudinal as well as transverse directions at the beginning of

grinding; afterward, pulp milling was performed mainly in a transverse direction. This change in the fiber length is a distinct feature of shear cutting. The typical mechanical refining processes do not have a significant effect on fiber shortening. For instance, fiber length was slightly reduced from 1.2 mm to 1 mm after pulp refining in a PFI mill at 10,000 revolutions (Jones et al., 2013). Other authors also reported that the refining in a PFI mill did not make an apparent reduction in fiber length (Marrakchi et al., 2011; Zhang et al., 2004). Regarding refining in a Valley beater, the effect on fiber shortening has not been confirmed. Zeng et al. (2012) refined bleached kraft softwood pulp in a Valley beater for one hour, and the average fiber length was almost same before and after the refining process; from 2.05 mm to 2.01 mm. However, Jones et al. (2013) demonstrated that the average length of hardwood pulp gradually decreased to 0.4-0.5 mm from 1.2 mm as the refining process continued up to 90 minutes. In addition, Spence (2011) described that fiber length was dramatically reduced after three-hour refining in a Valley beater, but the exact fiber length was not reported. Consequently, the shear cutting process tends to reduce the fiber length more efficiently than the refining process in a PFI mill or a Valley beater, and cellulose fibers with decreased length can be easily delaminated into cellulose nanofibrils, preventing plugging in a homogenizer.

3.3. Physical properties of cellulose precursors/powders

We investigated size distribution of knife-milled powders to evaluate the effect of grinding amount on fiber size. First of all, a geometric mean diameter decreased with increasing grinding amount. The geometric mean diameter for one-cycle and two-cycle knife-milled powders were 91.97 μm and 87.10 μm, respectively, and the geometric mean diameter was further reduced to 70.33 μm after the third cycle. Figure 3.5. shows a particle size distribution of the powders. The graphs of size distribution moved left with increasing grinding cycle, indicating the obtained

powder had smaller dimensions as the shear cutting proceeded. Besides, 2.7% of the first cycle powder was larger than 250 μm, which could impede the production of cellulose nanofibrils although the grinding process was performed with a screen size of 250 μm. This may be because raw fluff pulp had knots, and the shear cutting process with one cycle was not sufficient to remove the knots. It is likely that three-cycle shear cutting process removed almost all knots as only 0.4% of the third cycle powder remained on the 250 μm sieve.

In addition, the shear cutting process produced more fines with increasing grinding amount. The fines percent for fluff pulp was 5.06% and dramatically increased to 25.84% for one-cycle knife-milled powder. The fraction of fines gradually increased to 33.96%, and 37.22% for two-cycle, and three-cycle knife-milled powder, respectively. One-way ANOVA test also supported that the fines percent depended on the number of the grinding cycles with a p-value of less than 0.0001. However, the Tukey test result indicated that there was no statistical significance in fines percentages between the second and third cycles. Fines in the pulps facilitate fiber disintegration because exposed cross-sections in fines are more accessible to process (Herrick et al., 1983; Spence et al., 2010a).

Bulk and tapped densities of grinds were also measured. Both densities increased with increasing grinding cycles. Three-cycle knife-milled powder had the highest bulk and tapped densities of 111.59kg m^{-3} and 202.63 kg m^{-3} followed by two-cycle knife-milled powder (96.79 kg m^{-3} and 175.72 kg m^{-3}) and one-cycle knife-milled powder (93.48 kg m^{-3} and 168.17 kg m^{-3}), One-way ANOVA test for both bulk and tapped densities also showed that bulk and tapped densities of knife-milled powders were dependent on the grinding amount ($p < 0.0001$). Such increase in bulk and tapped densities suggests that the particle size was reduced with increasing grinding amount. As particle size decreased, the pore spaces between particles decreased,

resulting in the increase in bulk and tapped density. This was also confirmed by Mani et al. (2004).

The shear cutting process did not affect other pulp properties, such as moisture content and crystallinity. Fluff pulp and knife-milled powders had a moisture content of approximately 6.9 wb%. With respect to the effects on cellulose crystal structure, the shear cutting process did not change cellulose crystal structure. All samples had the crystallinity in range of 73-75% and showed similar X-ray diffraction patterns with three peaks at 2θ angles of approximately 14.6° ($1\bar{1}0$), 16.5° (110) and 22.5° (200), which were characteristic of cellulose I structure (Figure 3.6).

3.4. Effect of shear cutting on CNF production

Finally, we investigated the effect of grinding amount on the production of cellulose nanofibrils. The increase in the grinding cycle tended to enhance the ease of cellulose fibrillation. In case of one- or two-cycle knife-milled powders, it is likely that some of the powders would remain inside the French press, leading to clogging the equipment because of their large size. In contrast, knife-milled powder prepared with three cycles was small enough to produce cellulose nanofibrils by passing through a French press 15 times without clogging. As shown in Figure 3.7, the obtained cellulose nanofibrils looked like a gel as standard CNF did. The fibrillated samples with 10 and 15 passes through the French press were observed using an optical microscope. The sample obtained with 10 passes was not well-fibrillated, consisting of large fibers. After additional 5 passes, the well-fibrillated cellulose was prepared as shown in Figure 3.8. Figure 3.9 shows a scanning electron microscopic image of the fibrillated cellulose with 15 passes through the French press and standard cellulose nanofibrils. Both samples consisted of well-delaminated fibers at the nano scale. Figure 3.10 presents the distribution of the fiber width of these two samples. In case of the CNF obtained through the French press, 67% of the cellulose

fibers had a width of below 100 nm. The average width was calculated to be 118.7 nm with a standard deviation of 113.5 nm. Such large standard deviation is because the fibers with a width of 500-700 nm existed although only 11% of the fibers had a width of larger than 200 nm. In case of standard CNF, 49% of the cellulose fibers had a width of below 100 nm, whereas 15% of the fibers had a width of larger than 200 nm. As a result, its average width was larger than that of CNF obtained from the French press; 134 nm with a standard deviation of 80.4 nm.

In addition, the specific surface area of the third cycle cellulose powder, CNF obtained through the French press and standard CNF was measured since it is an indirect indicator of the fibrillation degree. When cellulose fibers are delaminated into nano-scale fibers, the specific surface area will be increased due to the change in external surface and internal pore structures of the fibers (Spence et al., 2010b). As expected, the three-cycle knife-milled powder had a specific surface area of 123 m^2g^{-1}, while two CNF samples had a much larger specific surface area. The cellulose nanofibrils obtained in this study had a specific surface area of 269 m^2g^{-1}, which is larger than that of the standard CNF (211 m^2g^{-1}). This suggests that the obtained CNF have a comparable fibrillation degree to standard CNF.

The stability of the 0.1wt% aqueous suspensions of the fibrillated cellulose was investigated by visual examination (Figure 3.11). The fibrillated cellulose prepared with 15 times through a French press did not present sedimentation within 10 minutes. After 90 minutes of standing, a small portion of the sample settled down to the bottom of the glass bottle, and most of the sample was still dispersed in water. This suggests that this sample contained nano-scale cellulose fibers, which can be dispersed in water for a long time. This is consistent with the results of SEM images. In case of standard cellulose nanofibrils (sample b), the sample started to settle down within 10 minutes after standing. Sedimentation further proceeded and two layers were clearly

formed after 90 minutes. This might be because that most of the cellulose fibers are too large to be dispersed in water.

4. Conclusions

Mechanical pretreatment using a shear cutting mill with three cycles was sufficient to produce cellulose precursors for cellulose nanofibrils production in the form of dry powder, which is favorable for storage and handling. The third cycle cellulose powder had the geometric mean diameter of 70.33 μm and the bulk and tapped densities of 111.59 kg m^{-3} and 202.63 kg m^{-3}, respectively. It was small enough to be disintegrated into cellulose nanofibrils without a clogging problem in a homogenizer, and the obtained cellulose nanofibrils showed comparable characteristics to standard CNF produced at pilot scale. In addition, three-cycle shear cutting of fluff pulp required a relatively low energy consumption (effective specific energy: 894 kWh/ton and total specific energy: 1,495 kWh/ton) compared with other mechanical pretreatments by set milling methods. The future global market size for nanocellulose is estimated to be 35 million tonnes/year (Cowie et al., 2014). If 50% of nanocellulose is in the form of cellulose nanofibrils at 2wt% solid content, up to 7.08 TWh of energy could be reduced per year globally by using a shear cutting mill over other methods.

References

Abe, K., Yano, H., 2009, Comparison of the characteristics of cellulose microfibril aggregates of wood, rice straw and potato tuber, Cellulose, 16:1017–1023.

ASABE, 2008, ANSI/ASAE- S319.4, Method of Determining and Expressing Fineness of Feed Materials by Sieving, American Society of Agricultural and Biological Engineers, Joseph, MI.

ASTM. 2015, ASTM-D4442-15, Standard Test Methods for Direct Moisture Content Measurement of Wood and Wood-Based Materials, American Society for Testing and Materials, West Conshohocken, PA.

Atic, C., Immamoglu, S., Valchev, I., 2005, Determination of specific beating energy-applied on certain pulps in a valley beater, J. Univ. Chem. Technol. Met., 40(3):199–204.

Besbes, I., Alila, S., Boufi, S., 2011, Nanofibrillated cellulose from TEMPO-oxidized eucalyptus fibers: Effects of the carboxyl content, Carbohydrate Polymers, 84:975-983.

Bitra, V.S.P., Womac, A.R., Igathinathane, C., Miu, P.I., Yang, Y.T., Smith, D.R., Chevanan, N., Sokhansanj, S., 2009, Direct measures of mechanical energy for knife mill size reduction of switchgrass, wheat straw, and corn stover, Bioresource Technology, 100:6578–6585.

Cadoche, L., López, G.D., 1989, Assessment of size reduction as a preliminary step in the production of ethanol for lignocellulosic wastes, Biological Wastes, 30:153–157.

Chakraborty, A., Sain, M., Kortschot, M., 2005, Cellulose microfibrils: A novel method of preparation using high shear refining and cryocrushing, Holzforschung, 59:102-107.

Chakraborty, A., Sain, M.M., Kortschot, M.T., Ghosh, S.B., 2007, Modeling energy consumption for the generation of microfibres from bleached kraft pulp fibres in a PFI mill, BioResources, 2(2):210-222.

Chen, W., Yu, H., Liu, Y., Chen, P., Zhang M., Hai, Y., 2011, Individualization of cellulose nanofibers from wood using high-intensity ultrasonication combined with chemical pretreatments, Carbohydrate Polymers, 83:1804-1811.

Chevanan, N., Womac, A.R., Bitra, V.S.P., Igathinathane, C., Yang, Y.T., Miu, P.I., Sokhansanj, S., 2010, Bulk density and compaction behavior of knife mill chopped switchgrass, wheat straw, and corn stover, Bioresource Technology, 101:207-214.

Cowie, J., Bilek, E.M., Wegner, T.H., Shatkin, J.A., 2014, Market projections of cellulose nanomaterial-enabled products – Part 2: Volume estimates, Tappi J., 13(6):57-69.

Dinand, E., Chanzy, H., Vignon, R.M., 1999, Suspensions of cellulose microfibrils from sugar beet pulp, Food hydrocolloids, 13:275-283.

Dufresne, A., Dupeyre, D., Vignon, M.R., 2000, Cellulose Microfibrils from Potato Tuber Cells: Processing and Characterization of Starch–Cellulose Microfibril Composites, Journal of Applied Polymer Science, 76:2080-2092.

Fukuzumi, H., Saito, T., Iwata, T., Kumamoto, Y., Isogai, A., 2009, Transparent and High Gas Barrier Films of Cellulose Nanofibers prepared by TEMPO-Mediated Oxidation, Biomacromolecules, 10:162-165.

Goodrich, J.D., Winter, W.T., 2007, α-Chitin Nanocrystals Prepared from Shrimp Shells and Their Specific Surface Area Measurement, Biomacromolecules, 8:252-257.

Herrick, F.W., Casebier, R.L., Hamilton, J.K., Sandberg, K.R., 1983, Microfibrillated cellulose: Morphology and accessibility, J. Appl. Polym. Sci. Appl. Polym. Symp., 37: 797-813.

Iwamoto, S., Nakagaito, A.N., Yano, H., Nogi, M., 2005, Optically transparent composites reinforced with plant fiber-based nanofibers, Appl. Phys. A, 81:1109-1112.

Jones, B.W., Venditti, R., Park, S., Jameel, H., Koo, B., 2013, Enhancement in enzymatic hydrolysis by mechanical refining for pretreated hardwood lignocellulosics, Bioresource Technology, 147:353-360.

Lavoine, N., Desloges, I., Dufresne, A., Bras, J., 2012, Microfibrillated cellulose - its barrier properties and applications in cellulosic materials: a review, Carbohydr Polym., 90(2):735-64.

Malainine, M.E., Mahrouz, M., Dufresne, A., 2005, Thermoplastic nanocomposites based on cellulose microfibrils from Opuntia ficus-indica parenchyma cell, Composites Sci. and Tech., 65:1520-1526.

Mani, S., Tabil, L.G., Sokhansanj, S., 2004, Grinding performance and physical properties of wheat and barley straws, corn stover and switchgrass, Biomass and Bioenergy, 27(4):339-352.

Marrakchi, Z., Khiari, R., Oueslati, H., Mauret, E., Mhenn, F., 2011, Pulping and papermaking properties of Tunisian Alfa stems (Stipa tenacissima)—Effects of refining process, Industrial Crops and Products, 34:1572-1582.

Miao, Z., Grift, T.E., Hansen, A.C., Ting, K.C., 2011, Energy requirement for comminution of biomass in relation to particle physical properties, Industrial Crops and Products, 33(2), 504-513.

Ougiya, H., Hioki, N., Watanabe, K., Morinaga, Y., Yoshinaga, F., Samejima, M., 1998, Relationship between the physical properties and surface area of cellulose derived from adsorbates of various molecular sizes, Bioscience, Biotechnology, and Biochemistry., 62(10):1880-1884.

Saito, T., Hirota, M., Tamura, N., Kimura, S., Fukuzumi, H., Heuz, L., Isogai, A., 2009, Individualization of nano-sized plant cellulose fibrils by direct surface carboxylation suing TEMPO catalyst under neutral conditions, Biomacromolecules, 7:1687-1691.

Spence, K.L., Benditti, R.A., Rojas, O.J., Habibi, Y., Pawlak, J.J., 2011, A comparative study of energy consumption and physical properties of microfibrillated cellulose produced by different processing methods, Cellulose, 18:1097-1111.

Spence, K.L., Benditti, R.A., Rojas, O.J., Habibi, Y., Pawlak, J.J., 2010a, The effect of chemical composition on microfibrillar cellulose films from wood pulps: mechanical processing and physical properties, Bioresource Tech., 101:5961-5968.

Spence, K.L., Venditti, R.A., Rojas, O.J., Habibi, Y., Pawlak, J.J., 2010b, The effect of chemical composition on microfibrillar cellulose films from wood pulps: water interactions and physical properties for packaging applications, Cellulose, 17:835-848.

Stelte, W., Sanadi, A.R., 2009, Preparation and characterization of cellulose nanofibers from two commercial hardwood and softwood pulps, Ind. Eng. Chen. Res., 48:11211-11219.

TAPPI, 2000, T248 sp-00, Laboratory beating of pulp (PFI mill method). Technical Association of the Pulp and Paper Industry, Norcross, GA.

TAPPI, 2001, T200 sp-01, Laboratory beating of pulp (Valley beater method). Technical Association of the Pulp and Paper Industry, Norcross, GA.

Turbak, A.F., Snyder, F.W., Sandberg, K.R., 1983, Microfibrillated cellulose, a new cellulose product: Properties, uses, and commercial potential., J. Appl. Polym. Sci. Appl. Polym. Symp., 37:815-827.

Welch, L.V., Kerekes, R.J., 1994, Characterization of the PFI mill by the C-factor, APPITA, 47(5):387-390.

Xhanari, K., Syverud, K., Chinga-Carrasco, G., Paso, K., Stenius, P., 2011, Reduction of water wettability of nanofibrillated cellulose by adsorption of cationic surfactants, Cellulose, 18:257-270.

Yano, H., Nakahara, S., 2004, Bio-composites produced from plant microfiber bundles with a nanometer unit web-like network, Journal of Materials Science, 39:1635-1638.

Zeng, X., Retulainen, E., Heinemann, S., Fu, S., 2012, Fibre deformations induced by different mechanical treatments and their effect on zero-span strength, Nordic Pulp and Paper Research Journal, 27(2):335-342.

Zhang, J., Song, H., Lin, L., Zhuang, J., Pang, C., 2012, Microfibrillated cellulose from bamboo pulp and its properties, Biomass and Bioenergy, 39:78-83.

Zhang, M., Hubbe, M.A., Venditti, R.A., Heitmann, J.A., 2004, Refining to Overcome Effects of Drying Unbleached Kraft Fibers in the Presence or Absence of Sugar, Progress in Paper Recycling, 13(2):1-8.

Table 3.1. Grinding rate and effective specific energy of shear cutting process with the different number of cycles.

Grinding cycle	Grinding rate (g/min)[a]	Effective specific energy (kWh/metric tonne)[a]	Total specific energy (kWh/ metric tonne) [a]
1	7.42 (0.27)	630.40 (95.02)	1053.30 (35.33)
2	23.07 (6.09)	186.29 (42.17)	257.50 (61.47)
3	34.73 (0.97)	77.51 (4.90)	147.74 (11.86)

*a: Number enclosed in the parenthesis were standard deviations with n=3.

Table 3.2. Average width, length and aspect ratio of fluff pulp and one to three-cycle knife-milled powders.

Grinding cycle	Average width (μm)	Average length (μm)	Average aspect ratio
0[*a]	41.69 (8.01)	3630 (747.9)	88.76 (18.64)
1[*b]	30.55 (9.37)	302.67 (138.35)	8.56 (5.47)
2[*b]	28.37 (9.23)	290.71 (97.69)	8.43 (4.54)
3[*b]	30.29 (8.65)	271.98 (87.79)	8.61 (5.13)

*a: Numbers enclosed in the parenthesis were standard deviations with n=30.

*b: In case of knife-milled powders, weight averaged width and length were calculated. Numbers enclosed in the parenthesis were standard deviations with n=90.

Table 3.3. Physical properties of one to three-cycle knife-milled powders.

Grinding cycle	Moisture content (%wb)[a]	Geometric mean diameter (μm) [a]	Fines (%)[a]	Bulk density (kg m^{-3})[b]	Tapped density (kg m^{-3})[b]	Crystallinity (%)[a]
0	6.95 (0.10)	-	5.06 (0.98)	-	-	75.19 (4.86)
1	6.90 (0.13)	91.97 (2.30)	25.84 (3.85)	93.48 (2.85)	168.17 (2.64)	73.40 (2.98)
2	6.82 (0.14)	87.10 (12.41)	33.96 (2.43)	96.79 (1.99)	175.72 (2.55)	75.12(3.76)
3	6.86 (0.15)	70.33 (3.05)	37.22 (3.48)	111.59 (3.06)	202.63 (1.19)	74.57 (1.77)

*****a: Number enclosed in the parenthesis were standard deviations with n=3.

*b: Number enclosed in the parenthesis were standard deviations with n=5.

Table 3.4. Average fiber width and specific surface area (SSA) for samples.

Sample	Average width (nm)[*a]	SSA (m^2/g)[*b]
Cellulose powder	30,290 (8,650)	112.07±0.70
CNF from French press	118.73 (113.52)	269.46±3.43
Standard CNF	133.96 (80.43)	210.62±0.00

*****a: Number enclosed in the parenthesis were standard deviations with n=90 for the cellulose powder and n=80 for the CNF samples, respectively.

*b: ±1 the difference between the smallest and largest values indicated

Figure 3.1. A laboratory heavy-duty shear cutting mill (Retsch SM 2000, Germany).

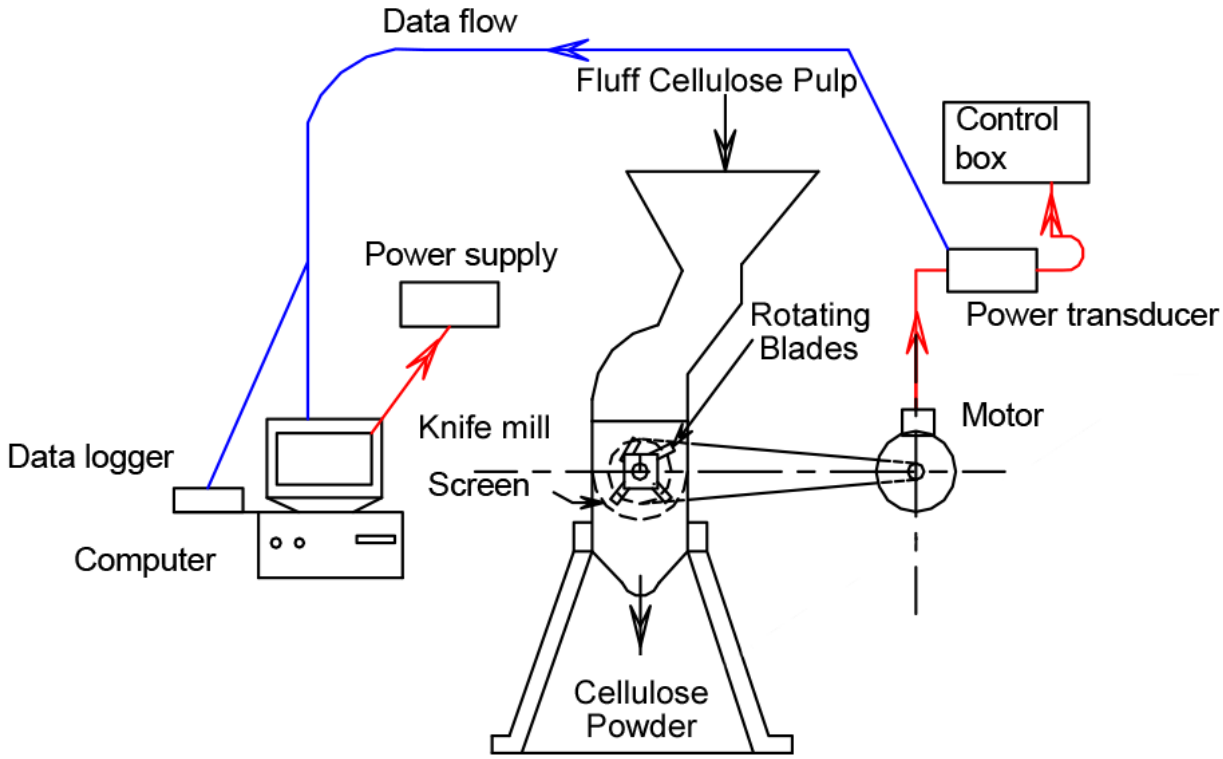

Figure 3.2. Complete flow diagram for shear cutting process

Figure 3.3. Fluff pulp (left) and three-cycle knife-milled powder (right).

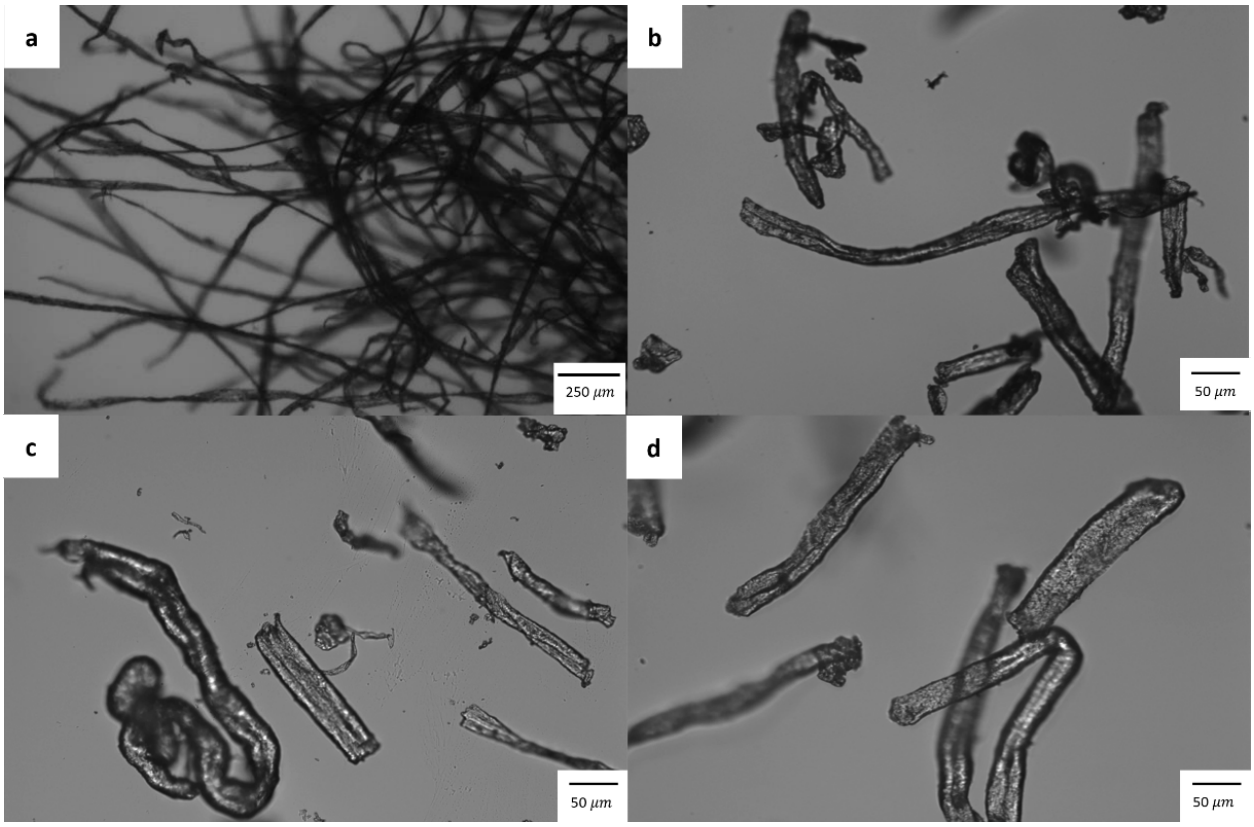

Figure 3.4. Optical microscopic images of (a) raw fluff pulp at 5 times magnification and (b) one-, (c) two-, and (d) three-cycle knife-milled powders at 20 times magnification.

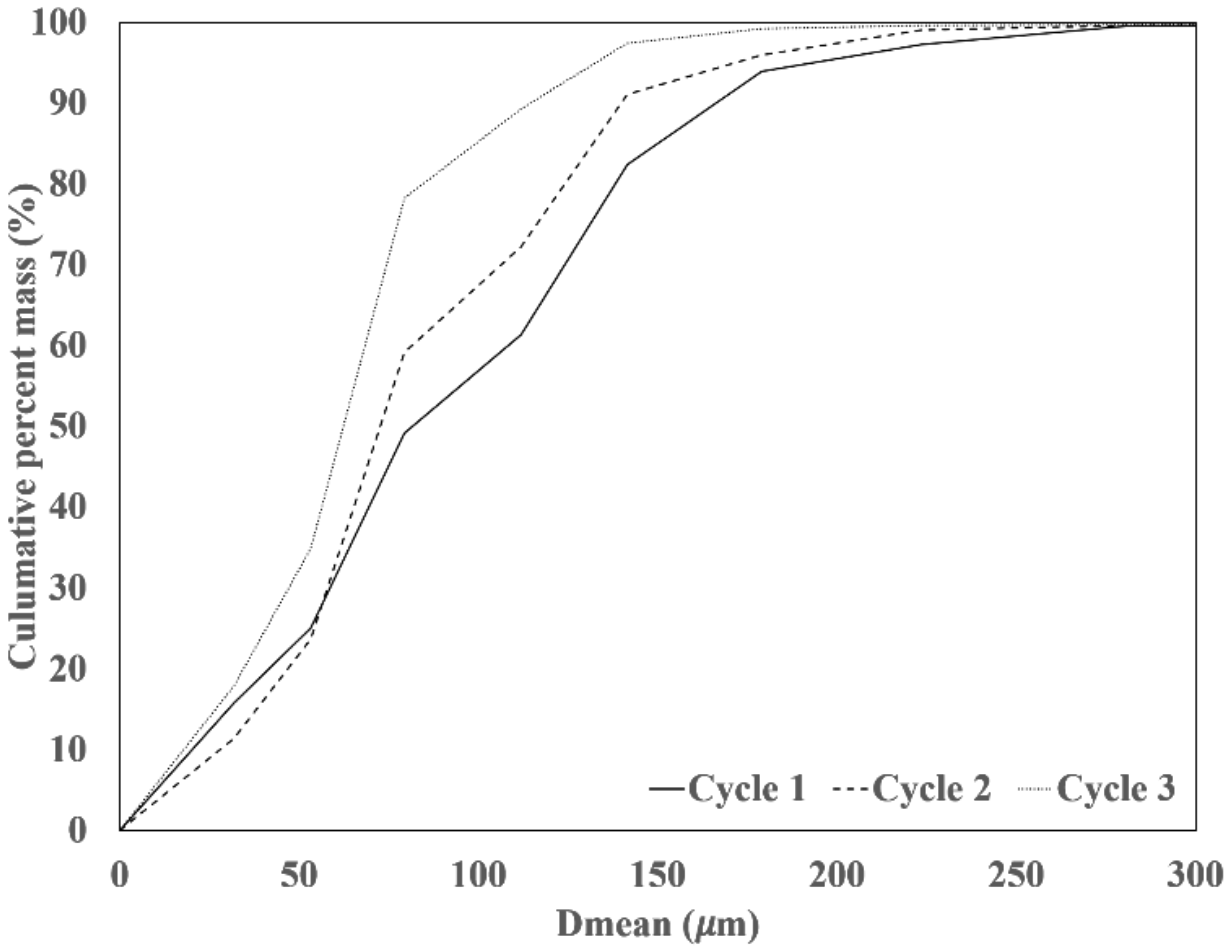

Figure 3.5. Particle size distributions of one- to three-cycle knife-milled powders.

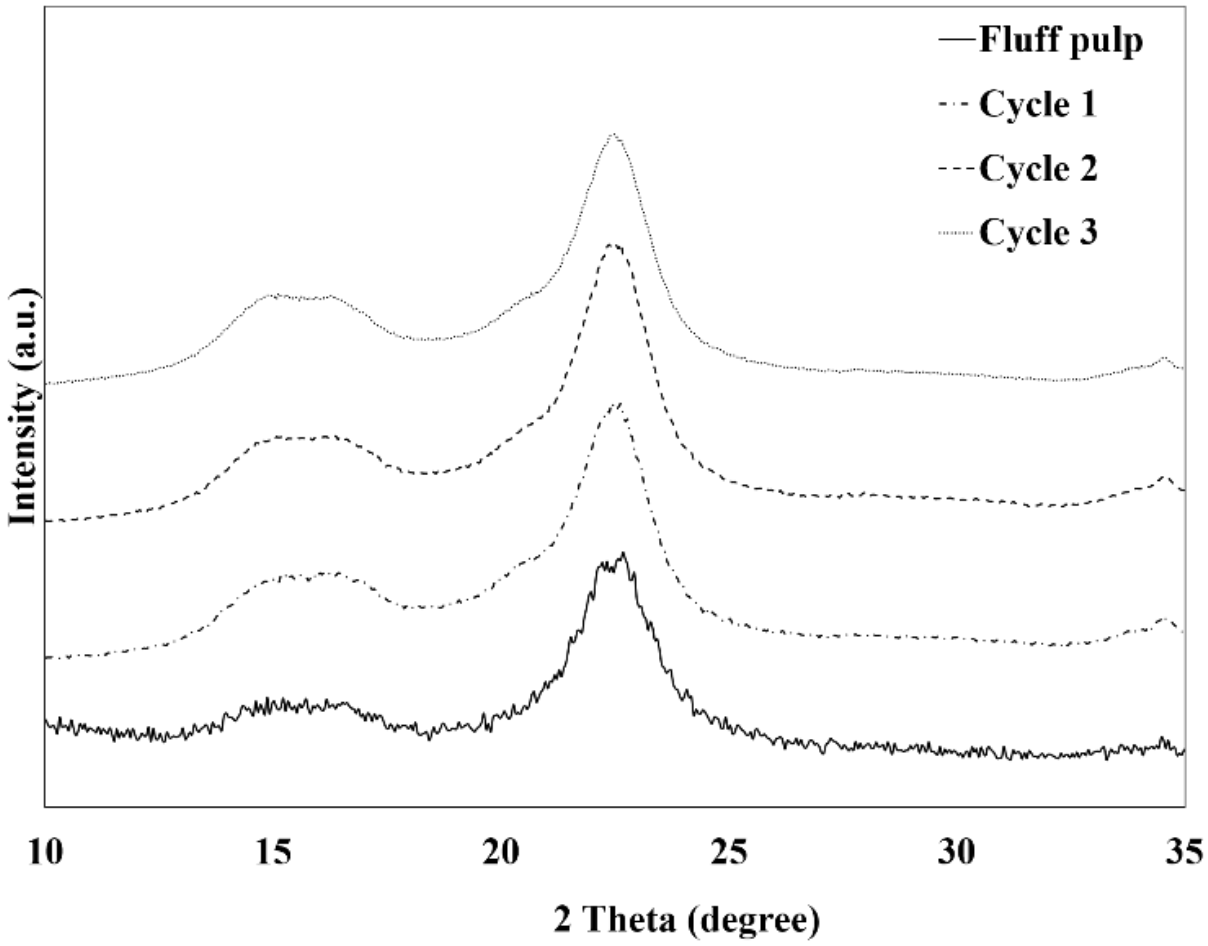

Figure 3.6. X-ray diffraction patterns of fluff pulp and knife-milled powders with one to three grinding cycles.

Figure 3.7. A photo of fibrillated cellulose gel after 15 passes through a French press (left) and standard CNF from University of Maine (right).

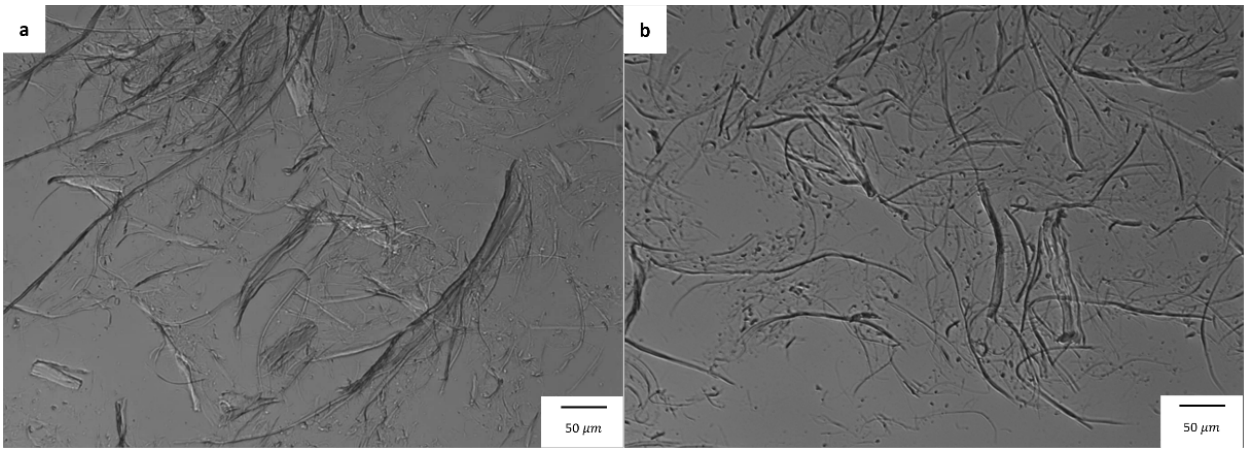

Figure 3.8. Optical microscopic images of the three-cycle knife-milled cellulose after passing through a French press with (a) 10 passes and (b) 15 passes.

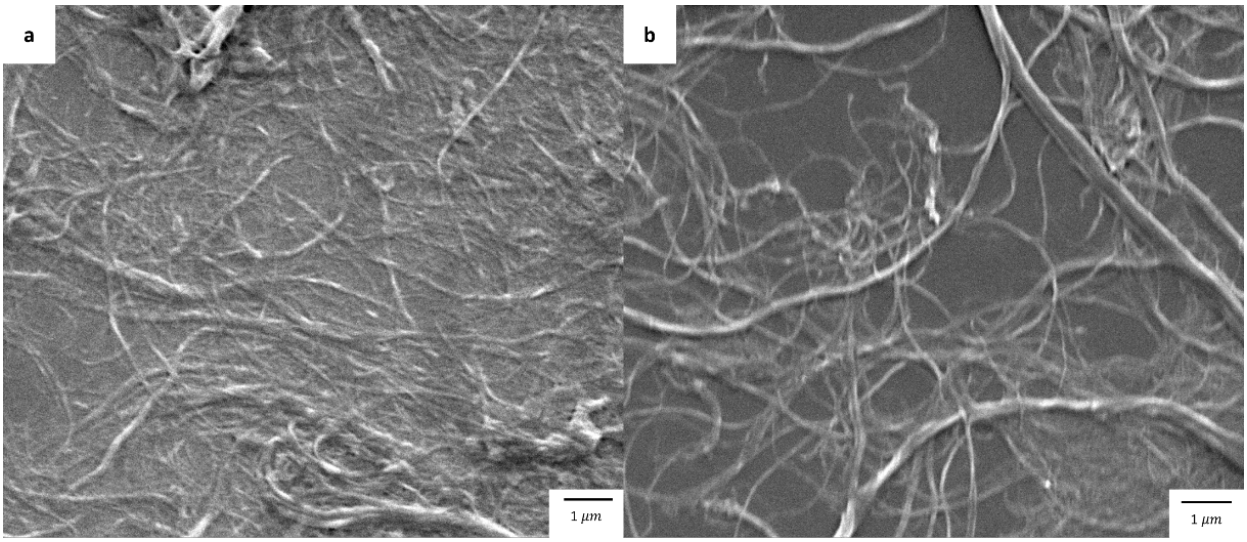

Figure 3.9. Scanning microscopic images of (a) the fibrillated cellulose with 15 passes through a French press and (b) standard cellulose nanofibrils from University of Maine.

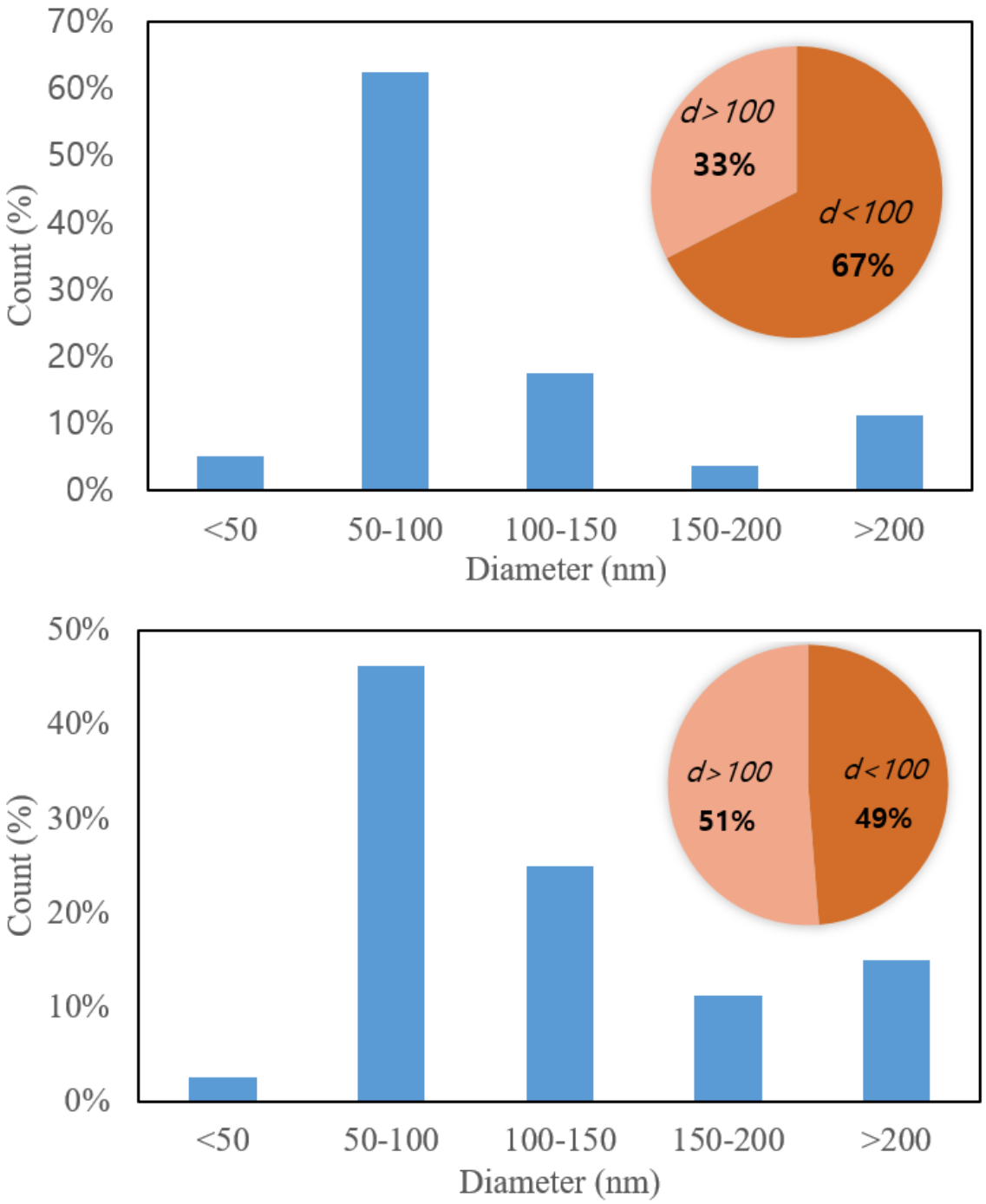

Figure 3.10. The distribution of fiber width for the fibrillated cellulose passed through a French press with 15 passes (top) and standard cellulose nanofibrils from University of Maine (bottom).

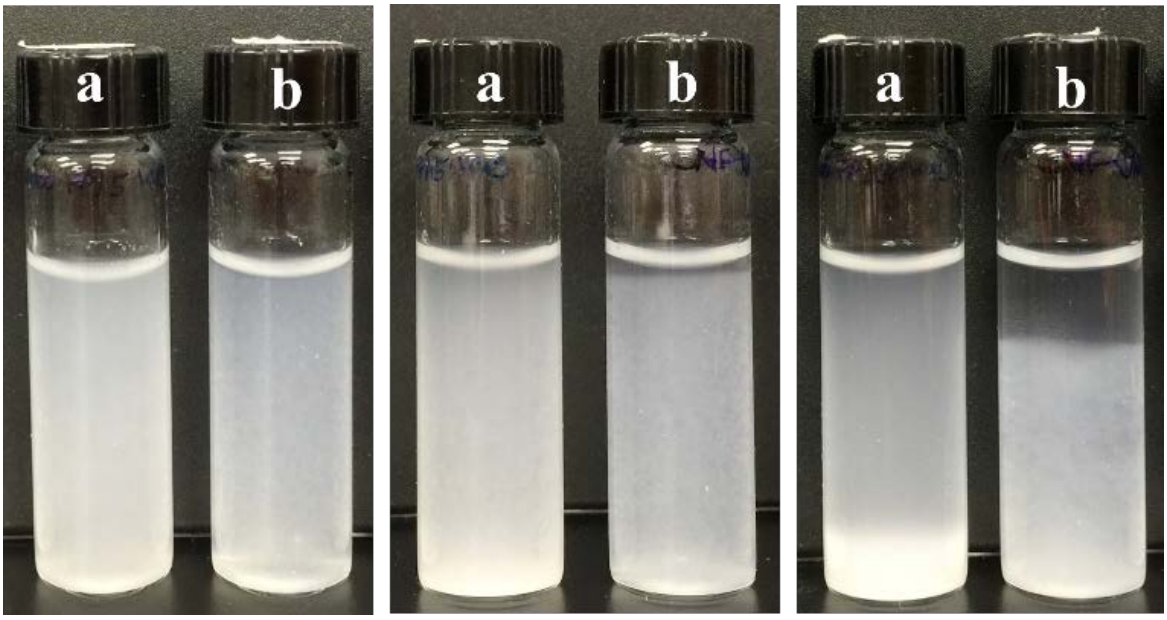

Figure 3.11. Dispersion states of the 0.1wt% suspensions of (a) the fibrillated cellulose passed through a French press with 15 passes, and (b) standard cellulose nanofibrils from University of Maine at 0, 10 and 90 minutes (from left to right).

CHAPTER 4

DEVELOPMENT OF THERMALLY STABLE CELLULOSE NANOFIBRILS USING LOW-CONCENTRATION ALKALINE TREATMENT

Lee, Hansol and Mani, Sudhagar

To be submitted to TAPPI Journal or ACS Sustainable Chemistry & Engineering

Abstract

High-concentration NaOH treatment has been used to prepare thermally stable cellulose nanofibrils (CNF) by converting cellulose crystal structure from cellulose I to cellulose II. However, a number of processing cycles was needed to obtain well-delaminated CNF, and a vast amount of water was required during neutralization. These problems can be reduced by using low-concentration NaOH treatment at low temperature. The objective of this study was to investigate the effects of low-concentration NaOH treatment on the production and properties of cellulose nanofibrils. Cellulose nanofibrils was successfully prepared by processing cellulose powder with 2wt.% NaOH solution at low temperature (below 0 ℃), followed by the mechanical disintegration through a French cell press with only ten passes. It had an average diameter of 90 nm and had a remarkable dispersion behavior in water. It also exhibited a comparatively high thermal stability with the mean onset thermal degradation temperature and DTG peak thermal degradation temperature of 305 ℃ and 343 ℃, respectively. Therefore, the low-concentration alkaline pretreatment conditions could be used to produce thermally stable CNF for nanocomposites applications.

Keywords: Cellulose nanofibrils, Cellulose II, Alkaline treatment, Thermal stability, French cell press.

1. Introduction

Cellulose is the most abundant renewable polymer on Earth as it is a naturally occurring polymer produced by numerous sources, such as plants, algae, and bacteria. Throughout human history, cellulose has been commonly used in the form of wood and plant fibers as fuel, building materials and clothing. It has also been used as a chemical raw material for about 150 years. Chemical modification of cellulose formed cellulose derivatives, such as cellulose ester and cellulose ethers, which contributes to expanding the range of industrial applications of cellulose, such as coating, films, new construction materials, pharmaceuticals, and food (Klemm et al. 2011). With increasing demand for environmentally friendly products as well as increasing interest in nanotechnology, the development of novel forms of cellulosic material with at least one dimension at the nanoscale has received considerable attention recently. Cellulose nanofibrils (CNF) is one type of nano-structured cellulose with a diameter below 100 nm and a length of several micrometers. Owing to its small dimentions, CNF is a lightweight material and can form extensive network structures that induce high strength over 200 MPa (Yano and Nakahara 2004; Fukuzumi et al. 2009; Saito et al. 2009; Abe and Yano, 2009). In addition, cellulose nanofibrils exhibits unique rheological properties. CNF is viscous under normal conditions, but flows once shear forces are introduced; thus, this shear-thinning behavior makes CNF injectable while maintaining its viscosity when forces are removed (Bhattacharya et al. 2012). Therefore, cellulose nanofibrils provides great opportunities in various applications, such as paper, films, food, automotive, electronic, and biomedical applications.

Cellulose nanofibrils can be obtained by mechanical methods where high shear and impact forces are applied. Such combination of forces allows large cellulose fibers to be disintegrated into nano-scale fibers Common disintegration methods include high-pressure homogenizers,

microfluidizers, and microgrinders. The disintegration process is responsible for the high energy consumption over 25,000 kwh/ton, which restricts the commercialization of CNF. Clogging in a homogenizer is another challenge for producing cellulose nanofibrils. In order to address these problems, several pretreatments have been developed, such as mechanical, chemical, and/or enzymatic pretreatment. Chemical pretreatment has been commonly used to produce high-quality cellulose nanofibrils. It introduces negative-charged groups on the surface of cellulose fibers, resulting in electrostatic repulsion between the fibers; therefore, the disintegration of cellulose fibers can occur much more easily. Carboxymethylation and TEMPO (2,2,6,6-tetramethylpiperidine-1-oxyl radical) oxidation are commonly used for the chemical pretreatment process. However, using the chemical pretreatment causes two major problems. Firstly, it requires various chemicals and organic solvents, which is far from environmentally benign technology. For instance, carboxymethylation is performed in organic solvents, such as ethanol, methanol and isopropanol. More specifically, this process requires 30 kg of organic solvents to produce one kg of CNF on dry basis (Arvidsson et al. 2015). In addition, the introduction of functional groups, such as carboxyl and carboxymethyl groups, decreases thermal stability of cellulose nanofibrils by decarbonation (Britto and Assis 2009; Fukuzumi et al. 2009 and 2010; Eyholzer et al. 2010). Fukuzumi et al. (2009) demonstrated that the TEMPO-oxidized cellulose nanofibrils had an onset thermal degradation temperature (T_o) of approximately 200 ℃, while original cellulose had a T_o of approximately 300 ℃. This low thermal stability of chemically-modified CNF is challenging for various applications because most commercial films are produced as composites with thermoplastic polymers at the processing temperature over 200 ℃ (Chen et al. 2011).

Thermally stable cellulose nanofibrils can be prepared by processing cellulose fibers with sodium hydroxide (NaOH). NaOH treatment is capable of converting cellulose crystal form into stable antiparallel cellulose II from parallel cellulose I (Simon et al. 1988). Cellulose II is believed to be more thermally stable than cellulose I. Wang et al. (2014) reported that cellulose nanofibrils from cellulose pulps treated in 17.5wt% NaOH solution was found in the crystalline form of cellulose II, and it had a higher onset and maximum thermal decomposition temperature at 326 ℃ and 353 ℃, respectively, compared to those for untreated CNF at 302 ℃ and 348 ℃, respectively. However, it would be difficult to use this NaOH treatment for the large-scale CNF production due to the following reasons: a number of processing cycles for disintegrating cellulose II fibers and high water consumption for neutralization. Firstly, it is difficult to produce well-dispersed cellulose II nanofibers due to the interdigitation and aggregation of cellulose II fibers (Shibazaki et al. 1997; Dinand et al. 2002; Abe and Yano 2012; Wang et al. 2014). Wang et al. (2014) obtained well-delaminated cellulose II nanofibers by a single grinder treatment followed by 50 homogenization treatments and centrifugation. Sharma et al. (2015) also reported that the higher number of passes through a microgrinder was required to produce cellulose II nanofibers than to produce cellulose I nanofibers. They found that cellulose II fibers at the submicron level could be obtained after microgrinding for 60 passes, while cellulose I fibers had diameters of the order of hundreds of nanometers after 20 passes and diameters of few nanometers after 60 passes. In addition, cellulose II fibers are obtained by processing cellulose I fibers in high concentration of NaOH solution. This results in the considerable water usage during neutralization. Moreover, this approach did not take advantage of swelling effect of NaOH. Cellulose fibers are swollen by treating in NaOH solutions, which are more accessible to be fibrillated. However, in this approach, neutralization was carried out prior to the mechanical

disintegration process, and it led to the aggregation of cellulose fibers, making the fiber disintegration a much more difficult task.

Instead of using high-concentration NaOH, low-concentration NaOH treatment with a dispersing agent, carboxymethylcellulose (CMC), can be an alternative to produce thermally stable cellulose nanofibrils, while reducing the number of passes through a homogenizer and water use during neutralization. It has been reported that low-concentration NaOH solutions (>4 wt.%) are able to swell and partially dissolve cellulose at low temperature from -10 ℃ to 4 ℃, converting the cellulose crystal structure of native cellulose to cellulose II (Sobue et al. 1939; Isogai and Atalla 1998; Cuissinat and Navard 2006; Wang 2008). Moreover, CMC addition would facilitate CNF production and prevent interdigitation of cellulose chains since it inhibits hydrogen bonds between cellulose fibers by introducing negative charged groups on cellulose backbone as well as acts as a lubricant between cellulose fibers, possibly between fibrils in the cell wall (Herrick 1984; Cantiani et al. 2001; Yan et al. 2006; Ankerfors 2015).

The objective of this study is to explore the preparation of cellulose nanofibrils by using low-concentration NaOH treatment and determine the best processing condition. This study also aims to understand its properties. The investigated properties include dispersion behavior, morphology, specific surface area, crystal structure crystallinity, and thermal stability.

2. Materials and Method

2.1. Materials and Chemicals

Fluff cellulose pulp was obtained from the commercial paper mill in Georgia, USA and milled into cellulose powder by passing through a heavy-duty knife mill three times with a screen size of 250 microns (Retsch SM 2000, Germany). The cellulose powder was used as a starting material for this study.

Sodium hydroxide was of reagent grade and in the form of beads, purchased from Amresco. Sodium carboxymethyl cellulose (CMC, DS=0.9 and Mw ~250K) was used, purchased from Aldrich. Congo red from Harleco was used at the total dye content of 80%. Sodium chloride was of reagent grade, purchased from Fisher chemical. All chemicals were used without further purification.

Cellulose nanofibrils obtained by using a high pressure homogenizer with CMC (0.25wt% in water) was kindly provided by Department of textiles, merchandising and interior, UGA. This CNF was produced from the same starting material (cellulose powder) used in this study; thus, it was used to evaluate the effect of CMC itself on CNF production and its properties. It is named as H-CMC-CNF. In addition, commercially available cellulose nanofibrils was purchased from the University of Maine and used as a standard CNF.

2.2. Alkaline treatment

Cellulose powder was treated with 2-6 wt.% sodium hydroxide (NaOH) aqueous solutions. The NaOH solutions were prepared with or without carboxymethylcellulose (CMC, 0.3wt% in water) and pre-cooled in a freezer. The frozen solid was broken into ice slush. A certain amount of cellulose powder was mixed with the ice slush at the solid content of 2 wt.%, and then placed in an ice bath at least for 15 minutes. Afterward, cellulose/NaOH aqueous slurry was completely thawed at room temperature prior to the following disintegration process.

2.3. Cellulose nanofibrils preparation

To produce cellulose nanofibrils, the alkali-treated cellulose was fibrillated through a French pressure cell press. 35 ml of cellulose suspension was passed through the French cell press ten times at operating pressure of 1,000-1,200 bar. The fibrillated cellulose was dialyzed

against deionized water until neutrality. Afterward, the sample was filtrated to make the solid content of 2wt%.

2.4. Characterization of alkali-treated cellulose

2.4.1. Solubility of cellulose in NaOH solutions

Solubility of cellulose in the NaOH solutions (2, 4 and 6wt%) was evaluated with or without CMC. To do so, 35 ml of cellulose/NaOH aqueous suspension was prepared with solid content of 2 wt.% as described in section 2.2. The samples were centrifuged at 6,000 rpm for 20 min. The sediments were filtered and neutralized by rinsing with deionized water, and then dried in an oven at 60 ℃ for 24 hours. The dry weight of the sediments was measured to calculate solubility ratio of cellulose as the weight of dissolved cellulose divided by the original weight of cellulose on dry basis as follow:

$$\text{Equation (1): Solubility ratio} = \frac{Wd}{Wo} \times 100 = \frac{Wo - Wund}{Wo} \times 100\ (\%)$$

where Wd is the weight of dissolved cellulose, Wund is the weight of undissolved cellulose and Wo is the original weight of cellulose. The value of solubility ratio represented three replicates.

2.4.2. Morphology of alkali-treated cellulose

The morphology of alkali-treated cellulose was determined using an optical microscope (DMI 3000B, Leica) at 20 times magnification. A drop of cellulose/NaOH aqueous suspension was placed on a glass side covered with a coverslip. The images presented were considered to be representative of the surfaces of alkali-treated cellulose fibers.

2.5. Characterization of fibrillated cellulose

We characterized the fibrillated cellulose produced by NaOH treatment and homogenization through the French cell press. The investigated properties were dispersion behavior, morphology, specific surface area, crystalline structure, crystallinity and thermal stability.

2.5.1. Visual examination

The dispersion behavior of the fibrillated cellulose was investigated through visual examination as described by other authors (Besbes et al., 2011; Chen et al., 2011), but at a lower solid content. The fibrillated cellulose was diluted with deionized water to 0.1 wt.% solid content. The diluted samples were placed motionlessly for 24 hours, and the photos were taken at 0, 10, 60 minutes and 24 hours.

2.5.2. Morphology of fibrillated cellulose

2.5.2.1. Optical microscopy

The fibrillated cellulose was observed using an optical microscope (DMI 3000B, Leica) at 20 times magnification. A drop of the fibrillated cellulose suspension was placed on a glass side covered with a coverslip. The images presented were considered to be representative of the fiber surfaces of the fibrillated cellulose.

2.5.2.2. Field-emission scanning electron microscopy (FE-SEM)

FE-SEM observation was performed to morphologically characterize the fibrillated cellulose using a FEI Inspect F FEG-SEM. The fibrillated cellulose suspension will be diluted to 0.1wt%. A drop of the diluted suspension was deposited on a silicon substrate and dried for 24 hours at room temperature. The samples were coated with a thin gold/palladium layer applied by ion sputtering with a thickness limited to 5 nm. To prevent damage on the samples, the relatively

low acceleration voltage was used at 5 kV. In case of the well-fibrillated samples, diameters of cellulose fibers were measured with 80 replicates.

2.5.2.3. Scanning transmission electron microscopy (STEM)

A scanning transmission electron microscopy was used to observe the fibrillated cellulose without sputtered metal coatings. The fibrillated cellulose suspension was diluted to 0.1wt%. A drop of the diluted suspension was deposited on a glow-discharged copper grid with formvar and carbon film (300 mesh). The samples were completely dried at room temperature and observed using a FEI Teneo FE-SEM operated at 30 kV.

2.5.3. Specific surface area study

Specific surface area (SSA) was measured using the Congo red adsorption method (Ougiya et al. 1998; Goodrich and Winter 2007; and Spence et al. 2010). SSA measurement was made only with raw cellulose powder and well-fibrillated samples. Samples was placed into a 0.1 M phosphate butter at pH 6 and treated with various concentrations of Congo red at a final solid content of 0.5%. The samples were incubated at 60 ℃ for 24 h. A small amount of NaCl (10wt% of cellulose weight on dry basis) was added to the samples at the beginning of the experiment in order to neutralize charged surface sites. After 24 hours, the samples were centrifuged at 12,000 rpm (14,000 rcf) for 5 min and 15 min for cellulose powder and the fibrillated samples, respectively. The supernatant was put into a quartz cuvette, and its absorbance was measured at 500 nm using an ultraviolet (UV)-visible spectrometer (Genesys 10S, Thermo Fisher Scientific). All runs were at least duplicated with the reported values being the averages. The maximum amount of Congo red absorbed was calculated from the equation (2) derived from Langmuir's absorption theory.

$$\text{Equation (2)}: \frac{[E]}{[A]} = \frac{1}{Kad[A]max} + \frac{[E]}{[A]max}$$

where [E] is the solution concentration of Congo red at adsorption equilibrium in mg/ml, [A] is the amount of Congo red adsorbed onto the cellulose surface in mg/g, $[A]_{max}$ is the maximum amount of Congo red adsorbed onto the cellulose surface in mg/g, and K_{ad} is the equilibrium constant. The specific surface area was determined as follows:

$$\text{Equation (3)} : SSA = \frac{[A]\,\text{max} \times N \times SA}{Mw \times 10^{21}}$$

where N is Avogadro's constant, SA is the surface area occupied by a single dye molecule (1.73 nm^2), and M_w is the molecular weight of Congo red (696 g/mole)

2.5.4. X-ray diffraction analysis (XRD)

The X-ray diffraction analysis was carried out to investigate the effect of NaOH treatment on cellulose crystal structure and to measure the crystallinity of fibrillated cellulose. To prepare the samples for XRD analysis, cellulose suspensions were poured onto a glass substrate and degassed under a sonicating bath and vacuum. Then, it was dried at 60 ℃ to make a film with a flat surface. The X-ray diffraction analysis was performed with the scanning region from 10° to 35° at scan rate of 1°/min, and crystallinity degree (CrD) was calculated using the Segal method as follows:

$$\text{Equation (4): CrD (\%)} = \left(\frac{\text{I200} - \text{Iam}}{\text{I200}}\right) \times 100$$

where I_{200} and I_{am} are the intensity value for the crystalline cellulose ($2\theta = 22.5°$) and the amorphous cellulose ($2\theta = 18.5°$), respectively. When cellulose crystal structure was converted to cellulose II, the intensity values of crystalline domain (200) and amorphous domain at 22.0° and 15.0°, respectively, were used to calculate the crystallinity.

2.5.5. Thermal analysis of fibrillated cellulose

Thermogravimetric analysis (TGA) was performed to determine the thermal stability of fibrillated cellulose. The dried samples were prepared as described in 2.5.4. and then cut into

small pieces for TGA. The sample weighing 4-5 mg was loaded, and the thermogravimetric analysis was performed at a heating rate of 10 ℃/min from room temperature to 600 ℃ under N_2 atmosphere with a 50ml/min flow rate. The weight-loss rate was obtained from the derivative thermogravimetric (DTG) data. The onset degradation temperature was defined as the intersection of tangent lines drawn from the TG curve; one before the cellulose degradation step and another from the degradation step.

2.6. Statistical analysis

Statistical analyses were performed using a scientific software (SAS, University Edition). The effects of CMC addition and NaOH concentration on cellulose solubility, crystallinity and thermal stability of the fibrillated cellulose were evaluated using two-way ANOVA. Multiple comparisons were also conducted using Tukey method. All differences were considered significant at $p<0.05$. Detailed results are provided in Appendix B.

3. Results and Discussion

3.1. Alkaline treatment

3.1.1. Solubility of cellulose in NaOH solutions

Overall, as the concentration of sodium hydroxide increased, the cellulose solubility increased. The weight loss of cellulose treated in NaOH solutions without carboxymethylcellulose increased from 5% to 24% when the NaOH concentration increased from 2wt% to 6wt%. The more cellulose is dissolved, the more regenerated cellulose would be obtained. The higher fraction of regenerated cellulose would lead to the reduction in thermal stability of cellulose since it has been reported that thermal degradation of regenerated cellulose takes place at lower temperature than that of original cellulose (Swatloski et al. 2002; Wu et al. 2009). In addition, the partial dissolution suggests that the NaOH treatment led to not only the

dissolution but also the swelling of cellulose fibers because the solvent system can dissolve cellulose only after swelling it. Particularly, only 5% of cellulose was dissolved in 2wt% NaOH solution, indicating that swelling was more dominant than dissolution. 2wt% NaOH treatemtn is could facilitate cellulose nanofibrils production as swollen fibers are more responsive to be disintegrated than untreated cellulose fibers.

In addition, CMC addition did not make any significant difference in cellulose solubility. The percent of cellulose dissolved in 2-6wt% NaOH solutions with CMC ranged from 8% to 23%. Two-way ANOVA test also showed that NaOH concentration significantly affected cellulose solubility ($p<.0001$), but CMC did not ($p=0.6047$), and it also showed that the effect of NaOH concentration on cellulose solubility would not depend on whether CMC is present or not ($p=0.3601$).

3.1.2. Morphology of alkali-treated cellulose

Figure 4.3 shows optical microscopic images of cellulose treated with various concentrations of aqueous NaOH solutions. Cellulose fibers were swollen in all NaOH solutions, but wer not in pure water or water containing CMC. The swelling behavior of cellulose fibers was different according to NaOH concentrations. Cellulose fibers treated with 2wt% NaOH were homogenously swollen without forming balloons; thereby, these fibers retained their fibrous structure. In contrast, those treated with 4wt% and 6wt% NaOH showed large swelling by ballooning, and some of these fibers completely lost their fibrous shapes and were fragmented. Such extensive swelling with fragmentation provides the plausible explanation for the increase in cellulose solubility with increasing NaOH concentration as described earlier. In addition, the addition of carboxymethylcellulose (CMC) did not apparently affect the morphology of cellulose

fibers. Therefore, we can conclude the NaOH concentration is the dominant factor to determine the morphology of cellulose fibers.

3.2. Characterization of fibrillated cellulose

Figure 4.4 shows the fibrillated cellulose fibers with various NaOH concentrations and with or without CMC at solid content of 2%. It was able to produce gel-like materials with 2wt% NaOH solution whether CMC is present or not. When NaOH concentration was 4wt%, cellulose gel was obtained only with CMC added, but it contained large round particles. The resultant cellulose samples prepared with other conditions did not look like gels.

3.2.1. Visual examination

The stability of the aqueous suspensions of the fibrillated cellulose was assessed by visual examination (Figure 4.5). Overall, the samples prepared with CMC were more homogenously dispersed in water compared to those without CMC. This indicates that CMC helped cellulose more nano-fibrillated as it introduced negative charges onto the cellulose surface and also created a lubricating effect between cellulose fibers (Yan et al. 2006; Ankerfors 2015). The effect of NaOH concentration on suspension stability was more influential than that of CMC. As NaOH concentration increased, the suspensions of the fibrillated cellulose showed a lower level of stability. When NaOH concentration was 4wt% or higher, a large portion of cellulose immediately settled down to the bottom within 10 minutes after standing whether CMC is present or not. This is because the alkaline treatment with 4wt% or higher NaOH solutions tends to convert the cellulose crystal form from parallel cellulose I to antiparallel cellulose II. The cellulose II chains have the opposite polarities to the adjacent chains, resulting in the irregular aggregation of cellulose. Only one of the fibrillated samples (pretreated with 2wt% NaOH solution containing CMC) was well-dispersed in water after one hour of standing. More

importantly, it showed a distinct dispersion behavior after 24 hours. Some fibers were still dispersed in water after 24 hours, implying these fibers are at the nanoscale and have smaller dimensions than standard CNF (sample a) and H-CMC-CNF (sample b) which completely settled down to the glass bottom after 24 hours. Consequently, the use of 2wt% NaOH solution with CMC seems desirable to produce cellulose nanofibrils.

3.2.2. Morphology of fibrillated cellulose

3.2.2.1. Optical microscopy

The optical microscopic images of the fibrillated cellulose before neutralization are shown in Figure 4.6. NaOH concentration had a strong influence on the morphology of the resultant cellulose, while the effect of CMC was not significant as mentioned earlier. Cellulose fibers treated with 2wt% NaOH solutions were well-fibrillated into individual fibrils. On the other hand, when NaOH concentration was 4wt% or higher, the resultant cellulose had cellulose fibrils as well as round-shaped particles. This is because the treatment with high-concentration NaOH solutions was strong enough to not only swell but also fragment cellulose fibers as described previously. The fragmented cellulose fibers tend to be broken into small round particles by the subsequent homogenization process.

Figure 4.7 shows the optical microscopic images of the fibrillated cellulose after neutralization. Only with 2wt% NaOH solution contacting CMC, it was able to prepare well-fibrillated cellulose fibers that kept their fibrous structure after neutralization. On the other hand, round-shaped particles were formed and clustered together in neutralized cellulose pretreated with higher NaOH concentrations. The higher NaOH concentrations, the more aggregates were formed. Such cellulose aggregation can be explained by the conversion of cellulose crystal form that induces interdigitation of cellulose during neutralization as described previously (Shibazaki

et al. 1997; and Dinand et al. 2002). Besides, CMC addition tends to minimize the formation of cellulose aggregates during neutralization because CMC introduce negative charges on cellulose surface, giving a gap between cellulose fibers as mentioned earlier. The CMC effect was clearly observed when NaOH concentration was 4wt%. The fibrillated cellulose treated in 4wt% NaOH solution with CMC did not contain as many cellulose aggregates as that without CMC. However, when NaOH concentration reached 6wt%, the extensive aggregation occurred even in presence of CMC. This indicates that the NaOH concentration is a more contributing factor to the aggregation than whether CMC is added or not. Consequently, 2wt% NaOH concentration with CMC seems the best condition to produce cellulose nanofibrils that has the same extent of fibrillation as standard CNF and H-CMC-CNF have.

3.2.2.2. Scanning electron microscopy (FE-SEM) and Scanning transmission electron microscopy (STEM)

Figure 4.8 represents the FE-SEM images of the fibrillated samples after neutralization. As expected, nano-scale cellulose fibers were produced when NaOH concentration was 2wt%; whereas, the samples with 4wt% and 6wt% NaOH solutions contained a number of large cellulose aggregates. SEM imaging also showed that the presence of CMC prevented the aggregation of cellulose fibers and improved the fibrillation degree of the resultant fibers. When NaOH centration was 2wt%, cellulose fibers prepared with CMC were uniformly fibrillated into nano-scale fibers; whereas, parts of cellulose fibers were clustered together when CMC was not used. This explains why the sample with 2wt% NaOH without CMC began to settle down within 10 minutes after standing as seen in section 3.2.1. In case of the samples with 4wt% NaOH solution, not only cellulose aggregates but also cellulose fibers with nano-scale widths were observed with CMC added; in contrast, only large aggregates of cellulose fibers were observed

when CMC was not added. Diameters of the fibers were measured on the fibrillated sample pretreated with 2wt% NaOH solution containing CMC, and those of standard CNF and H-CMC-CNF were also measure for comparison. Among these three samples, the fibrillated sample had the smallest average diameter of 89.8 nm with a standard deviation of 67.7 nm. The average diameter was 134 nm and 97.1 nm with a standard of 80.4 nm and 73.1 nm for standard CNF and H-CMC-CNF, respectively. Figure 4.9 exhibits the diameter distribution of these three samples. Except standard CNF, fiber diameters generally ranged from several tens of nanometer to 200 nm, and more than 70% of cellulose fibers had a diameter below 100 nm. It is worth mentioning that the sample with 2wt% NaOH together with CMC had the largest fraction of cellulose fibers with a diameter below 50 nm (17.5%); whereas, in case of other samples, less than 4% of cellulose fibers had a diameter of smaller than 50 nm. This indicates that the alkaline treatment facilitates the delamination of cellulose fibers into nano-scale fibers by swelling. In addition, the STEM images provided the morphological information of these three samples without sputtered metal coating (Figure 4.10). The fibrillation degree of the sample obtained in this study (Figure 4.10-a) was comparable to that of standard CNF (Figure 4.10-b) and H-CMC-CNF (Figure 4.10-c). All samples consisted of nanofibers although there existed large fibers with a diameter of several hundred nanometers.

3.2.3. Specific surface area study

Specific surface area (SSA) was measured on the fibrillated cellulose prepared with 2wt% NaOH solution together with CMC using the Congo red adsorption method and compared to those of starting material and two control CNF materials (standard CNF and H-CMC-CNF). As can be seen in Figure 4.11, the fibrillated cellulose obtained in this study and two control CNFs had a higher SSA than cellulose powder (122.07 m^2g^{-1}), indicating the surface area of

cellulose increased as fibrillation progressed. SSA was 248.05 m^2g^{-1}, 210.62 m^2g^{-1}, and 232.52 m^2g^{-1} for the fibrillated cellulose sample, standard CNF, and H-CMC-CNF respectively, which is a little higher than the value reported in literature (up to 202 m^2g^{-1}, Spence et al. 2010). Thus, it can be concluded that the fibrillation degree of the fibrillated cellulose would be comparable to that of other standard CNF materials.

3.2.4. X-ray diffraction analysis (XRD)

X-ray diffraction patterns of the fibrillated cellulose samples are shown in Figure 4.12. Figure 4.12-(1) and Figure 4.12-(2) represent XRD patterns of the samples prepared without or with CMC, respectively. Figure 4.12-(3) shows XRD patterns of cellulose powder (case g), standard CNF (case h) and H-CMC-CNF (case i). NaOH concentration strongly affected the cellulose crystalline structure. NaOH concentration of 2wt% was not sufficient to transform the cellulose crystal structure. The samples (case a and d) had peaks at 2θ angles of approximately 14.6° ($1\bar{1}0$), 16.5° (110) and 22.5° (200), which were characteristic of cellulose I structure as the case g, h and I had. The alkaline treatment with 4wt% or higher NaOH concentrations converted the cellulose crystal structure. The peaks were shifted to 12.2° ($1\bar{1}0$), 20.0° (110) and 22.0° (200), indicating the formation of cellulose II structure. This result gives the reason for the extensive aggregation in the samples prepared with 4wt% and 6wt% NaOH solutions. Cellulose II chains of the opposite polarities are able to attract each other and form large cellulose aggregates. The influence of CMC on the conversion of cellulose crystal structure was not strong as that of NaOH concentration. However, it is likely to inhibit the conversion of cellulose crystal form as seen in case e, which shows the signature peaks of both cellulose I and cellulose II. CMC could increase the mobility of cellulose chains by giving a gap between cellulose fibers and possible cellulose chains inside the fibers. Therefore, cellulose chains could preserve their

original parallel structure. This explains why the samples with CMC contained fewer cellulose aggregates than those without CMC.

In addition, NaOH concentration plays a big role in cellulose crystallinity. With 2wt% NaOH, the fibrillated cellulose samples had the cellulose crystallinity of 75.0 % and 75.6 % without or with CMC, respectively. These values are higher than those of raw cellulose powder (74.6%), standard CNF (73.1%) and H-CMC-CNF (73.3%). The increase in the crystallinity is because at low NaOH concentrations, NaOH hydrates cannot penetrate the internal crystalline regions and only can disrupt amorphous inter-fibrillar regions, leading to the increased crystallinity. Other authors also reported that cellulose crystallinity was slightly increased by 2-3% until cellulose crystal structure was converted to cellulose II (Liu and Hu 2008; Yue 2011). When NaOH concentration was 4wt% or higher, the crystallinity significantly dropped to 56-58%. As NaOH concentration increased, cellulose fibers were more swollen, which made it for NaOH hydrates easier to penetrate and disrupt the internal crystals. It was reported that the crystallinity sharply fell down when the conversion of the crystal structure occurred (Liu and Hu 2008; Wang et al. 2008; Mirahmadi et al. 2010; Yue 2011). Two-way ANOVA test confirmed that there was a significant difference in crystallinity across NaOH concentration ($p<0.0001$). On the other hand, CMC addition did not make any significant difference in CNF crystallinity as confirmed by the two-way ANOVA result ($p=0.6059$).

3.2.5. Thermal analysis of fibrillated cellulose

Thermogravimetric analysis (TGA) and derivative thermogravimetric analysis (DTGA) were performed to investigate thermal stability of the fibrillated cellulose samples. TG and DTGA curves are shown in Figure 4.13. The mean onset thermal degradation temperature (T_o) and mean DTG peak thermal degradation temperature (T_{max}) are summarized in Table 4.1. First

of all, it should be noted that the alkaline treatment with 2wt% NaOH solution has a potential to improve the thermal stability of cellulose. Among the fibrillated cellulose samples, the sample treated in 2wt% NaOH solution without CMC showed the best thermal stability with T_o and T_{max} of 320.05 ℃ and 353 ℃, respectively. Such relative high thermal stability can be explained by the increased crystallinity of this sample compared with other samples. It was reported that thermal stability of cellulose was closely associated with its crystallinity, and the cellulose sample with higher crystallinity exhibited better thermal stability (Liu and Hu 2008; Yue 2011). It is worth mentioning that this sample had a comparable thermal stability to original cellulose powder although it was reported that thermal stability of cellulose decreased as fibrillation proceeded (Sharma et al. 2015). Moreover, this sample presented a much higher onset thermal decomposition temperature (304.83 ℃) than the sample prepared only with CMC (H-CMC-CNF, 286.51 ℃). The Tukey test results also showed that there is a significant difference in thermal stability between these two samples ($p=0.0003$). These results support that 2wt% NaOH treatment potentially improves thermal stability of cellulose. One possible reason for this is that 2wt% NaOH treatment might reduce the carboxyl content of CMC adsorbed onto cellulose. Fukuzumi et al. (2010) reported that the repeated alkaline treatments with 1M NaOH removed approximately 86% of the carboxyl groups present in TEMPO-oxidized cellulose, resulting in the increase in the thermal stability.

Besides, the thermal stability of the fibrillated cellulose samples gradually decreased with increasing NaOH concentrations even though the increase in NaOH concentration led to the conversion of native cellulose I to cellulose II. In case of the samples without CMC, T_o was decreased from 320.05 ℃ to 314.98 ℃; likewise, T_{max} was decreased from 353 ℃ to 344.33 ℃ as NaOH concentration increased from 2wt% to 6wt%. This trend was also observed in the samples

prepared with CMC. Two-way ANOVA test also provided a strong evidence that NaOH concentration significantly affected the thermal stability of the samples ($p<0.0001$). Such decrease with increasing NaOH concentration is due to the low thermal stability of dissolved/regenerated cellulose as described earlier. It has been reported that the onset and maximum thermal decomposition temperatures of regenerated cellulose is 20-50 ℃ lower than those of pure cellulose (Swatloski et al. 2002; Wu et al. 2009). The percent of dissolved cellulose was increased with increasing NaOH concentrations as shown in Figure 4.2; therefore, the cellulose fibers treated with a higher NaOH concentration contained a higher fraction of regenerated cellulose fibers, resulting in the reduction in thermal stability. Another explanation is the reduced crystallinity with higher NaOH concentration. Lower crystallinity indicates that cellulose is less organized and therefore more vulnerable by heating process.

Regarding the effects of CMC, CMC addition significantly reduced thermal stability of the resultant cellulose samples. This is attributed to the carboxymethyl groups of CMC. Other authors also reported that the cellulose containing charged groups was decomposed at lower temperature than pure cellulose due to decarbonation (Britto and Assis 2009; Fukuzumi et al. 2010). Two-way ANOVA test supported that the addition of CMC made a significant difference in cellulose thermal stability ($p<.0001$ for the onset thermal degradation temperature and $p=0.0097$ for the maximum thermal degradation temperature).

4. Conclusions

Cellulose nanofibrils was successfully produced by treating cellulose fibers with low-concentration NaOH solution (2wt.%) containing CMC at low temperature, followed by homogenization using a French cell press with only ten passes. Its characteristics were comparable to standard CNF produced at pilot scale. It had an average diameter of 89.8 nm and a

specific surface area of 248.05 m^2g^{-1} and showed a remarkable dispersion behavior in water. In addition, it has a relatively high thermal stability with the mean onset thermal degradation temperature of 305 ℃ and the mean DTG peak thermal degradation temperature of 343 ℃. Therefore, it could be concluded that low-concentration NaOH treatment (2wt.%) was a promising alternative way to produce thermally stable cellulose nanofibrils with reduced homogenization cycles and water use for neutralization.

Acknowledgement

We thank Dr. Eric Freeman from College of Engineering, Dr. Yiping Zhao from Department of Physics, Dr. Albin F. Turbak and Dr. Suraj Sharma from Department of textiles, merchandising and interiors, UGA for providing technical assistance. We also thank Dr. Hari P. Singh from Fort Valley State University for his financial support on electron microscopic studies.

References

Abe, K., Yano, H., 2009, Comparison of the characteristics of cellulose microfibril aggregates of wood, rice straw and potato tuber, Cellulose, 16:1017–1023.

Abe, K., Yano, H., 2012, Cellulose nanofiber-based hydrogels with high mechanical strength, Cellulose, 19:1907-1912.

Ankerfors, M., 2015, Microfibrillated cellulose: Energy-efficient preparation techniques and key properties, PhD. Dissertation, KTH Royal Institute of Technology.

Arvidsson, R., Nguyen, D., Svanstrom M., 2015, Life cycle assessment of cellulose nanofibrils production by mechanical treatment and two different pretreatment processes, Environ. Sci. Technol., 49:6681-6890.

Bhattacharya, M., Malinen, M.M., Lauren, P., Lou, Y., Kuisma, S.W., Kanninen, L., Corlu, A., GuGuen-Guillouzo, C., Ikkala, O., Laukkanen, A., Urtti, A., Yliperttula, M., 2012, Nanofibrillar cellulose hydrogel promotes three-dimensional liver cell culture, Journal of Controlled Release, 164(3):291-298.

Britto, D., and Assis, O.B.G., 2009, Thermal degradation of carboxymethylcellulose in different salty forms, Thermochimica Acta, 494:115-122.

Cantiani, R., Knipper, M., Vaslin, S., 2002, Use of cellulose microfibrils in dry form in food formulations, US Patent 6,485,767 B1.

Chen, W., Yu, H., Liu, Y., Chen, P., Zhang M., Hai, Y., 2011, Individualization of cellulose nanofibers from wood using high-intensity ultrasonication combined with chemical pretreatments, Carbohydrate Polymers, 83:1804-1811.

Cuissinat, C., Navard, P., 2006, Swelling and dissolution of cellulose part II: free floating cotton and wood fibres in NaOH–water–additives Systems, Macromolecular Symposia, 244(1):19-30.

Dinand, E., Vignon, M., Chanzy, H., Heux, L., 2002, Mercerization of primary wall cellulose and its implication for the conversion of cellulose I to cellulose II, Cellulose, 9:7-18.

Eyholzer, Ch., Bordeanu N., Lopez-Suevos, F., Rentsch D., Zimmermann T., Oksman, K., 2010, Preparation and characterization of water-redispersible nanofibrillated cellulose in powder form, Cellulose 17:19-30.

Fukuzumi, H., Saito, T., Iwata, T., Kumamoto, Y., Isogai, A., 2009, Transparent and high gas barrier films of cellulose nanofibers prepared by TEMPO-mediated oxidation, Biomacromolecules, 10:162-165.

Fukuzumi, H., Saito, T., Okita, Y., Isogai, A., 2010, Thermal stabilization of TEMPO-oxidized cellulose, Polymer Degradation and Stability, 95:1502-1508.

Goodrich, J.D., Winter, W.T., 2007, α-Chitin Nanocrystals Prepared from Shrimp Shells and Their Specific Surface Area Measurement, Biomacromolecules, 8:252-257.

Herrick, F.W., 1984, Redispersible microfibrillated cellulose, US patent 4,481,076.

Isogai, A., Atalla, R.H., 1998, Dissolution of cellulose in aqueous NaOH solutions, Cellulose, 5, 309-319.

Klemm, D., Kramer, F., Mortiz, S., Lindstrom, T., Ankerfors, M., Gray, D., Dorris, A., 2011, Nanocelluloses: a new family of nature-based materials, Angew. Chem. Int. Ed., 50(24):5438-5466.

Liu, Y., Hu, H., 2008, X-ray diffraction study of bamboo fibers treated with NaOH, Fibers and Polymers, 9(6):735-739.

Mirahmadi, K., Kabir, M.M., Jeihanipour, A., Karimi, K., Taherzadeh, M.J., 2010, Alkaline pretreatment of spruce and birch to improve bioethanol and biogas production, Bioresources, 5(2):928-938.

Nair, S.S., Zhu, J.Y., Deng, Y., Ragauskas, A.J., 2014, Characterization of cellulose nanofibrillation by micro grinding, Journal of Nanoparticle Research, 16:2349.

Ougiya, H., Hioki, N., Watanabe, K., Morinaga, Y., Yoshinaga, F., Samejima, M., 1998, Relationship between the physical properties and surface area of cellulose derived from adsorbates of various molecular sizes, Bioscience. Biotechnology, and Biochemistry., 62(10):1880-1884.

Saito, T., Hirota, M., Tamura, N., Kimura, S., Fukuzumi, H., Heuz, L., Isogai, A., 2009, Individualization of nano-sized plant cellulose fibrils by direct surface carboxylation suing TEMPO catalyst under neutral conditions, Biomacromolecules, 7:1687-1691.

Sharma, S. Nair, S.S., Zhang, Z., Ragauskas, A.J., Deng, Y., 2015, Characterization of micro fibrillation process of cellulose and mercerized cellulose pulp, RSC Advances, 5:63111-63122.

Shibazaki, H., Kuga, S., Okano, T., 1997, Mercerization and acid hydrolysis of bacterial cellulose, Cellulose, 4:75-87.

Simon, I., Glasser, L., Scheraga, H. A., Manley, R. S. J., 1998, Structure of cellulose. 2. low-energy crystalline arrangements, Macromolecules, 21:990–998.

Sobue, H., Kiessig, H., Hess, K., 1939, The cellulose-sodium hydroxide-water system as a function of the temperature, Z. Physik. Chem. B, 43:309–328.

Spence, K.L., Venditti, R.A., Rojas O.J., Habibi, Y., Pawlak, J.J., 2010, The effect of chemical composition on microfibrillar cellulose films from wood pulps: water interactions and physical properties for packaging applications, Cellulose, 17:835-848.

Swatloski, R.P., Spear, S.K., Holbrey, J.D., Rogers, R.D., 2002, Dissolution of Cellulose with Ionic Liquids, Journal of American Chemical Society, 124:4974-4975.

Wang, H., Li, D., Yano, H., Abe, K., 2014, Preparation of tough cellulose II nanofibers with high thermal stability from wood, Cellulose, 21:1505-1515.

Wang, Y., 2008, Cellulose fiber dissolution in sodium hydroxide solution at low temperature: dissolution kinetics and solubility improvement, PhD dissertation, Georgia Institute of Technology.

Wu, R.L., Wang, X., Li, F., Li, H., Wang, Y., 2009, Green composite films prepared from cellulose, starch and lignin in room-temperature ionic liquid, Bioresource Technology, 100:2569–2574.

Yan, H. Lindstrom, T., Christiernin, M., 2006, Some ways to decrease fibre suspension flocculation and improve sheet formation, Nordic Pulp & Paper Research Journal, 21(1):36-43.

Yano, H., Nakahara, S., 2004, Bio-composites produced from plant microfiber bundles with a nanometer unit web-like network, Journal of Materials Science, 39:1635-1638.

Yue, Y., 2011, A comparative study of cellulose I and II fibers and nanocrystals, Master's thesis, Louisiana State University.

Table 4.1. Onset and DTG peak thermal degradation temperature of fibrillated cellulose fibers prepared with various NaOH solutions with or without CMC

Sample	Crystallinity (%)	Onset thermal degradation temperature (°C)	DTG peak thermal degradation temperature (°C)
f2NaOH	75.02 (1.86)	320.05 (3.93)	353.00 (2.41)
f4NaOH	57.23 (1.58)	318.69 (2.69)	347.22 (2.34)
f6NaOH	58.08 (9.52)	314.98 (1.57)	344.33 (4.67)
fCMC2NaOH	75.64 (1.89)	304.83 (3.13)	342.78 (3.91)
fCMC4NaOH	N/A	305.73 (2.43)	345.67 (2.91)
fCMC6NaOH	56.50 (4.85)	301.27 (0.53)	341.44 (1.02)
Cellulose powder	74.57 (1.77)	327.60 (1.04)	360.11 (1.02)
Standard CNF	73.12 (2.55)	316.78 (1.19)	348.56 (1.02)
H-CMC-CNF	73.36 (0.36)	286.51 (0.28)	326.33 (0.00)

*Samples starting with “f” are fibrillated cellulose using a French cell press.

*Numbers enclosed in the parenthesis were standard deviations with n=3.

*N/A: Not available.

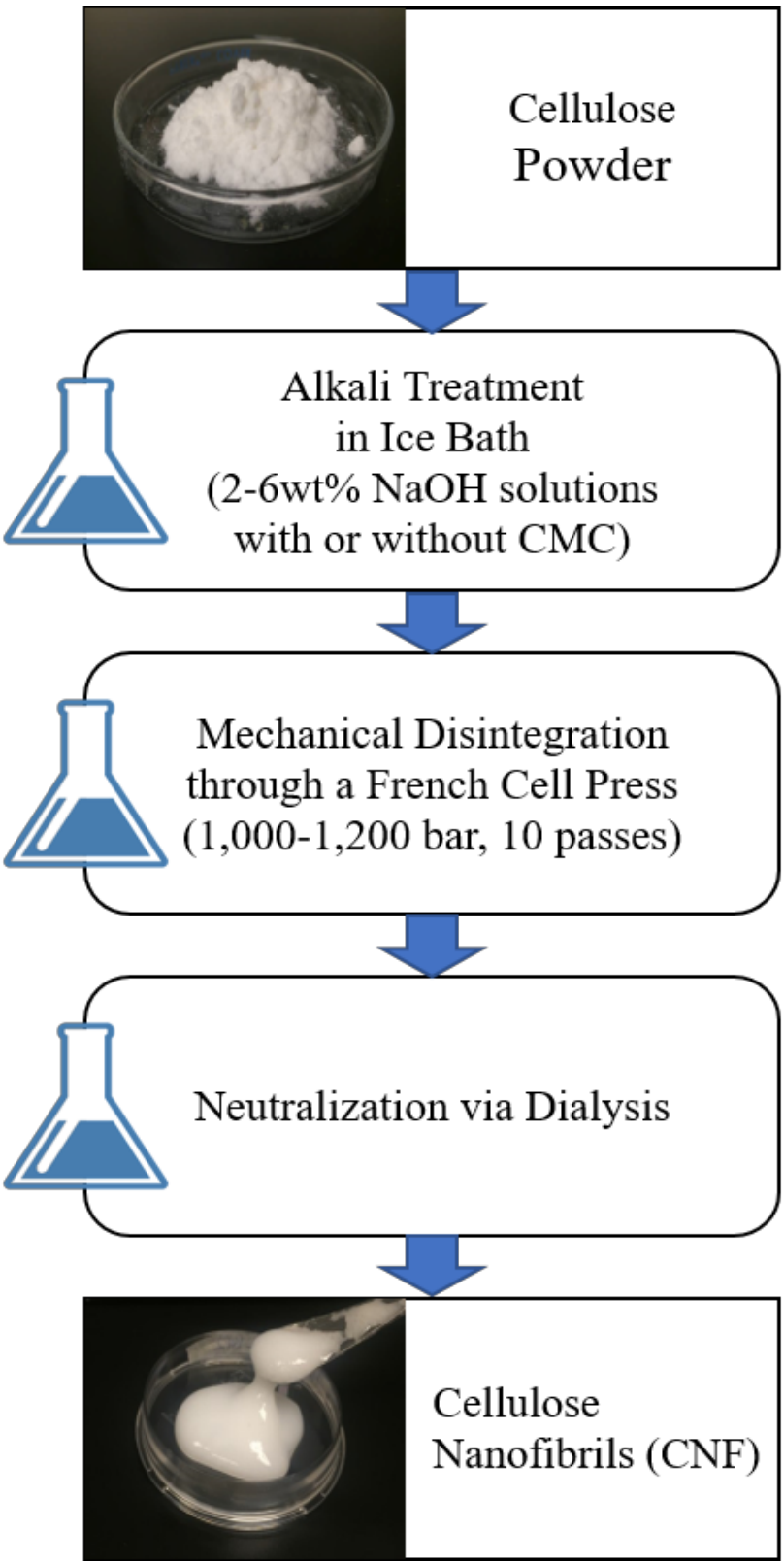

Figure 4.1. Summary of cellulose nanofibrils production procedure in this study

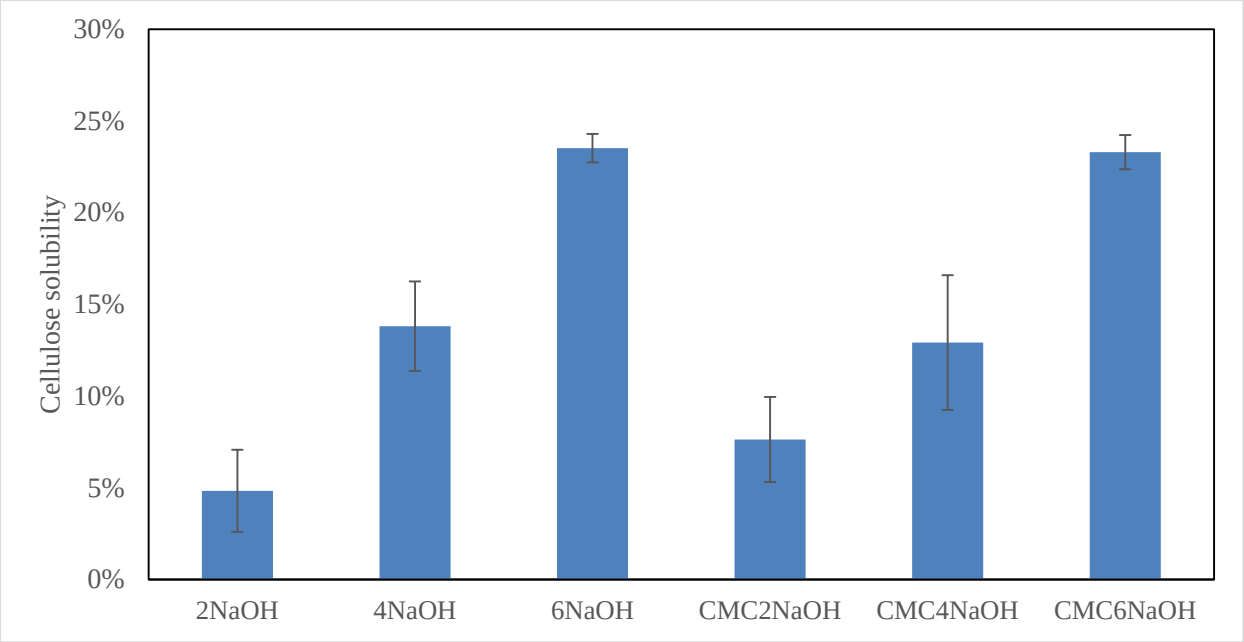

Figure 4.2. Cellulose Solubility in various concentrations of NaOH solutions with or without CMC.

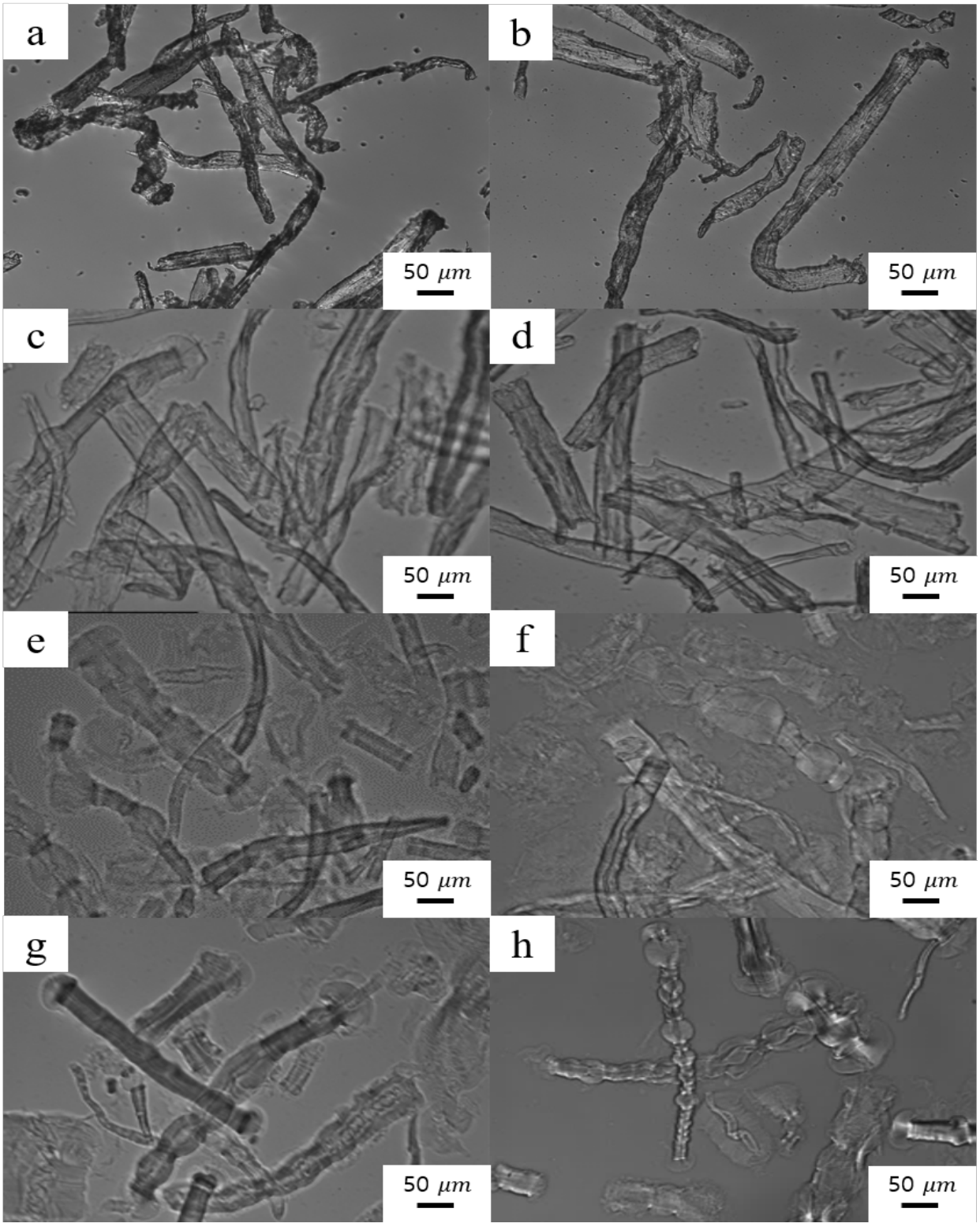

Figure 4.3. Optical microscopic images of cellulose fibers treated with 2-6wt% NaOH solutions without (left) or with CMC (right) (a,b : 0wt%, c,d : 2wt%, e,f : 4wt%, g,h : 6wt% NaOH solutions)

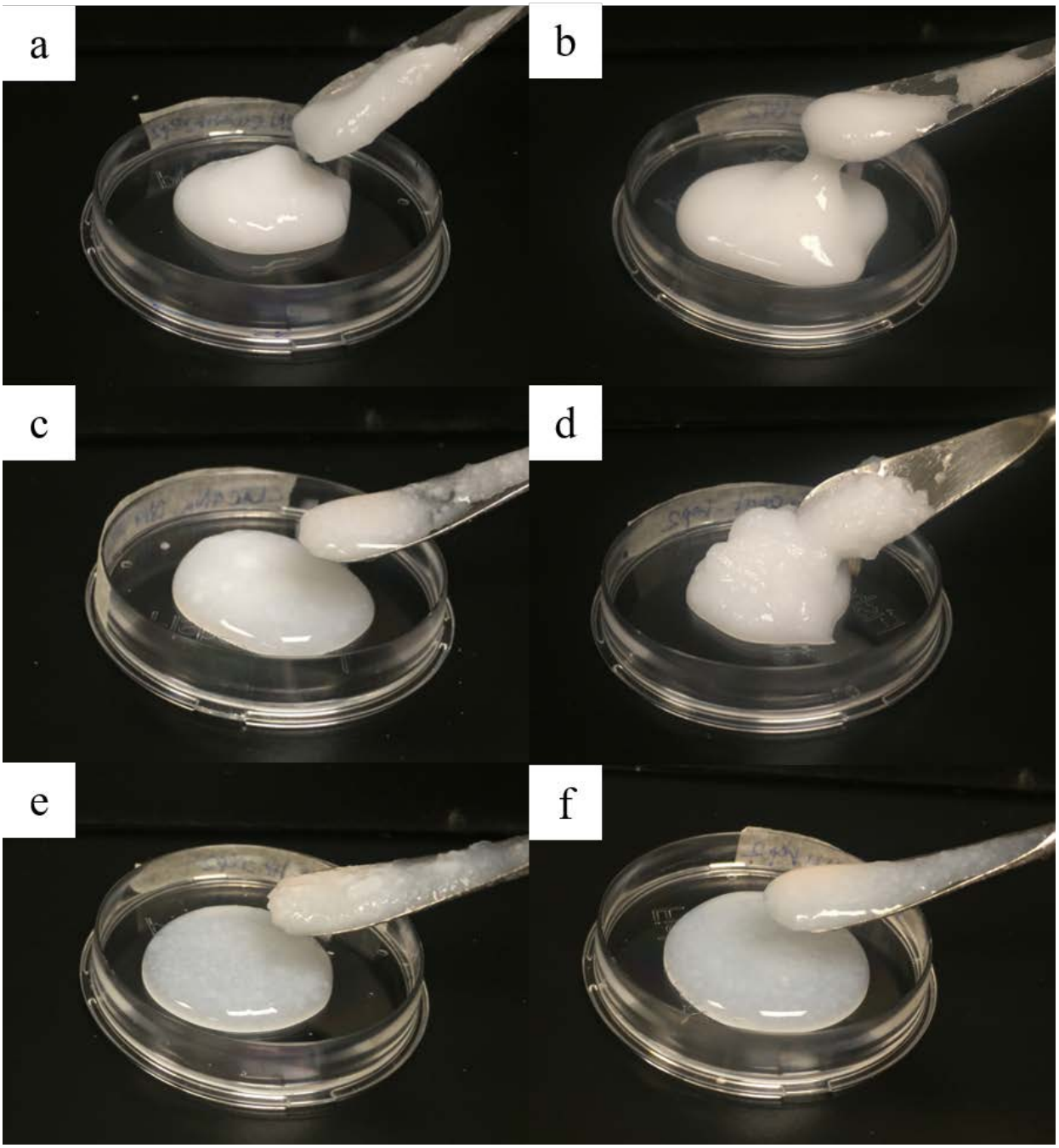

Figure 4.4. Fibrillated cellulose samples treated with 2-6wt% NaOH solutions without (left) or with CMC (right) (a,b : 2wt%, c,d : 4wt%, e,f : 6wt% NaOH solutions)

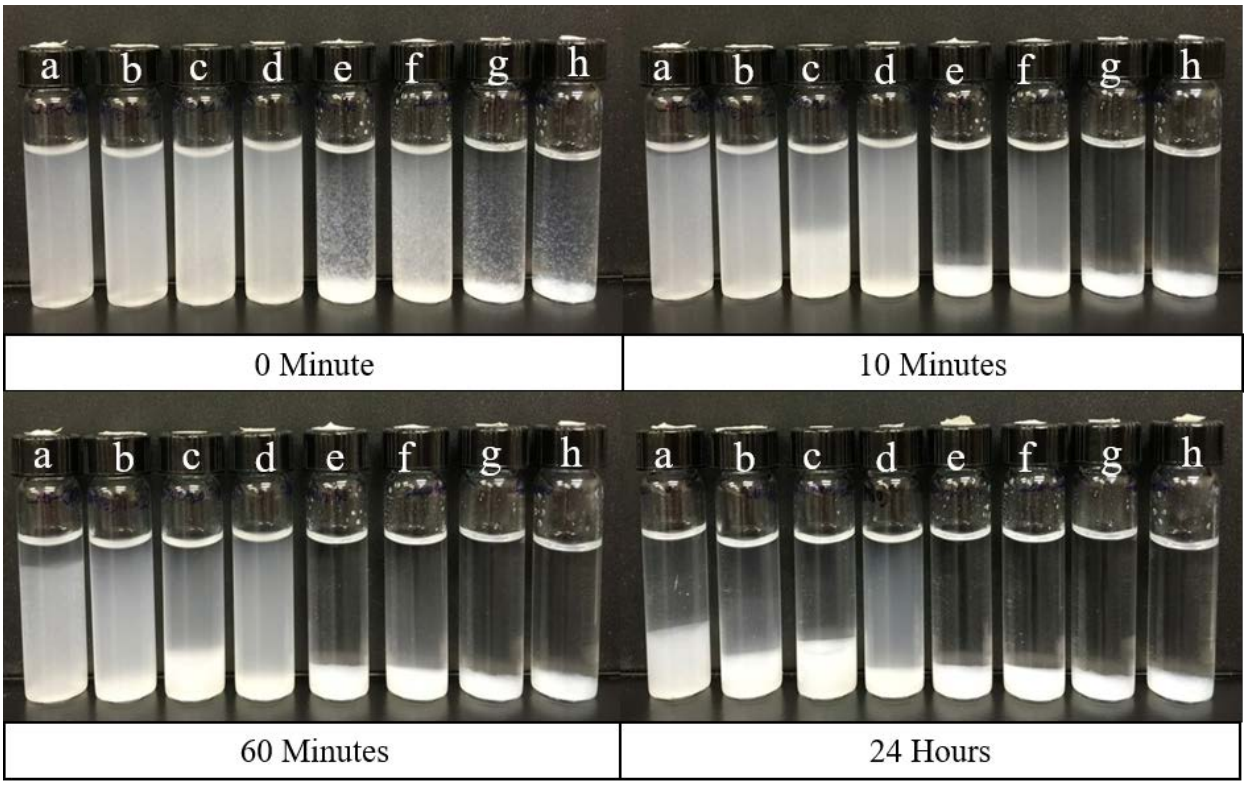

Figure 4.5. Dispersion states of the 0.1wt% fibrillated cellulose suspensions at 0, 10, 60 minutes and 24 hours (a: standard CNF, b: H-CMC-CNF, c: 2NaOH, d: CMC-2NaOH, e: 4NaOH, f: CMC-4NaOH, g: 6NaOH, and h: CMC-6NaOH)

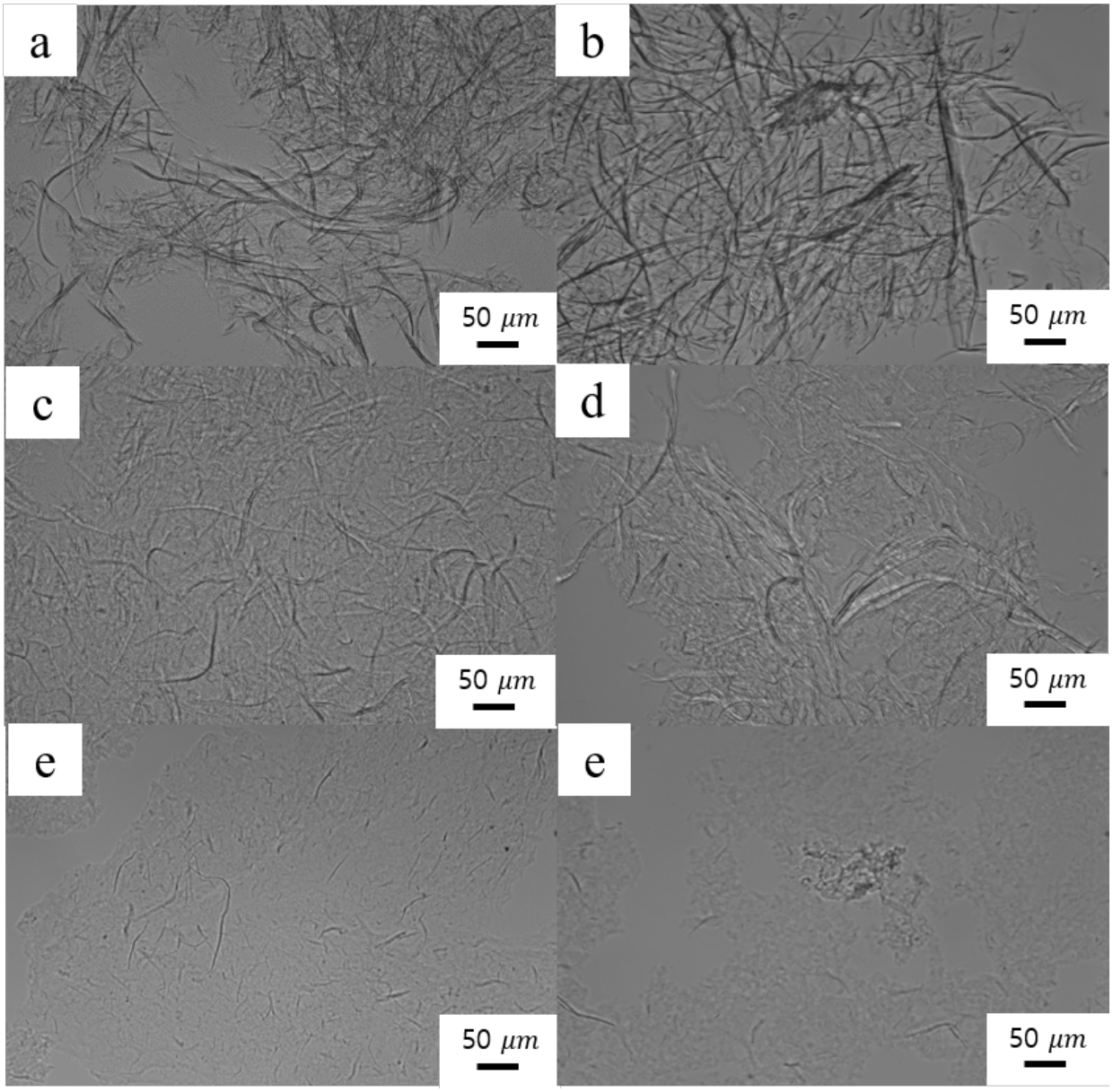

Figure 4.6. Optical microscopic images of alkali-treated cellulose without (left) or with CMC (right) after the fibrillation process through a French cell press 10 times (a,b : 2wt%, c,d : 4wt%, e,f : 6wt% NaOH solutions)

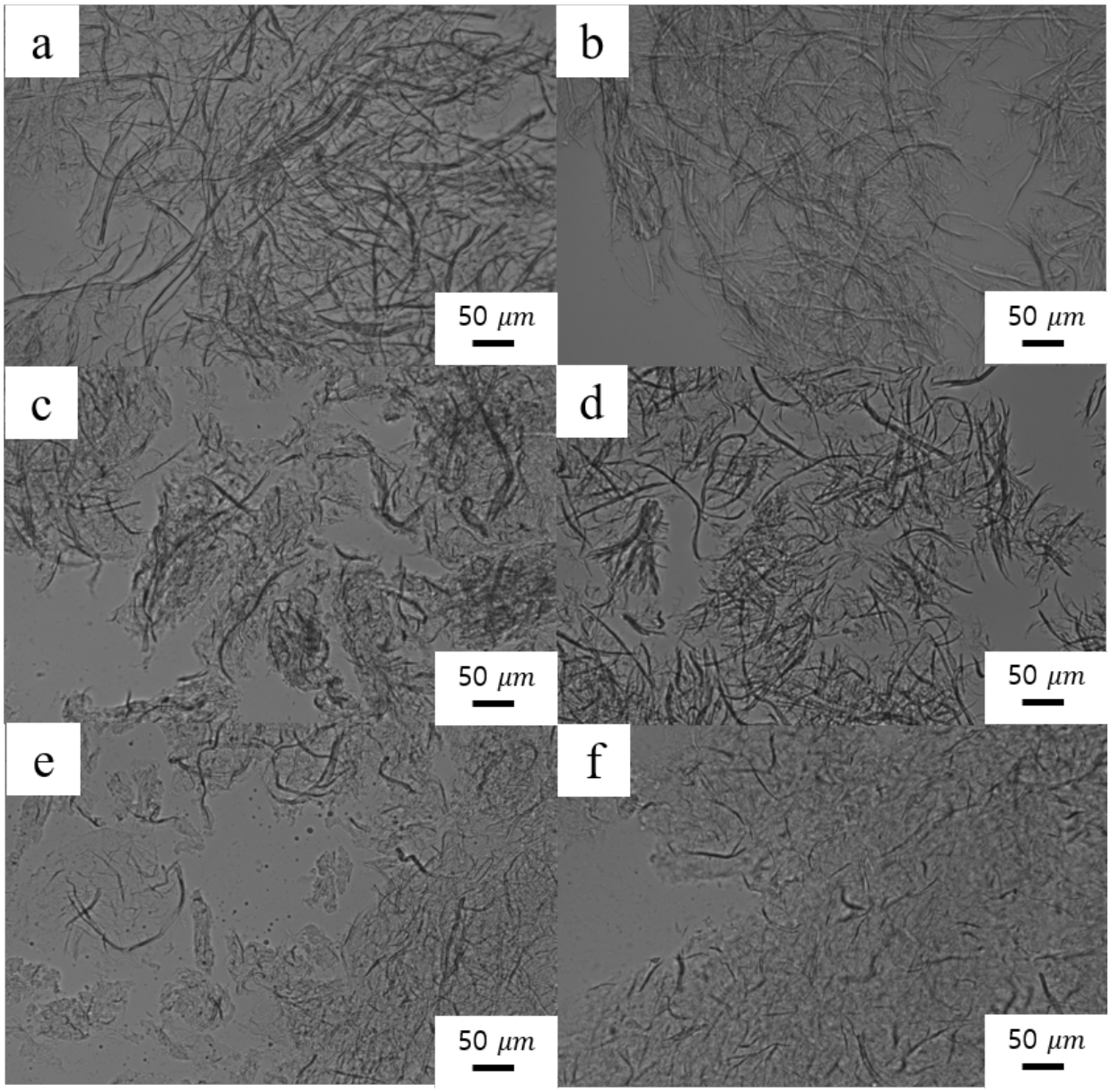

Figure 4.7. Optical microscopic images of fibrillated cellulose samples treated with 2-6wt% NaOH solutions without (left) or with CMC (right) (a,b : 2wt%, c,d : 4wt%, e,f : 6wt% NaOH solutions)

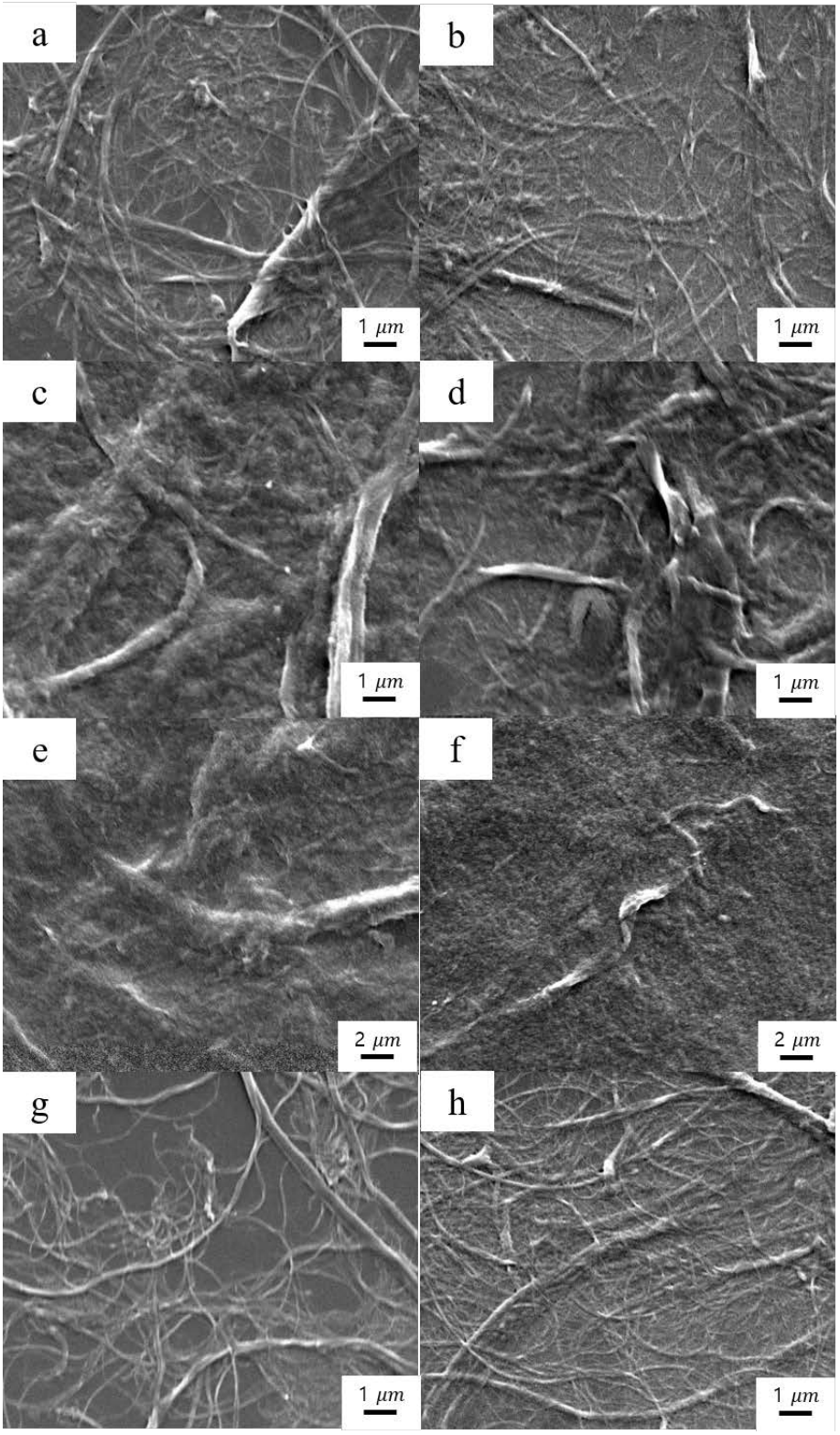

Figure 4.8. SEM images of fibrillated cellulose samples treated with 2-6wt% NaOH solutions without (left) or with CMC (right) (a,b: 2wt%, c,d : 4wt%, e,f : 6wt% NaOH solutions), (g) standard CNF and (h) H-CMC-CNF

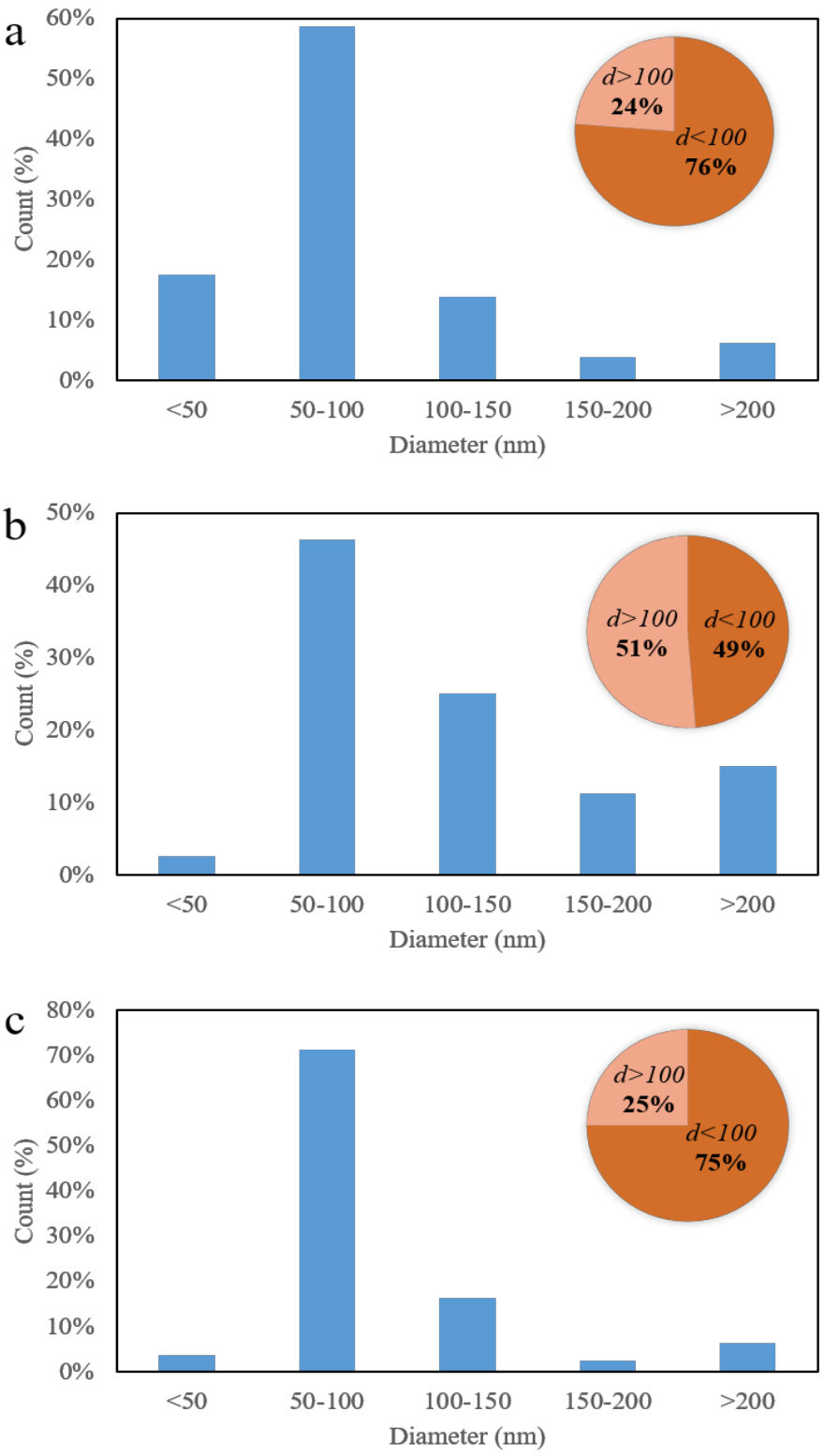

Figure 4.9. Diameter distribution of (a) the fibrillated cellulose treated with 2wt% NaOH solution containing CMC, (b) standard CNF and (c) H-CMC-CNF.

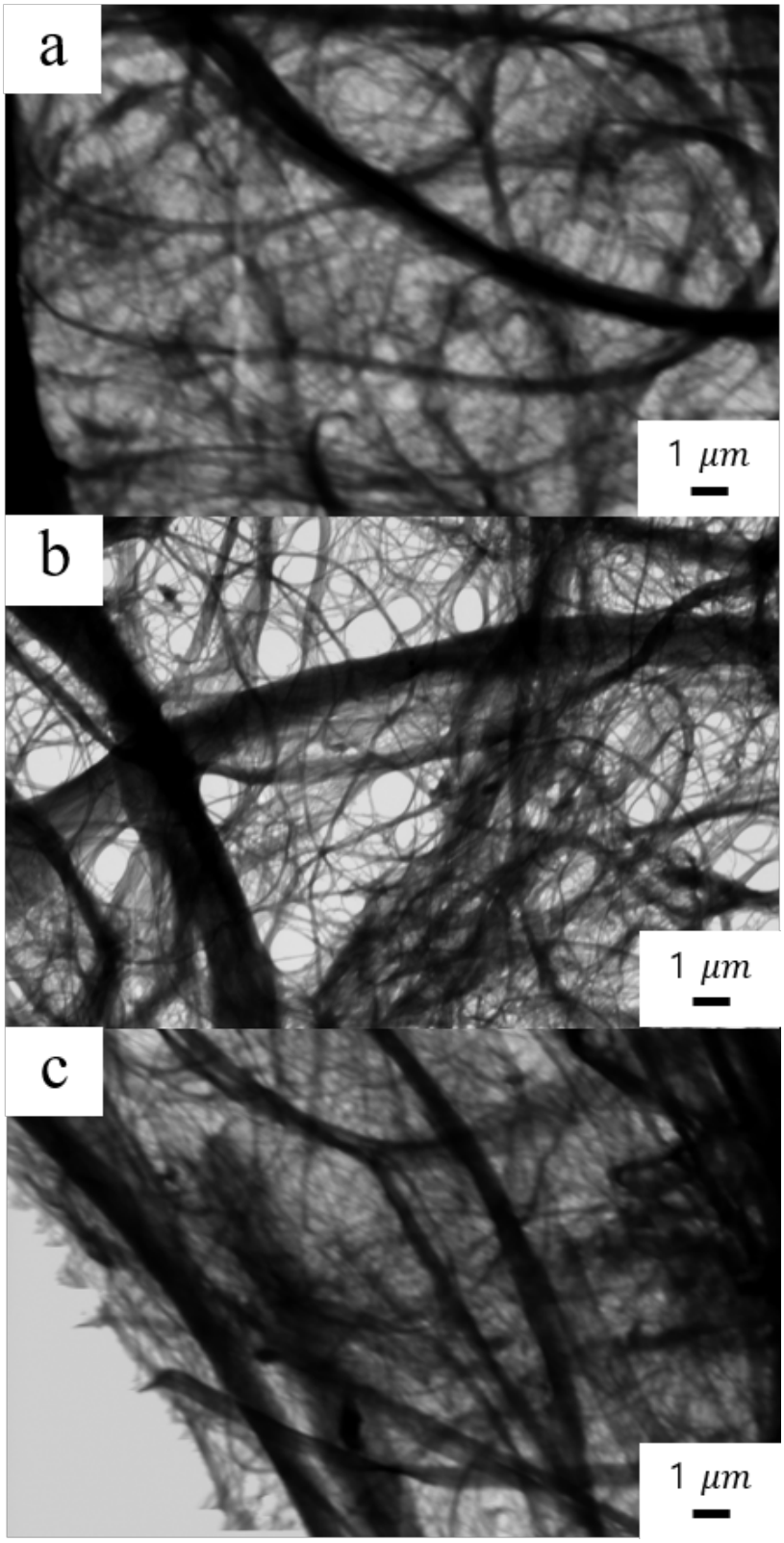

Figure 4.10. STEM images of (a) the fibrillated cellulose treated with 2wt% NaOH solution containing CMC, (b) standard CNF and (c) H-CMC-CNF.

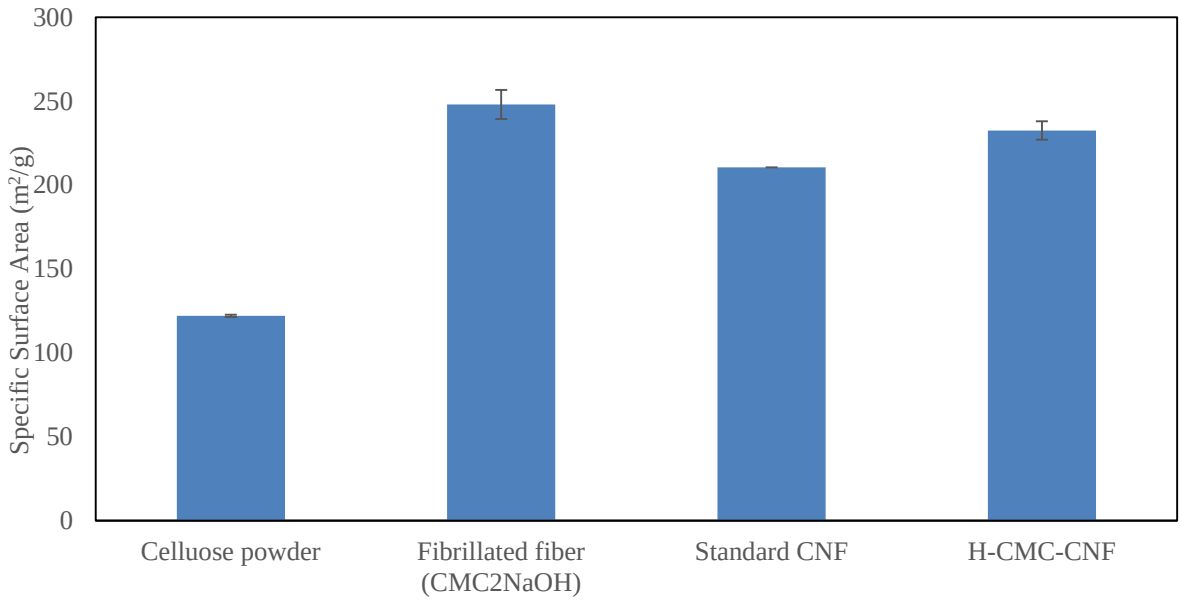

Figure 4.11. Specific surface area of cellulose powder, the fibrillated cellulose treated with 2wt% NaOH solution containing CMC, standard CNF and H-CMC-CNF.

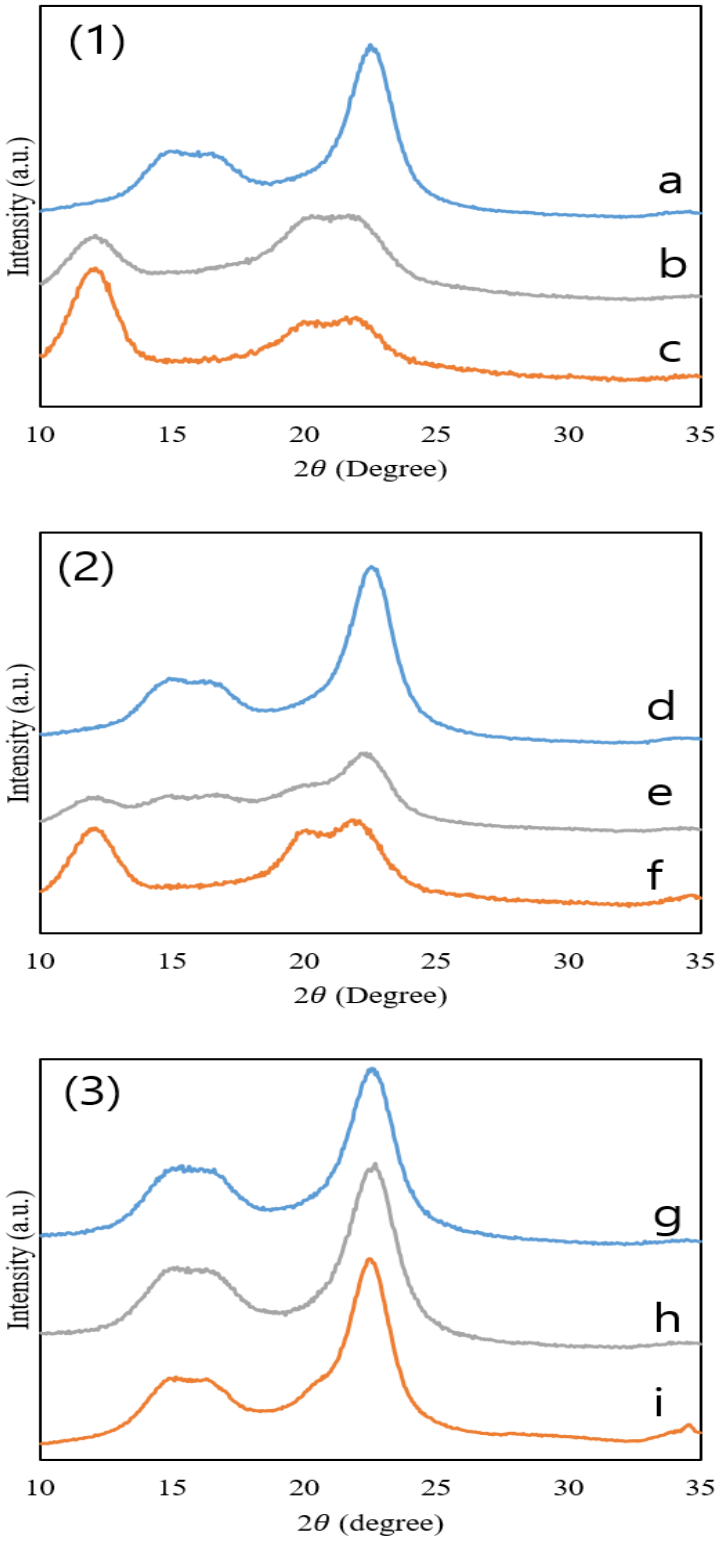

Figure 4.12. XRD patterns of fibrillated cellulose treated with 2-6wt% NaOH solution (1) without or (2) with CMC (a,d :2wt%, b,e : 4wt%, c,f : 6wt% NaOH solution), (g) cellulose powder, (h) standard CNF, (i) H-CMC-CNF.

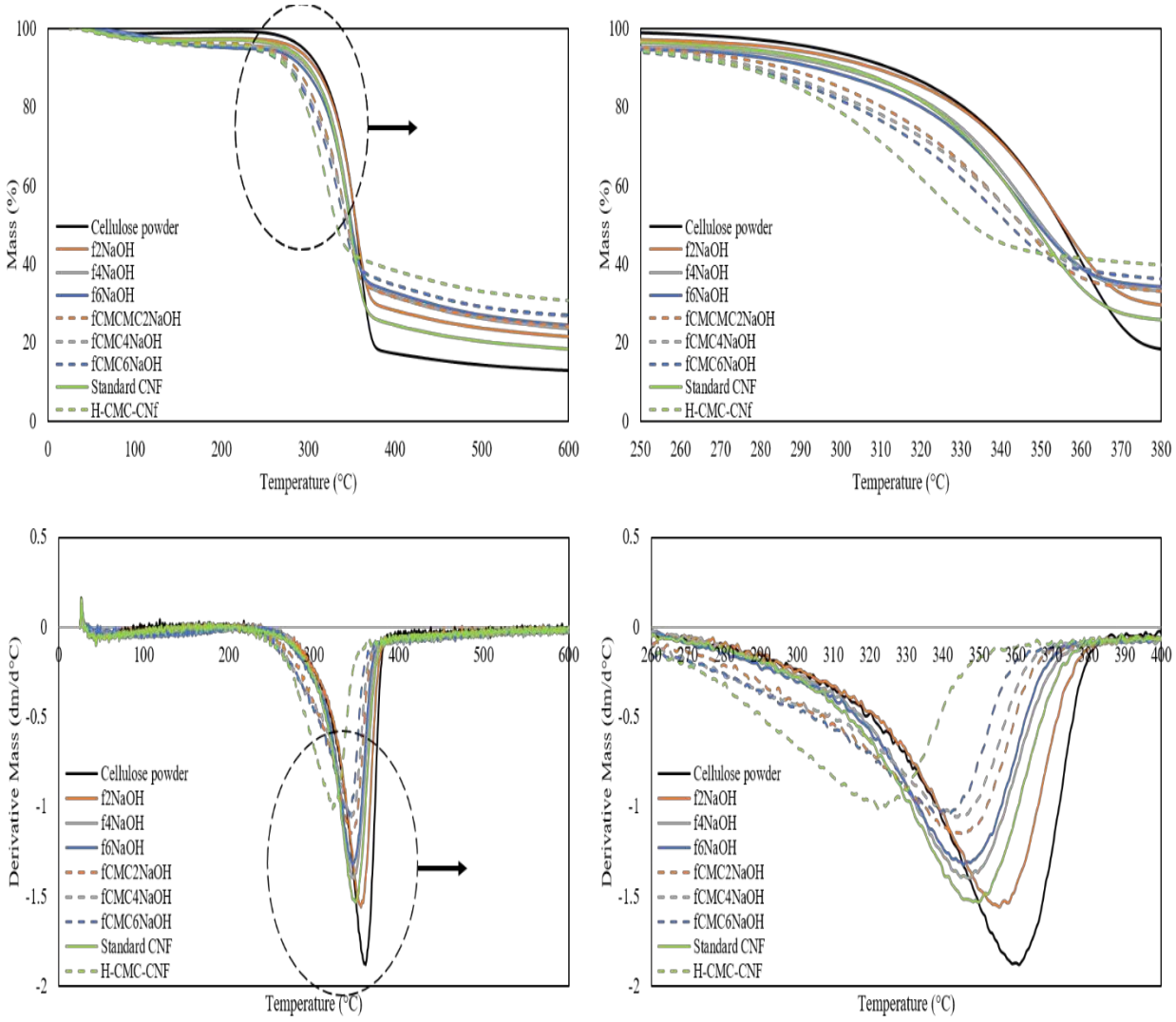

Figure 4.13. TG (top) and DTG (bottom) curves of fibrillated cellulose treated with 2-6wt% NaOH solution with or without CMC, standard CNF and H-CMC-CNF.

.

CHAPTER 5

LIFE CYCLE ASSESSMENT OF PRODUCING CELLULOSE NANOFIBRILS WITH MECHANICAL AND ALKALINE PRETREATMENT

Lee, Hansol and Mani, Sudhagar

To be submitted to ACS Sustainable Chemistry & Engineering

Abstract

Cellulose nanofibrils (CNF) has received considerable attention due to its remarkable mechanical properties and biodegradability. However, CNF production is still under development owing to high energy consumption (as high as 70,000 kWh/ton). Therefore, it is important to investigate life cycle energy use for producing CNF and its impacts on environment and human. The objective of this study was to assess cradle-to-gate life cycle environmental impacts of CNF produced from three different production routes: (1) the Valley beating route, which includes mechanical pretreatment with a Valley beater, (2) the shear cutting route, which includes mechanical pretreatment with a shear cutting mill and (3) alkaline pretreatment route, which includes alkaline pretreatment using 2wt% NaOH solution. The results indicated that the Valley beating route had the highest impact values relevant to energy input, such as global warming potential and cumulative energy demand, followed by the shear cutting route and the alkaline pretreatment route. On the other hand, the highest impact values relevant to water usage were obtained from the alkaline pretreatment route due to high water input during neutralization. When comparing the previous LCA results of CNF, all three routes had a relatively low environmental impacts compared with the routes including chemical pretreatments and had impacts of similar magnitude as the route without any pretreatment. In addition, a sensitive analysis showed that the increase in CNF solid content was the most obvious way to reduce environmental impacts of CNF production. Therefore, opportunities likely exist to reduce environmental impacts for manufacturing CNF by using efficient methods to increase the solid content of CNF.

Keyword: Life cycle assessment, Cellulose nanofibrils, Alkaline treatment, Valley beater, Shear cutting mill, Homogenization, Environmental impacts.

1. Introduction

Nanocellulose is an emerging bionanomaterial and has been increasingly produced in recent years. The future global market size for nanocellulose is estimated to be 35 million tonnes/year (Cowie et al. 2014). Cellulose nanofibrils (CNF) is one type of nanocellulose which typically has a width of below 100 nm and a length of several micrometers. Due to its nano-scale dimensions, it can form extensive network structures, and CNF film has a tensile strength of up to 310 MPa with high transparency and low density of 0.8-1.5 gcm^{-3} (Yano and Nakahara 2004; Fukuzumi et al. 2009; Saito et al. 2009; Abe and Yano, 2009). CNF can be used in various application fields, such as food packaging, electronics, automotive, and biomedical applications. In addition, CNF is renewable and biodegradable as forest biomass and energy grasses are abundantly renewable feedstock and potential raw materials for manufacturing CNF.

The production process of cellulose nanofibrils involves pretreatment process and mechanical disintegration process. Pretreatment process is where cellulose fibers become more susceptible to be disintegrated using mechanical, chemical or/and enzymatic methods. In the mechanical disintegration process, pretreated cellulose fibers are subjected to high impact and shear forces and delaminated into individual nanofibrils. However, there are some challenges that restrict CNF commercialization, such as high energy consumption (12,000-70,000 kwh/ton) and clogging in the mechanical disintegration process (Klemm et al. 2011). Specifically, the high energy requirement increases not only CNF manufacturing cost but also its environmental impacts.

Life cycle assessment (LCA) is a reliable tool to evaluate environmental impacts of a product on its entire life cycle, generally covering all relevant processes from raw material extraction to final product disposal. LCA is used in new product research and development to

identify which step creates environmental impacts the most and what improvement can be made against the benchmarking product. Three LCA studies related to cellulose nanofibrils have been conducted (Hohenthal et al. 2012, Li et al. 2013; Arvidsson et al. 2015). Hohenthal et al. (2012) assessed environmental impacts of CNF production from three different processing routes, including 2,2,6,6,-tetramethylpiperidine-1-oxyl (TEMPO) oxidation or enzymatic pretreatment with homogenization, and TEMPO oxidation with Cavitron dispersion. Unfortunately, this LCA report did not clearly describe the source for quantitative inventory data. The LCA study conducted by Li et al. (2013) investigated the environmental impacts of CNF production in the United States using four different processing routes including two chemical pretreatment processes (TEMPO oxidation and chloroacetic acid etherification) and two mechanical disintegration processes (high pressure homogenization and sonication). The results showed that the production route with TEMPO oxidation and homogenization had the lowest environmental impacts; while the production route with etherification and sonication had the highest impacts. Moreover, Arvidsson et al. (2015) assessed the life cycle environmental impacts of CNF produced from three different production routes; (1) enzymatic pretreatment with microfluidization, (2) carboxymethylation with microfluidization, and (3) high pressure homogenization with no pretreatment. Carboxymethylation route had a comparatively high impacts for all impact categories due to its high chemical consumption (30 kg of organic solvents per one kg CNF). Although these three LCA study assessed the environmental impacts of producing cellulose nanofibrils with various pretreatment techniques, the environmental impacts of CNF production with a mechanical or an alkaline pretreatment process has been not studied. Therefore, additional LCA study is needed to verify the environmental impacts of CNF production using a mechanical or an alkaline pretreatment.

This LCA study assessed life cycle environmental impacts of CNF produced from three different routes: (1) the Valley beating route, where a mechanical pretreatment in a Valley beating and a mechanical disintegration are involved; (2) the shear cutting route, with a mechanical pretreatment using a shear cutting mill and a mechanical disintegration process; and (3) the alkaline pretreatment route, which includes a low-concentration NaOH treatment (2wt%) and a mechanical disintegration process. The first production route is commonly used and therefore is considered as a benchmarking process.

The ultimate goal of this LCA study is to assess the life cycle environmental impacts of producing cellulose nanofibrils from the three different routes. This study also aims to investigate the effects of mechanical pretreatment process on environmental impacts of CNF and to find opportunities to reduce CNF environmental impacts by using alkaline pretreatment instead of other chemical pretreatments.

2. LCA Scope and Functional unit definition

The scope of this LCA study is defined as “cradle-to-gate”, including all processes from raw material (bleached kraft pulp) production to CNF production as shown in Figure 5.1. This boundary indicates that the use and disposal of CNF is not included since CNF has a wide range of applications and its disposal would be different for every application. The inputs considered in this study are bleached kraft pulp, direct processing energy (in the form of electricity), water and chemicals, and the outputs include cellulose nanofibrils (final product), direct processing wastes and emissions related to the production of raw materials and energy. The functional unit is defined as one kg of cellulose nanofibrils on a dry basis, which is a common functional unit for cradle-to-gate studies of nanomaterials (Figueirêdo et al. 2012; Kim and Fthenakis 2013;

Arvidsson et al. 2015). All input and output data were scaled up for producing one kg (dry weight) of cellulose nanofibrils.

3. Process description

3.1. Pulp production

Wood pulps are the most commonly-used feedstock for manufacturing CNF. In 2015, 19 out of 31 pilot or commercial-scale plants used wood pulps as a starting material (TAPPI Nano, 2015). Among various wood pulps, bleached kraft pulp is a dominating raw material for CNF production. Data for manufacturing bleached kraft pulp is available in the US LCA database. This data includes all input and output for all related processes to produce bleached kraft pulp sheets from wood, such as forest operations, off-site chip production, on-site production of chips, production of pulps, papermaking operations and transportation (AF&PA, 2010).

3.2. Valley beating route

A Valley beater is one of the common mechanical pretreatment methods for CNF production where the pulps are looped around a well and refined between a rotor bar and loaded bedplate (TAPPI T200 sp-01). Prior to the mechanical pretreatment process, bleached kraft pulp sheets were assumed to be cut into small pieces and soaked in deionized water at least for four hours. The mechanical pretreatment with a Valley beater is described by Spence et al. (2011). The process was performed for three hours at the initial pulp consistency of 2%. Total energy necessary for this process was calculated based on the report by Atic et al. (2005). The pretreated cellulose pulp was assumed to be loaded into a high pressure homogenizer without drying and passed through the homogenizer five times at operating pressure of 500-800 bar. Energy required by the homogenizer was assumed to be 25,000 kWh/ton, which is considered as an average value of energy required for the high pressure homogenization.

3.3. Shear cutting route

Shear cutting process is a proposed mechanical pretreatment in this study. The raw material for this route was bleached kraft pulp sheets produced as described above. The pulp sheet pieces were cut into small pieces and milled three times through a shear cutting mill, known as a knife mill with a screen size of 0.25 mm. Energy required for shear cutting process was measured using an energy data logger. Knife-milled cellulose powder was suspended and heated with deionized water at a solid content of 2 wt.% together with carboxymethylcellulose (CMC, 0.25wt% in water, average molecular weight: 250 kD). The cellulose suspension was passed five times through a high pressure homogenizer at 500-800 bar. Energy for the high pressure homogenization was assumed to be 25,000 kWh/ton as same as for the Valley beating route. Other than energy, data for this processing route was obtained from experiments.

3.4. Alkaline pretreatment route

The alkaline pretreatment route started with bleached kraft pulp as other routes. Cellulose powder was obtained using a shear cutting mill as described earlier. 2wt% NaOH solution was prepared with carboxymethylcellulose (CMC, 0.25wt% in water, average molecular weight: 250 kD) and pre-cooled in a freezer. The frozen solid was broken into ice slush at room temperature. Afterward, cellulose powder was added and mixed with the ice slush at the cellulose solid content of 2wt.%, and then placed in an ice bath at least for 15 minutes. Cellulose/NaOH aqueous slurry was left at room temperature to make sure all ice fragments were thawed. The high pressure homogenization with three or four passes at 500-800 bar would be sufficient to produce CNF from cellulose/NaOH suspension. Alkali-treated CNF was dialyzed against deionized water until neutrality and filtrated to make a CNF gel at the solid content of 2wt%. Data for this route was obtained from experiments.

3.5. Key assumptions

1. We assumed that high pressure homogenization in the Valley beating route and shear cutting route is performed under the same operating conditions (e.g. the number of processing cycles, operating pressure and cellulose solid content). Energy required for this process is assumed to be 25,000 kWh/ton, which is considered as the average value of energy for the high pressure homogenization.

2. Cellulose nanofibrils (CNF) was successfully prepared from alkali-treated cellulose suspension after passing through a French cell press with 10 passes, while additional 5 passes were needed to obtain CNF from the cellulose aqueous suspension with CMC. Thus, we can expect that alkali-treated cellulose nanofibrils would be prepared using a high pressure homogenizer with the fewer number of processing cycles than untreated cellulose nanofibrils was prepared. We assumed that the mechanical disintegration process in the alkaline pretreatment route required two-thirds of the energy required by the mechanical disintegration process in the shear cutting route.

3. We assumed that cellulose nanofibrils was produced at the same plant where the raw material (bleached kraft pulp) was produced. Therefore, transportation from the pulp mill to the CNF plant was excluded in this study. Transportation for chemicals (sodium hydroxide and carboxymethylcellulose) was not included as the production routes with chemicals used are still at laboratory stage and the location of the production units have not been determined. In addition, process equipment manufacturing was also excluded since its contributions are considered negligible over the life of the equipment.

4. Regarding the percent loss in mass during processing, it was basically assumed to be 3%. However, the mass lose percent was higher than 3% in some processes. In case of the shear cutting process, the sample weight was measured before and after every cycle, and approximately 5% of pulp in mass was lost after each cycle; thus, the total mass loss percent after shear cutting with three cycles is estimated to be 15%. With respect to the alkaline pretreatment route, total mass loss was measured and determined to be 10% during homogenization, rinsing, and filtration.

5. For calculating the energy to freeze 2wt% NaOH solution, we assumed that heat capacity and crystallization energy of 2wt% NaOH solution were the same as those of water (4.18 kJ/kg ℃ and 333kJ/kg, respectively) for simplicity. Detailed information is provided in the supporting information (SI) in Appendix C.

6. We assumed that 20% of energy used is released as heat to atmosphere during all processes.

4. Life cycle inventory analysis (LCI)

This LCA study was performed using the method as described by the ISO standard (ISO 14040, 2006). All input and output data used in this study were obtained from bench scale experimental data, the LCI databases within Simapro version 8 (Ecoinvent v 3 and USLCI v.1.6.0), and literature sources (Atic et al. 2005; AF&PA 2010; Spence 2011). USLCI database was used to extract data for chemicals and materials used in this study. For some chemicals that are not available from USLCI database, the European database was selected as similar technologies are used to manufacture those selected chemicals. Electricity mix used in this study was assumed to be a low-voltage average for the US grid (approximately 57% coal, 22% nuclear, 17% natural gas and 4% others) obtained from the USLCI database.

Table 5.1 summarizes the inputs for manufacturing one kg of cellulose nanofibrils using three different production routes. Detailed input and output data is provided in the SI. The yield of cellulose nanofibrils depended on the production route used. The mass yield of the final product was 94%, 83% and 77% in the Valley beating route, shear cutting route and alkaline pretreatment route, respectively (1.06 kg, 1.20 kg and 1.30 kg of the bleached kraft pulp was used to prepare one kg of CNF, respectively). The difference between the Valley beating and shear cutting routes is mainly attributed to that the shear cutting process was repeated three times with 5% mass loss per every cycle. Thus, total 15% of pulp was lost after three-cycle shear cutting process as mentioned earlier. The further decrease in the yield of alkali-treated CNF is because the alkaline pretreatment route required additional neutralization and filtration process.

Major air emissions for producing one kg of cellulose nanofibrils in all three production routes were described in Table 5.2. Fossil CO_2 eq. emission was much higher than other air emissions and ranged from 23.7 to 27.3 kg per kg of CNF. It was mainly generated from the fossil fuels burned to produce electricity; therefore, the more energy-consuming route, the more fossil CO_2 was generated. If the electricity is generated from renewable sources, total CO_2 eq. emission would be greatly reduced by 60%. Biogenic CO_2 came from hog fuel or natural gas combusted for pulp production. As the alkaline pretreatment route required the highest amount of bleached kraft pulp to produce CNF, this route had the largest biogenic CO_2 eq. emission.

5. Life cycle impact assessment (LCIA)

Life cycle impact assessment was performed using the impact assessment methods in the Simapro package (TRACI v 4, BEES v 4.02 and CED v 1.08). Total eleven different impact categories were evaluated. TRACI allowed us to analyze nine environmental impacts: global warming, acidification, carcinogenics, non- carcinogenics, respiratory effects, eutrophication,

ecotoxicity, smog, and ozone depletion. Water intake and fossil energy consumption were calculated by using BEES and CED method, respectively. Table 5.3 shows the cradle-to-gate life cycle impacts of producing one kg of CNF from three different production routes, and Figure 5.2 presents the comparative life cycle impact assessment of these three routes. The Valley beating route had the highest impacts for five impact categories: global warming, smog, acidification, respiratory effects and fossil energy consumption since its total required energy was higher compared with that of other two routes. The alkaline pretreatment route showed the lowest impact values for these five categories as this route was the least energy-demanding route; while it had the highest impact values for other six categories due to the high water consumption during neutralization. In case of the shear cutting route, this route had the impact values in the middle of the values of other two routes. The most investigated impact categories for nanocellulose production, such as fossil energy consumption, global warming potential, water intake, and eutrophication potential were further discussed in the following sections, see the SI for the detailed results.

5.1. Fossil energy consumption

Fossil energy consumption is an important impact category since high energy use in the mechanical disintegration process has been a main challenge in CNF production. The life cycle assessment result showed that 95-99% of total energy for producing CNF was generated from fossil-based resources. 403.73 MJ, 371.46 MJ and 350.96 MJ of fossil energy was required to produce one kg of CNF from the Valley beating route, shear cutting route, and alkaline pretreatment route, respectively. As expected, most of fossil energy (70%, 87%, and 58% for each route) was consumed to generate electricity used for the mechanical disintegration process. The Valley beating route consumed a higher amount of fossil energy than the shear cutting route

because the Valley beater is more energy-intensive compared with the shear cutting mill. Besides, the alkaline pretreatment route had a lower fossil energy consumption than the shear cutting route although it included additional steps for alkaline pretreatment. This is because the alkaline pretreatment helps cellulose fibers to be delaminated, reducing the number of cycles and thus energy requirement for the disintegration process. The effect of energy required for the mechanical disintegration process on fossil energy consumption is further studied in the sensitive analysis.

5.2. Global warming potential (GWP)

Global warming impact is calculated based on the global warming potentials due to different greenhouse gases (GHG) produced during the life cycle of products manufactured, mainly CO_2, CH_4 and N_2O. The total global warming potential for the Valley beating route was 28.84 kg CO_2 eq. as compared with 26.49 kg CO_2 eq. and 25.07 kg O_2 eq. for the shear cutting route and the alkaline pretreatment route, respectively. The electricity usage for the mechanical disintegration process was the main contributor to the global warming, producing 70%, 87%, and 58% of total greenhouse gases in the Valley beating route, shear cutting route, and alkaline pretreatment route, respectively. In the first route, the electricity required for mechanical pretreatment also contributed to the increase in GWP, generating 25% of total GHG emissions. This indicated that replacing a Valley beater to a shear cutting mill could reduce total GHG emissions of cellulose nanofibrils production. It is worth noting that the alkaline pretreatment route had a less significant impact on global warming than the shear cutting route. This is because using alkaline pretreatment reduced energy required for the mechanical disintegration process as mentioned previously. Consequently, reducing the energy for the mechanical

disintegration process is the key to reduce total GWP of CNF production. This is further studied in the sensitive analysis.

5.3. Water intake

The cradle-to-gate water intake of one kg of cellulose nanofibrils was 2,121 L, 4,319 L, and 14,933 L for the Valley beating route, shear cutting route and the alkaline pretreatment route, respectively. For the first route, the pulp production was the main process responsible for water use, requiring 1,630 L of water. More specifically, 72% of total water (1,521 L) was needed to produce sodium chlorate used for pulp bleaching. The shear cutting route requires a higher amount of water than the Valley beating route due to the use of carboxymethylcellulose (CMC), A total of 1,998 L water was used for CMC production. In addition, high water intake for the alkaline pretreatment route was attributed to the neutralization process where 69% of the total water required in this route was used. The total volume of water needed for neutralization was approximately 20 times larger than the volume of alkali-treated cellulose nanofibrils as the nano-scale structure of CNF would make difficulties in removing ions. If the water in this process is recycled, the total water usage in the alkaline pretreatment route would be significantly reduced. The effects of water recovery are further discussed in the sensitive analysis.

5.4. Eutrophication potential

Eutrophication potential is calculated based on the total amount of the substances that contain available nitrogen or phosphorus. The eutrophication potential for the Valley beating route was 6.40 g N eq. as compared with 8.45 g N eq. and 14.1 g N eq. for the shear cutting route and the alkaline pretreatment route, respectively. The main process responsible for eutrophication was different for each route. For the first route, the pulp production was the major contributing factor to eutrophication. 43% of total N eq. emissions was generated from the pulp

production, mostly derived from the production of sodium chlorate used for pulp bleaching. The shear cutting route had a higher eutrophication potential than the Valley beating route although the energy required by a shear cutting mill was lower than by a Valley beater. This is mainly because this route needed carboxymethylcellulose (CMC) of which production contributed to the eutrophication. Specifically, 61% of total N eq. emissions (4.9 g N eq.) was released from the mechanical disintegration process; 33% (2.8 g N eq.) from the electricity production and 25% (2.1 g N eq.) from the CMC production. The highest eutrophication potential of the alkaline pretreatment route was because this route included the neutralization process where a vast amount of deionized water was consumed. Deionized water production generated approximately 5.5 g N eq. emission. As mentioned earlier, the reduced water use during neutralization would be critical to reduce the impacts of the third cycle on eutrophication.

6. Sensitive analysis

A sensitive analysis was conducted to investigate the uncertainties in the production routes as the CNF production system is still under development (Figure 5.3). Four factors were discussed in the sensitive analysis; (1) energy use for the mechanical pretreatment process (MP energy) (2) energy use for the mechanical disintegration process (MD energy), (3) the final solid content of cellulose nanofibrils, and (4) water use for neutralizing alkali-treated cellulose nanofibrils. Firstly, we found the deviation in energy demand for both mechanical pretreatment process and mechanical disintegration process. For instance, energy necessary for shear cutting of bleached kraft pulp ranged from 1,096 kWh/ton to 1,727 kWh/ton. It was reported that energy for high pressure homogenization reached as high as 70,000 kWh/ton (Eriksen et al. 2008). Thus, the sensitivity of the energy required for the mechanical pretreatment process and mechanical disintegration process was conducted using 20% deviation. Besides, cellulose nanofibrils is

usually produced at solid contents of 0.5-5%, mostly 2-3% using a high pressure homogenizer (Turbak et al. 1983; Pääkkö et al. 2007; Kekäläinen et al. 2015). The increase in the solid content could reduce specific energy consumption for producing CNF, leading to the reduction in the environmental impacts. To analyze the effect of CNF solid content on the environmental impacts of CNF, the sensitive analysis was performed with increased solid content of 5%. Lastly, the high water use for neutralization is a major obstacle in the alkaline pretreatment route. As mentioned earlier, if the water recycling system is introduced during the neutralization process, the water consumption in this route would be significantly reduced; thus, the corresponding environmental impacts would be also reduced. To investigate the sensitivity of water required for neutralizing alkali-treated CNF, it is designed as the total water volume for the neutralization process would be reduced by 80% if the water is efficiently recovered during the process.

6.1. Fossil energy consumption

Among the four factors, the change in CNF solid content made the remarkable change in fossil energy consumption. With CNF solid content of 5%, fossil energy consumption was reduced by 43%, 54%, and 53% for the Valley beating route, shear cutting route and alkaline pretreatment route, respectively, since the increased CNF solid content led to the reduction in specific energy for the mechanical disintegration process. Fossil energy consumption was also sensitive to energy required for the mechanical disintegration process. When the energy for the disintegration process was reduced by 20%, the total fossil energy consumption was reduced by between 12% and 15%. Other two factors did not have a significant influence on fossil energy consumption. Therefore, the considerable reduction in fossil energy use could be achieved by increasing solid content of CNF and reducing energy use in the mechanical disintegration process.

6.2. Global warming potential (GWP)

Overall, CNF solid content had a significant effect on global warming potential. For the Valley beating route, GWP value was reduced by 39% when the solid content of CNF increased from 2wt% to 5wt.%. Other production routes also reduced GWP values approximately by 50% with increasing the solid content to 5wt.%. This is because the increase in CNF solid content results in the reduction in total electricity use for the mechanical disintegration process per kg of CNF as mentioned above. Change in the energy required for the mechanical disintegration process also affected the global warming potential in all three routes. 20% change in the disintegration energy caused around 14%, 15%, and 11% change in GWP values for each route. On the other hand, the effects of energy used for the mechanical pretreatment process and water used for the neutralization process were not significant. Consequently, increasing CNF solid content is the most obvious way to reduce its global warming potential.

6.3. Water intake

The change in energy input did not make any difference in total water intake of CNF production since water was not needed to generate electricity used in this study (a low-voltage average for the US grid). Water intake is sensitive to CNF solid content. Total water intake value could be reduced by 15%, 36% and 53% with the increased solid content of 5% for the Valley beating route, shear cutting route and alkaline pretreatment route, respectively. The more significant effect of CNF solid content for the third route can be explained by the fact that increased solid content reduces the water use not only to prepare cellulose suspension but also to neutralize alkali-treated cellulose nanofibrils. In addition, the reduction in water consumption for neutralization by recycling also greatly decreased the water intake value by 55%. Consequently, the increase in the solid content of CNF would significantly reduce cradle-to-gate water demand

for producing CNF. For the alkaline pretreatment route, the water recovery during neutralization would be an additional way to reduce water intake.

6.4. Eutrophication potential

Eutrophication potential was sensitive to the solid content of cellulose nanofibrils as other impacts. When CNF solid content was increased to 5wt% from 2wt%, eutrophication potential was reduced by 26%, 37%, and 46% for Valley beating route, shear cutting route, and alkaline pretreatment route, respectively. This is because the increased CNF solid content reduced specific energy consumption as well as the total required amount of chemicals, such as carboxymethylcellulose and sodium hydroxide. The introduction of water recovery system during neutralization also notably reduced eutrophication potential for the alkaline pretreatment route by 31%. In addition, 20% change in energy for the mechanical disintegration process caused 8%, 9%, and 3% change in eutrophication for each route, while the change in energy for mechanical pretreatment process did not significantly affect the eutrophication potential. Consequently, all three routes could reduce their eutrophication potential by increasing CNF solid content. The alkaline pretreatment route could further reduce by introducing the water recovery system during neutralization.

7. Comparison to other carbon nanomaterials

The LCA results obtained in this study were compared with the previous LCA results of producing carbon nanomaterials, such as cellulose nanofibrils (Li et al. 2013; Arvidsson et al. 2015); cellulose nanocrystals (Figueirêdo et al. 2012; Gu et al. 2015); and carbon nanotubes (Gavankar et al. 2014).

The LCA study by Li et al. (2013) showed that GWP of lab-scale CNF production ranged from 190 kg CO_2 eq./kg to 1,160 kg CO_2 eq./kg. The lowest value was obtained from TEMPO

oxidation and homogenization (TOHO) route, and the highest value was from chloroacetic acid etherification and sonication (CESO) route. The cumulative energy demand (CED) value of TOHO and CESO routes was 3,500 MJ/kg and 17,600 MJ/kg, respectively. Such high GWP and CED values of CESO route are attributed to a high input of organic solvents (70 kg of ethanol and isopropanol per kg CNF) and the absence of solvent recovery system. Arvidsson et al. (2015) also demonstrated the CNF fabrication with chemical pretreatment by carboxymethylation had the high impacts on GWP and CED. The carboxymethylation route caused 100 kg CO_2 eq./kg for GWP and 1,800 MJ/kg for CED. These values are much lower than those reported by Li et al. since this route required a relatively low chemical input (30 kg per kg CNF) and included solvent recovery. In this LCA study, CNF production route without any pretreatment was also investigated. The results obtained were 1.2-23 kg CO_2 eq./kg for GWP and 240-320 MJ/kg for CED. The environmental impacts of CNF from the no pretreatment route strongly depended on the electricity mix used since the electricity use for the mechanical disintegration process is the main contributor to the CNF environmental impacts. The lowest values were obtained with Swedish electricity mix, which has approximately half hydro and half nuclear, and the highest values were obtained with a coal-dominated electricity mix which has >90% coal.

Regarding the LCA results of cellulose nanocrystals (CNC) production, Figueirêdo et al. (2012) reported that CNC production required a high amount of energy and water. 1,800-16,000 MJ of energy and 131-138 m^3 of water were required, while 120-1,100 kg CO_2 eq. emissions was generated to produce one kg of CNC. Gu et al. (2015) assessed the life cycle impacts of pilot-scale CNC production. The result obtained were 1,000 MJ for energy use, 29.6 kg CO2 eq. for global warming potential and 50 g N eq. for eutrophication potential.

In addition, Gavankar et al. (2014) reviewed the energy use for CNT production. The required energy for manufacturing one kg of CNT ranged from 480 MJ to 630,000 MJ. They also reported the impacts of CNT production on global warming and eutrophication. The results showed that direct and indirect CO_2 eq. emission was 64,400 kg and 754,000 kg, respectively, and total N eq. emission was 356 kg to manufacture one kg of single wall carbon nanotubes (SWCNT). When comparing these previous LCA results for carbon nanomaterials, cellulose nanofibrils produced from the three production routes in this study has low environmental impacts compared with CNF produced with the chemical pretreatment and other carbon nanomaterials, such as cellulose nanocrystals and carbon nanotubes. Its environmental impacts were comparable to those of CNF produced without any pretreatment.

8. Conclusions

The present LCA study assessed the cradle-to-gate life cycle environmental impacts for bench-scale cellulose nanofibrils production from three different production routes: (1) Valley beating route, (2) Shear cutting route, and (3) Alkaline pretreatment route. The results of this study showed that the alkaline pretreatment route had the highest values for water-related impact categories, such as eutrophication and water intake, due to high water use during neutralization. In contrast, this route had the lowest values for the energy-related impact categories, such as global warming and fossil energy consumption. This is because that integration of mechanical pretreatment with a shear cutting mill and alkaline pretreatment facilitates the mechanical disintegration process easily, reducing the energy required for this process. Moreover, the sensitive analysis results indicated that the increase in CNF solid content caused the most significant reductions in environmental impacts of CNF produced from all three production

routes. Thus, opportunities exist to reduce environmental impacts of producing CNF by using efficient disintegration methods which can increase CNF solid content.

References

Abe, K., Yano, H., 2009, Comparison of the characteristics of cellulose microfibril aggregates of wood, rice straw and potato tuber, Cellulose, 16:1017–1023.

AF&PA, 2010, Printing & Writing Papers Life-Cycle Assessment Summary Report, American Forest & Paper Association, Washington, DC, United States.

Arvidsson, R., Nguyen, D., Svanstrom M., 2015, Life cycle assessment of cellulose nanofibrils production by mechanical treatment and two different pretreatment processes, Environ. Sci. Technol., 49:6681-6890.

Atic, C., Immamoglu, S., Valchev, I., 2005, Determination of specific beating energy-applied on certain pulps in a valley beater, J. Univ. Chem. Technol. Met., 40(3):199–204.

Cowie, J., Bilek, E.M., Wegner, T.H., Shatkin, J., 2014, Market projections of cellulose nanomaterial-enabled Products-Part 2: Volume estimates, Tappi Journal, 13(6):57-67.

Figueirêdo, M.C.B., Rosa, M.F., Ugata, C.N.L., Filho M.S.M.S., Braid A.C.C.S., Melo, L.F.L., 2012, Life cycle assessment of cellulose nanowhiskers, Journal of Cleaner Production, 35:130-139.

Fukuzumi, H., Saito, T., Iwata, T., Kumamoto, Y., Isogai, A., 2009, Transparent and high gas barrier films of cellulose nanofibers prepared by TEMPO-mediated oxidation, Biomacromolecules, 10:162-165.

Gavankar, S., Suh, S., Keller, A.A., 2014, The role of scale and technology maturity in life cycle assessment of emerging technologies, Journal of Industrial Ecology, 19(1):51-60.

Gu, H., Reiner, R., Bergman, R., Rudie, A., 2015, LCA study for pilot scale production of cellulose nano crystals (CNC) from wood pulp, In:Proceedings from the LCA XV Conference – A bright green future, Vancouver, British Columbia, Canada, 33-42.

Hohenthal, C., Ovasakainen, M., Bussini, D., Sadocco, P., Pajula, T., Hannele, L., Kautto, J., Salmenkivi, K., 2012, Final assessment of nanoenhanced new products, VTT Technical Research Centre of Finland.

ISO 14040, 2006, Environmental Management – Life Cycle Assessment – Principle and framework, International Organization for Standardization, Geneva, Switzerland.

Kekäläinen, K., Liimantainen, H., Biale, F., Niinimäki, J., 2015, Nanofibrillation of TEMPO-oxidized bleached hardwood kraft cellulose at high solids content, Holzforschung, 69(9):1077-1088.

Kim, H.C., Fthenakis, V., 2013, Life cycle energy and climate change implications of nanotechnologies, Journal of Ind. Ecol., 17(4):528-541.

Klemm, D., Kramer, F., Mortiz, S., Lindstrom, T., Ankerfors, M., Gray, D., Dorris, A., 2011, Nanocelluloses: a new family of nature-based materials, Angew. Chem. Int. Ed., 50(24):5438-5466.

Li, Q., McGinnis, S., Sydnor, C., Wong, A., Renneckar, S., 2013, Nanocellulose life cycle assessment, ACS Sustainable Chem.Eng., 1:919-928.

Pääkkö, M., Ankerfors, M., Kosonen, H., Nykänen, A., Ahola, S., Österberg, M., Ruokolainen, J., Laine, J., Larsson, P., Ikkala, O., Lindström, T., 2007, Enzymatic hydrolysis combined with mechanical shearing and high-pressure homogenization for nanoscale cellulose fibrils and strong gels, Biomacromolecules, 8:1934–1941.

Saito, T., Hirota, M., Tamura, N., Kimura, S., Fukuzumi, H., Heuz, L., Isogai, A., 2009, Individualization of nano-sized plant cellulose fibrils by direct surface carboxylation suing TEMPO catalyst under neutral conditions, Biomacromolecules 7:1687-1691.

Spence, K.L., Benditti, R.A., Rojas, O.J., Habibi, Y., Pawlak, J.J., 2011, A comparative study of energy consumption and physical properties of microfibrillated cellulose produced by different processing methods, Cellulose, 18:1097-1111.

TAPPI, 2001, T200 sp-01, Laboratory beating of pulp (Valley beater method), Technical Association of the Pulp and Paper Industry, Norcross, GA.

TAPPI NANO, 2015, Summary of International Activates on Cellulosic Nanomaterials, Technical Association of the Pulp and Paper Industry, Norcross, GA, Available from: http://www.tappinano.org/media/1096/tc6-world-cnm-activities-summary-july-29-2015.pdf, Last assessed on 06/04/16.

Turbak, A.F., Snyder, F.W., Sandberg, K.R., 1983, Microfibrillated cellulose, a new cellulose product: properties, uses, and commercial potential, J. Appl. Polym. Sci., 37: 815–827.

Yano, H., Nakahara, S., 2004, Bio-composites produced from plant microfiber bundles with a nanometer unit web-like network, Journal of Materials Science, 39:1635-1638.

Table 5.1. Input inventory for producing 1kg of cellulose nanofibrils with three different processing routes.

Production Route	Input	Unit	Quantity
Valley Beating Route	Mechanical Pretreatment		
	Bleached kraft pulp	kg	1.06
	Deionized water	L	52.03
	Electricity	kWh	9.54
	Mechanical Disintegration		
	Electricity	kWh	25.75
Shear Cutting Route	Mechanical Pretreatment		
	Bleached kraft pulp	kg	1.2
	Electricity	kWh	1.79
	Mechanical Disintegration		
	Deionized water	L	50.47
	Carboxymethylcellulose	kg	0.13
	Electricity	kWh	29.57
Alkaline Pretreatment Route	Mechanical Pretreatment		
	Bleached kraft pulp	kg	1.3
	Electricity	kWh	1.929634
	Alkaline Pretreatment		
	Deionized water	L	53.36
	Sodium hydroxide	kg	1.09
	Carboxymethylcellulose	kg	0.14
	Electricity	kWh	6.3
	Mechanical Disintegration		
	Electricity	kWh	18.52
	Neutralization		
	Deionized water	L	1088.89
	Electricity	kWh	0.0022

Table 5.2. Emissions to air per kg cellulose nanofibrils from three production routes.

Substance	Unit	Valley beating route	Shear cutting route	Alkaline pretreatment route
Carbon dioxide, fossil	kg	27.2690	25.0398	23.6769
Carbon dioxide, biogenic	kg	1.2273	1.4074	1.7347
Sulfur dioxide	kg	0.1808	0.1633	0.1513
Nitrogen oxides	kg	0.0733	0.0670	0.0625
Methane	kg	0.0564	0.0507	0.0467
Particulates, unspecified	kg	0.0177	0.0161	0.0147
Carbon monoxide, fossil	kg	0.0158	0.0151	0.0154
Isoprene	kg	0.0122	0.0109	0.0097
Sulfur oxides	kg	0.0082	0.0075	0.0068
Carbon dioxide	kg	0.0049	0.0055	0.0060
Methane, fossil	kg	0.0046	0.0054	0.0068
Particulates, > 10 um	kg	0.0002	0.1704	0.1843

Table 5.3. Life cycle impact assessment of producing one kg of cellulose nanofibrils with three different processing routes.

Impact category	Unit	Valley beating route	Shear cutting route	Alkaline pretreatment route
Ozone depletion	kg CFC-11 eq.	1.57.E-07	2.95.E-07	8.81.E-07
Global warming	kg CO2 eq.	28.84	26.49	25.07
Smog	kg O3 eq.	1.95	1.79	1.67
Acidification	mol H+ eq.	12.88	11.68	10.82
Eutrophication	kg N eq.	6.40.E-03	8.45.E-03	1.41.E-02
Carcinogenics	CTUh	2.88.E-07	3.41.E-07	4.71.E-07
Non carcinogenics	CTUh	1.12.E-06	1.16.E-06	1.75.E-06
Respiratory effects	kg PM10 eq.	3.54.E-02	3.27.E-02	3.13.E-02
Ecotoxicity	CTUe	13.90	13.67	15.10
Water intake (BEES)	liters	2120.80	4319.14	14933.48
Fossil energy consumption (CED)	MJ	403.73	371.46	350.96

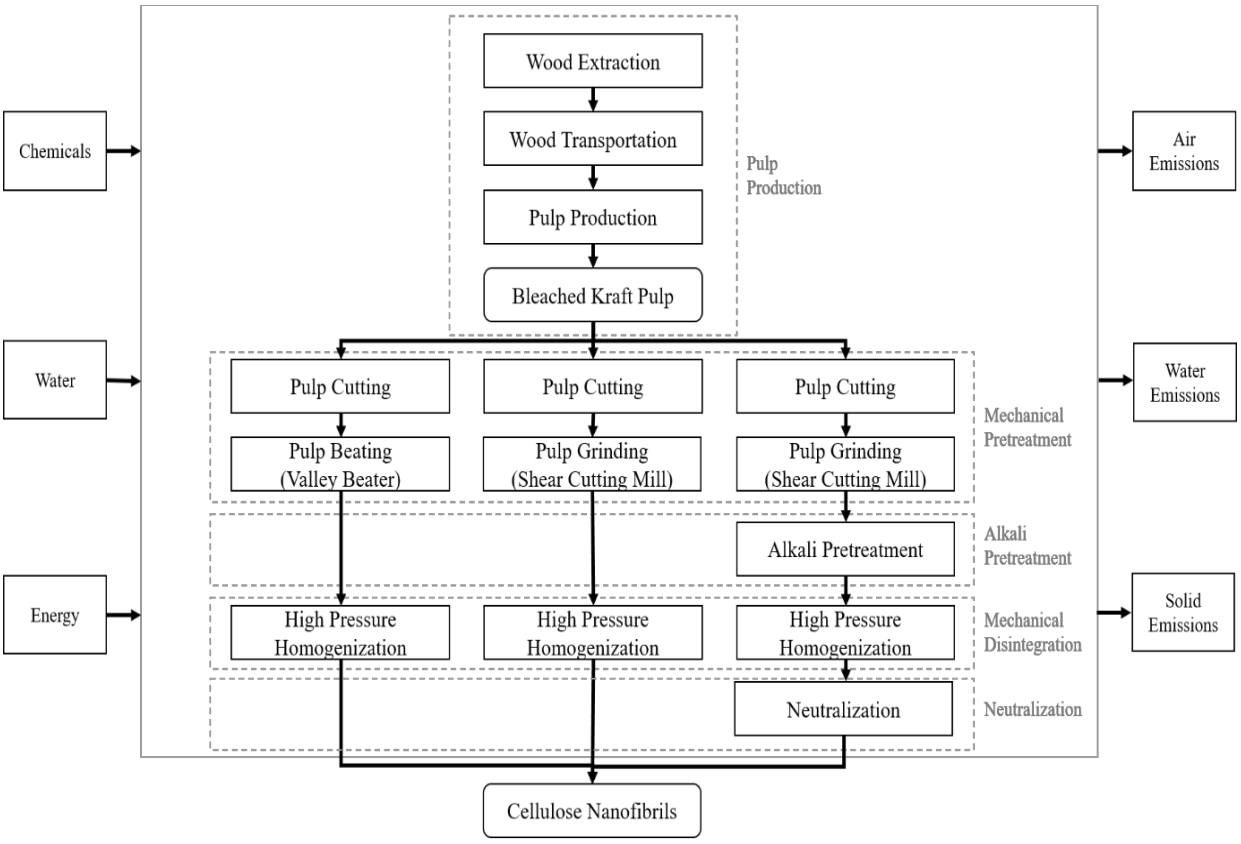

Figure 5.1. A flowchart of CNF production with three different production routes: (1) the Valley beating route (to the left), (2) the shear cutting route (in the middle), and (3) the alkaline pretreatment route (to the right).

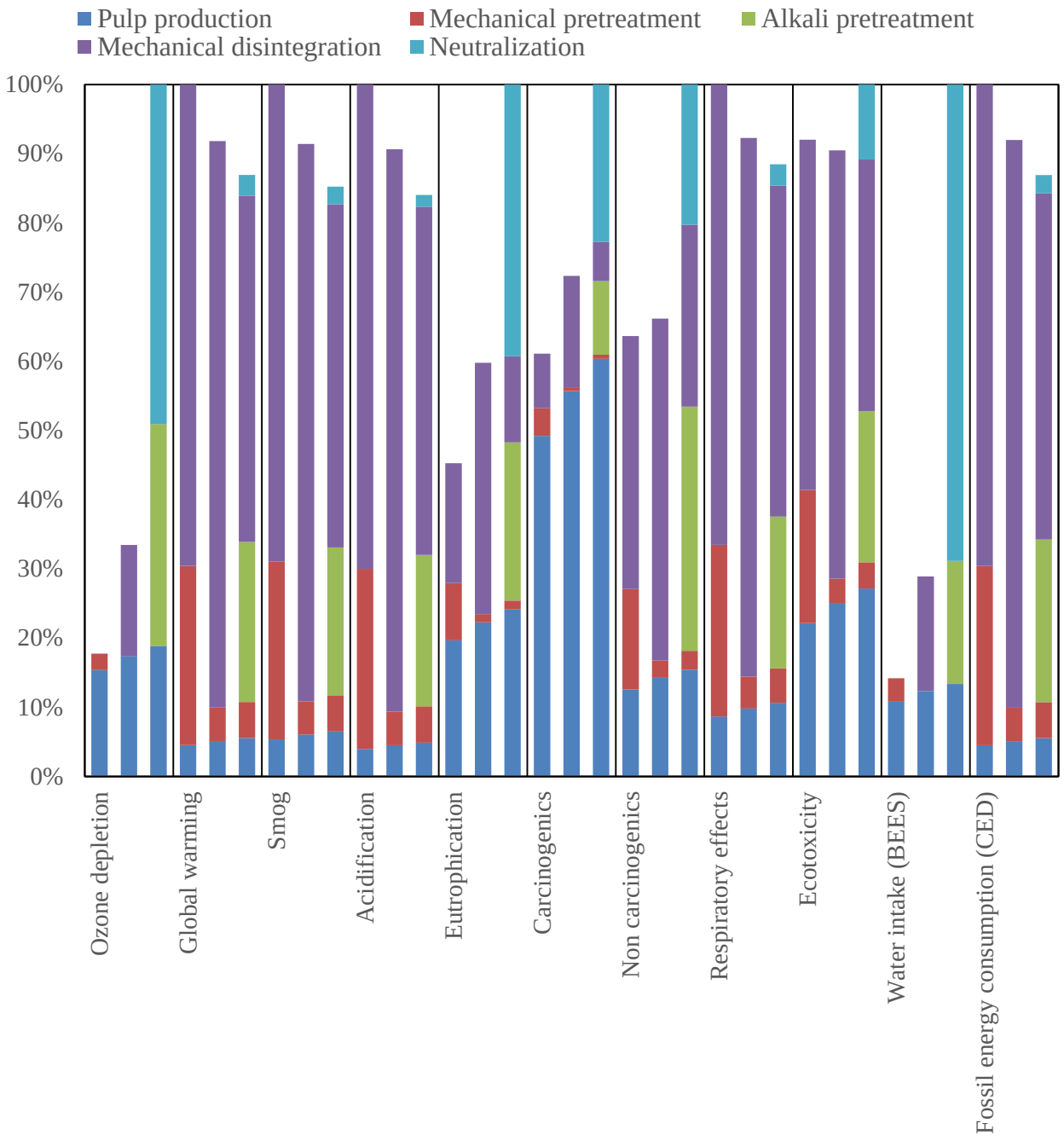

Figure 5.2. Comparative life cycle impact assessments of three different routes; Valley beating route, shear cutting route and alkaline pretreatment route (left to right in each impact category).

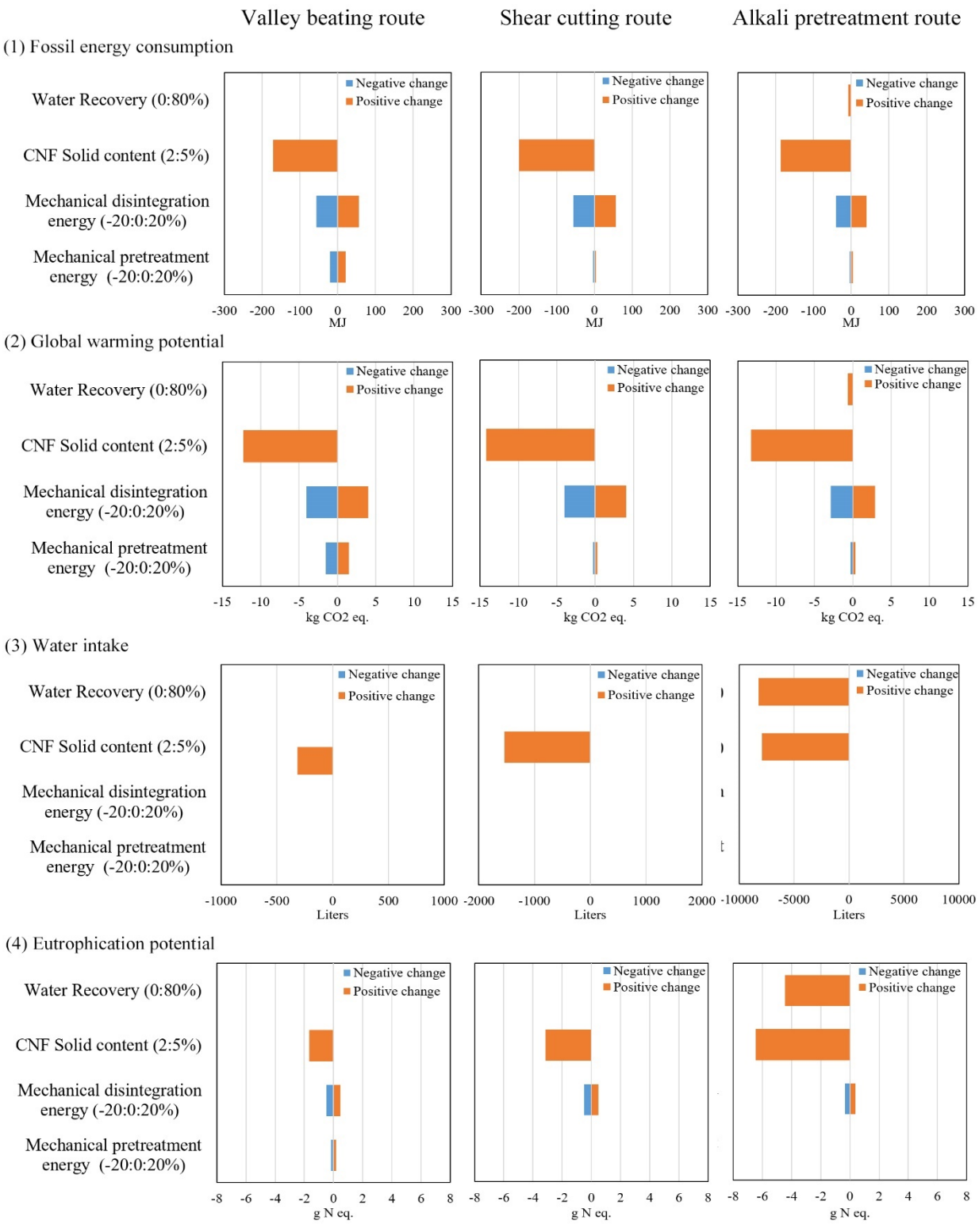

Figure 5.3. Sensitive analysis of four different factors on fossil energy consumption, global warming potential, water intake and eutrophication potential.

CHAPTER 6

CONCLUSIONS AND RECOMMENDATIONS

Cellulose nanofibrils (CNF) is a promising biomaterial for manufacturing of biodegradable composites, flexible electronics and biomedical scaffolds, but the commercial production of CNF is still at an early stage due to high energy consumption and standardization of CNF for specific applications. Several pretreatment methods have been developed to make consistent grade CNF. In this study, cellulose nanofibrils was prepared from fluff cellulose pulp with two alternative pretreatments: mechanical pretreatment using a shear cutting mill and alkaline treatment with low-concentration NaOH (2wt.%). Firstly, shear cutting of fluff pulp with three cycles produced very fine cellulose powder, which can be used as a precursor for CNF production. The three-cycle cellulose powder had a geometric mean diameter of 70 μm and the bulk and tapped densities of 112 kg m^{-3} and 203 kg m^{-3}, respectively and was successfully disintegrated into cellulose nanofibrils using a French cell press without clogging issues. The specific energy required by the shear cutting mill was relatively low (894 kWh/ton) compared with that of other mechanical pretreatment methods. In addition, the shear cutting method produces CNF precursors in the form of dry powder, which can be easily handled and stored. Consequently, the shear cutting method is a potentially effective and economically favorable mechanical pretreatment method for CNF production over other wet milling methods.

Cellulose nanofibrils with improved thermal stability was successfully produced by processing cellulose powder with low-concentration NaOH solution (2wt.%) containing carboxymethylcellulose (CMC) at low temperature, followed by mechanical disintegration

through a French cell press. Its characteristics were comparable with those of standard CNF manufactured at pilot scale. It had an average diameter of 90 nm and a specific surface area of 248 m^2g^{-1} and also presented an excellent dispersion behavior in water. It also exhibited a relatively high thermal stability with the mean onset thermal degradation temperature of 305 ℃ and the mean DTG peak thermal degradation temperature of 343 ℃. In addition, low-concentration NaOH had several advantages over conventional NaOH treatment (17-20 wt.%). It used a lower amount of NaOH and therefore required a lower amount of water during neutralization. CNF produced with low-concentration NaOH was obtained with a lower number of homogenization cycles than that of CNF with high-concentration NaOH.

A cradle-to-gate life cycle assessment (LCA) for the production of CNF using three different routes was conducted to evaluate energy and environmental impacts. The production routes include conventional pretreatment using Valley beating, mechanical pretreatment using shear cutting and a combination of shear cutting and low-concentration alkaline pretreatment. The LCA results showed that the alkaline pretreatment route, which included mechanical pretreatment with a shear cutting mill and alkaline pretreatment, had the lowest environmental impacts on global warming and fossil energy consumption as the electricity energy required for the mechanical disintegration was relatively low. However, the water usage during the neutralization was a shortcoming in this route, leading to increased water intake and eutrophication impacts. Sensitive analysis study showed that opportunities exist to reduce the environmental impacts of CNF production by increasing CNF solid content and introducing water recovery system during alkaline pretreatment.

An integration of pretreatment techniques with shear cutting and low-concentration treatment is a promising approach to produce cellulose nanofibrils with low energy consumption,

improved thermal stability and overall reduction in environmental impacts. Nevertheless, the proposed approach requires further research to validate at pilot-scale production and to evaluate the economic feasibility of producing CNF at commercial scale. Future work can be focused on optimizing the operating parameters and pilot scale testing of this approach to determine its commercial potential.

APPENDIX A

Statistical analysis for Chapter 3:

"Mechanical pretreatment of fluff pulp to produce cellulose nanofibrils (CNF) precursors"

Summary

This appendix includes statistical analysis to determine the effects of grinding amount on the grinding energy and rate, and the properties of the ground samples (Fines percentage, bulk density and tapped density).

Criteria

Null hypothesis: There is no significant difference across the number of the grinding cycles (one to three; zero to three for fines percentage).

One-way ANOVA test was performed with multiple comparisons by Tukey test.

F statistic is smaller than the critical value (p-value is smaller than 0.05), then we fail to reject the null.

1. Specific grinding energy

Table A.1. One-way ANOVA result for specific grinding energy.

Source	DF	Sum of Squares	Mean Square	F Value	Pr > F
Model	2	514762.5675	257381.2838	71.28	<.0001
Error	6	21663.7538	3610.6256		
Corrected Total	8	536426.3213			

Table A.2. Least Squares Means and Adjustment for Multiple Comparisons (Tukey) of specific grinding energy

Cycle	Grinding energy LSMEAN	LSMEAN Number
1	630.401200	1
2	186.290133	2
3	77.505367	3

Least Squares Means for effect cycle
Pr > $|t|$ for H0: LSMean(i)=LSMean(j)

Dependent Variable: Grinding energy

i/j	1	2	3
1		0.0003	<.0001
2	0.0003		0.1464
3	<.0001	0.1464	

2. Grinding rate

Table A.3. One-way ANOVA result for grinding rate.

Source	DF	Sum of Squares	Mean Square	F Value	Pr > F
Model	2	1126.913360	563.456680	44.39	0.0003
Error	6	76.153372	12.692229		
Corrected Total	8	1203.066732			

Table A.4. Least Squares Means and Adjustment for Multiple Comparisons (Tukey) of grinding rate.

Cycle	Grinding rate LSMEAN	LSMEAN Number
1	7.4191667	1
2	23.0713333	2
3	34.7315000	3

Least Squares Means for effect cycle
Pr > $|t|$ for H0: LSMean(i)=LSMean(j)

Dependent Variable: Grinding rate

i/j	1	2	3
1		0.0041	0.0002
2	0.0041		0.0166
3	0.0002	0.0166	

3. Fines percentage

Table A.5. One-way ANOVA result for fines percentage.

Source	DF	Sum of Squares	Mean Square	F Value	Pr > F
Model	3	1879.876092	626.625364	74.11	<.0001
Error	8	67.641200	8.455150		
Corrected Total	11	1947.517292			

Table A.6. Least Squares Means and Adjustment for Multiple Comparisons (Tukey) of fines percentage.

Cycle	Fines percentage LSMEAN	LSMEAN Number
0	5.0633333	1
1	25.8433333	2
2	33.9600000	3
3	37.2166667	4

Least Squares Means for effect cycle Pr > $\|t\|$ for H0: LSMean(i)=LSMean(j) Dependent Variable: Fines percentage				
i/j	1	2	3	4
1		0.0001	<.0001	<.0001
2	0.0001		0.0369	0.0060
3	<.0001	0.0369		0.5482
4	<.0001	0.0060	0.5482	

4. Bulk density

Table A.7. One-way ANOVA result for bulk density.

Source	DF	Sum of Squares	Mean Square	F Value	Pr > F
Model	2	858.8527281	429.4263640	70.74	<.0001
Error	12	72.8438954	6.0703246		
Corrected Total	14	931.6966235			

Table A.8. Least Squares Means and Adjustment for Multiple Comparisons (Tukey) of bulk density.

Cycle	Bulk density LSMEAN	LSMEAN Number
1	94.106360	1
2	96.692620	2
3	111.294120	3

Least Squares Means for effect cycle
Pr > $|t|$ for H0: LSMean(i)=LSMean(j)

Dependent Variable: Bulk density

i/j	1	2	3
1		0.2599	<.0001
2	0.2599		<.0001
3	<.0001	<.0001	

5. Tapped density

Table A.9. One-way ANOVA result for tapped density.

Source	DF	Sum of Squares	Mean Square	F Value	Pr > F
Model	2	3215.056105	1607.528052	369.86	<.0001
Error	12	52.155509	4.346292		
Corrected Total	14	3267.211613			

Table A.10. Least Squares Means and Adjustment for Multiple Comparisons (Tukey) of tapped density.

Cycle	Tapped density LSMEAN	LSMEAN Number
1	169.403040	1
2	176.268400	2
3	203.317960	3

Least Squares Means for effect cycle
Pr > $|t|$ for H0: LSMean(i)=LSMean(j)

Dependent Variable: Tapped density

i/j	1	2	3
1		0.0006	<.0001
2	0.0006		<.0001
3	<.0001	<.0001	

APPENDIX B

Statistical analysis for Chapter 4:

"Development of thermally stable cellulose nanofibrils using low-concentration alkaline treatment"

Summary

This appendix includes statistical analysis to determine the effects of NaOH concentrations and CMC addition on cellulose solubility and the properties of the fibrillated cellulose samples (crystallinity, and onset and DTG peak thermal degradation temperate).

Criteria

Null hypothesis: There is no significant difference across the NaOH concentration (0, 2, 4, and 6 wt.%) and whether CMC is added or not.

Two-way ANOVA test was performed with multiple comparisons by Tukey test.

F statistic is smaller than the critical value (p-value is smaller than 0.05), then we fail to reject the null.

1. Cellulose solubility

Table B.1. Two-way ANOVA result for cellulose solubility.

Source	DF	Type III SS	Mean Square	F Value	Pr > F
CMC	1	1.4964500	1.4964500	0.28	0.6047
NaOH	2	890.9083444	445.4541722	84.12	<.0001
CMC*NaOH	2	11.7919000	5.8959500	1.11	0.3601

Table B.2. Least Squares Means and Adjustment for Multiple Comparisons (Tukey) of cellulose solubility.

CMC	NaOH	Cellulose solubility LSMEAN	LSMEAN Number
N	2	4.8366667	1
N	4	13.8000000	2
N	6	23.5000000	3
Y	0	7.6666667	4
Y	2	12.9000000	5
Y	6	23.3000000	6

Least Squares Means for effect cycle
Pr > $|t|$ for H0: LSMean(i)=LSMean(j)

Dependent Variable: Cellulose solubility

i/j	1	2	3	4	5	6
1		0.0047	<.0001	0.6672	0.0104	<.0001
2	0.0047		0.0025	0.0586	0.9961	0.0030
3	<.0001	0.0025		<.0001	0.0012	1.0000
4	0.6672	0.0586	<.0001		0.1279	<.0001
5	0.0104	0.9961	0.0012	0.1279		0.0014
6	<.0001	0.0030	1.0000	<.0001	0.0014	

2. Cellulose crystallinity

Table B.3. Two-way ANOVA result for cellulose crystallinity.

Source	DF	Type III SS	Mean Square	F Value	Pr > F
CMC	1	5.736296	5.736296	0.28	0.6059
NaOH	3	1215.046897	405.015632	19.92	<.0001
CMC*NaOH	1	11.760000	11.760000	0.58	0.4629

Table B.4. Least Squares Means and Adjustment for Multiple Comparisons (Tukey) of cellulose crystallinity

CMC	NaOH	Cellulose crystallinity LSMEAN	LSMEAN Number
N	2	75.0333333	1
N	4	57.2000000	2
N	6	58.0666667	3
Y	0	73.3666667	4
Y	2	75.6666667	5
Y	6	54.5000000	6

Least Squares Means for effect cycle
Pr > $|t|$ for H0: LSMean(i)=LSMean(j)

Dependent Variable: Cellulose crystallinity

i/j	1	2	3	4	5	6
1		0.0052	0.0074	0.9969	1.0000	0.0041
2	0.0052		0.9999	0.0104	0.0040	0.9835
3	0.0074	0.9999		0.0151	0.0057	0.9471
4	0.9969	0.0104	0.0151		0.9866	0.0077
5	1.0000	0.0040	0.0057	0.9866		0.0033
6	0.0041	0.9835	0.9471	0.0077	0.0033	

3. Onset thermal degradation temperature

Table B.5. Two-way ANOVA result for onset thermal degradation temperature.

Source	DF	Type III SS	Mean Square	F Value	Pr > F
CMC	1	754.9203857	754.9203857	110.42	<.0001
NaOH	3	712.8935092	237.6311697	34.76	<.0001
CMC*NaOH	2	3.8123744	1.9061872	0.28	0.7614

Table B.6. Least Squares Means and Adjustment for Multiple Comparisons (Tukey) of onset thermal degradation temperature.

CMC	NaOH	Onset thermal degradation temp. LSMEAN	LSMEAN Number
N	2	320.046667	1
N	4	318.686667	2
N	6	314.980000	3
Y	0	286.510000	4
Y	2	304.833333	5
Y	4	305.850000	6
Y	6	301.060000	7

Least Squares Means for effect cycle
Pr > $|t|$ for H0: LSMean(i)=LSMean(j)

Dependent Variable: Onset thermal degradation temp.

i/j	1	2	3	4	5	6	7
1		0.9939	0.2872	<.0001	0.0002	0.0010	<.0001
2	0.9939		0.6076	<.0001	0.0004	0.0023	0.0001
3	0.2872	0.6076		<.0001	0.0063	0.0291	0.0012
4	<.0001	<.0001	<.0001		<.0001	<.0001	0.0008
5	0.0002	0.0004	0.0063	<.0001		0.9993	0.6959
6	0.0010	0.0023	0.0291	<.0001	0.9993		0.5531
7	<.0001	0.0001	0.0012	0.0008	0.6959	0.5531	

4. DTG peak thermal degradation temperature

Table B.7. Two-way ANOVA result for DTG peak thermal degradation temperature.

Source	DF	Type III SS	Mean Square	F Value	Pr > F
CMC	1	85.3856679	85.3856679	9.45	0.0097
NaOH	3	716.4207021	238.8069007	26.42	<.0001
CMC*NaOH	2	67.8668423	33.9334212	3.75	0.0542

Table B.8. Least Squares Means and Adjustment for Multiple Comparisons (Tukey) of DTG peak thermal degradation temperature.

CMC	NaOH	DTG Peak thermal degradation temp. LSMEAN	LSMEAN Number
N	2	353.000000	1
N	4	347.223333	2
N	6	344.333333	3
Y	0	326.330000	4
Y	2	342.776667	5
Y	4	346.665000	6
Y	6	341.000000	7

Least Squares Means for effect cycle
Pr > $|t|$ for H0: LSMean(i)=LSMean(j)

Dependent Variable: DTG Peak thermal degradation temp

i/j	1	2	3	4	5	6	7
1		0.2952	0.0475	<.0001	0.0166	0.3137	0.0117
2	0.2952		0.8900	<.0001	0.5648	1.0000	0.3311
3	0.0475	0.8900		0.0001	0.9940	0.9739	0.8758
4	<.0001	<.0001	0.0001		0.0003	0.0001	0.0024
5	0.0166	0.5648	0.9940	0.0003		0.7839	0.9934
6	0.3137	1.0000	0.9739	0.0001	0.7839		0.5238
7	0.0117	0.3311	0.8758	0.0024	0.9934	0.5238	

APPENDIX C

Supporting Information for Chapter 5:

"Life cycle assessment of producing cellulose nanofibrils with mechanical and alkaline pretreatment"

Summary

This appendix contains the calculation for freezing energy needed to freeze the alkali solutions (Section 1), the inventory data for producing cellulose nanofibrils from three different production routes (Section 2 and Tables C1-C3) and the detailed results of the life cycle impact assessment (Section 3 and Table C4) and the sensitive analysis (Section 4 and Table C5).

1. Energy calculation for freezing alkali solutions

In the alkaline pretreatment route, 2wt% NaOH solution was prepared and frozen before cellulose powder was added. The energy required for freezing the NaOH solution was calculated with the assumption that heat capacity and crystallization energy of the NaOH solution are the same as those of water. First, the energy needed to cool it down from room temperature (20 ℃) to 0 ℃ was calculated using the following equation:

$$\mathrm{E} = c \times \mathrm{m} \times \Delta\mathrm{T}$$

where E is the required energy for the temperature change, *c* is the heat capacity of the solvent, m is the mass of the solvent, and ΔT is the temperature change.

In this case, the heat capacity of the solvent is assumed to be the same as that of water (4.18kJ/kg ℃), and the weight of the NaOH solution required for producing 1kg of cellulose nanofibrils is 54.44 kg. Therefore, the required energy for the temperature change is estimated to be 4,552 kJ per 1kg of CNF.

Moreover, the energy for changing from liquid to solid is also needed. It takes 333 kJ to crystallize 1kg of water, thus, 18,130 kJ of energy would be required to crystallize 54.44kg of NaOH solution for manufacturing 1kg of CNF. Consequently, the total energy necessary for freezing the NaOH solution is calculated as 22,682 kJ for producing 1kg of CNF.

2. Inventory data for producing cellulose nanofibrils from three different production routes

Table C1. Inventory data for Valley beating route.

Operation			
Pulp cutting	Inputs	Unit	Quantity
	Bleached Kraft pulp	kg	1.06
	Electricity, Pulp cutter	kwh	0.0062
	Outputs	Unit	Quantity
	Pulp sheet pieces	kg	1.06
	Heat (Air)	MJ	0.0045
Pulp Beating (Valley beater)	Inputs	Unit	Quantity
	Pulp sheet pieces	kg	1.06
	Deionized water	L	52.03
	Electricity, Valley beater	kwh	9.54
	Outputs	Unit	Quantity
	Beaten pulp	kg	1.03
	Heat, waste (Air)	MJ	6.87
	Pulp lost (Water)	kg	0.03
	Water (Water)	kg	1.56
High pressure homogenization	Inputs	Unit	Quantity
	Beaten pulp	kg	1.03
	Electricity, High pressure homogenizer	kwh	25.75
	Outputs	Unit	Quantity
	Cellulose nanofibrils	kg	1.00
	Heat, waste (Air)	MJ	18.54
	Cellulose nanofibrils lost (Water)	kg	0.03
	Water (Water)	kg	1.47

Table C2. Inventory data for shear cutting route

Operation			
Pulp Cutting	Inputs	Unit	Quantity
	Bleached Kraft pulp	kg	1.20
	Electricity, Pulp cutter	kwh	0.0070
	Outputs	Unit	Quantity
	Pulp sheet pieces	kg	1.20
	Heat (Air)	MJ	0.0051
Pulp Grinding (Shear cutting mill)	Inputs	Unit	Quantity
	Pulp sheet pieces	kg	1.20
	Electricity, Shear cutting mill	kwh	1.78
	Outputs	Unit	Quantity
	Cellulose powder	kg	1.03
	Cellulose powder lost (Air)	kg	0.17
	Heat (Air)	MJ	1.28
High pressure homogenization	Inputs	Unit	Quantity
	Cellulose powder	kg	1.03
	Deionized water	L	50.47
	Carboxymethylcellulose	kg	0.13
	Electricity, High pressure homogenizer	kwh	25.75
	Electricity, Heater	kwh	3.52
	Electricity, Stirrer	kwh	0.30
	Outputs	Unit	Quantity
	Cellulose nanofibrils	kg	1.00
	Heat, waste (Air)	MJ	22.48
	Cellulose nanofibrils lost (Water)	kg	0.03
	Water (Water)	kg	1.47

Table C3. Inventory data for alkaline pretreatment route

Operation			
Pulp cutting	Inputs	Unit	Quantity
	Bleached Kraft pulp	kg	1.30
	Electricity, Pulp cutter	kwh	0.0076
	Outputs	Unit	Quantity
	Pulp sheet pieces	kg	1.30
	Heat (Air)	MJ	0.0055
Pulp Grinding (Shear cutting mill)	Inputs	Unit	Quantity
	Pulp sheet pieces	kg	1.30
	Electricity, Shear cutting mill	kwh	1.92
	Outputs	Unit	Quantity
	Cellulose powder	kg	1.11
	Cellulose powder lost (Air)	kg	0.18
	Heat (Air)	MJ	1.38
Alkaline pretreatment	Inputs	Unit	Quantity
	Cellulose powder	kg	1.11
	Deionized water	L	53.36
	Sodium hydroxide	kg	1.09
	Carboxymethylcellulose	kg	0.14
	Electricity, Freezer	kwh	6.30
	Outputs	Unit	Quantity
	Alkali-treated cellulose (Intermediate product)	kg	1.11
High pressure homogenization	Inputs	Unit	Quantity
	Alkali-treated cellulose	kg	1.11
	Electricity, High pressure homogenizer	kwh	18.52
	Outputs	Unit	Quantity
	Alkali-treated cellulose nanofibrils (Intermediate product)	kg	1.03
	Heat, waste (Air)	MJ	13.33
Neutralization	Inputs	Unit	Quantity
	Alkali-treated cellulose nanofibrils	kg	1.03
	Deionized water	L	1088.89
	Electricity, Peristaltic pump	kwh	0.022
	Outputs	Unit	Quantity
	Cellulose nanofibrils	kg	1.00
	Heat, waste (Air)	MJ	0.02
	Waste water (Water)	L	1094.33
	Cellulose nanofibrils lost (Water)	kg	0.11
	Na+ (Water)	kg	0.63

3. Detailed results for the life cycle impact assessment

Table C4. Results for the life cycle impact assessment of producing cellulose nanofibrils from three different production routes.

Unit process	Valley beating route	Shear cutting route	Alkaline pretreatment route
Fossil energy consumption (MJ/kg CNF)			
Pulp production	18.2590	20.6706	22.3931
Mechanical pretreatment	104.6183	19.4911	21.0054
Alkaline pretreatment	0.0000	0.0000	94.9101
Mechanical disintegration	280.8562	331.2942	201.9983
Neutralization	0.0000	0.0000	10.6523
Sum	403.7334	371.4558	350.9592
Global warming potential (kg CO_2 eq./kg CNF)			
Pulp production	1.3101	1.4832	1.6068
Mechanical pretreatment	7.4746	1.3915	1.4996
Alkaline pretreatment	0.0000	0.0000	6.6696
Mechanical disintegration	20.0512	23.6118	14.4213
Neutralization	0.0000	0.0000	0.8763
Sum	28.8359	26.4865	25.0736
Water intake (Liters/kg CNF)			
Pulp production	1629.6159	1844.8482	1998.5855
Mechanical pretreatment	491.1880	0.0000	0.0000
Alkaline pretreatment	0.0000	0.0000	2655.2505
Mechanical disintegration	0.0000	2474.2885	0.0000
Neutralization	0.0000	0.0000	10279.6413
Sum	2120.8039	4319.1366	14933.4773
Eutrophication potential (g N eq./kg CNF)			
Pulp production	2.7822	3.1497	3.4121
Mechanical pretreatment	1.1720	0.1698	0.1830
Alkaline pretreatment	0.0000	0.0000	3.2318
Mechanical disintegration	2.4463	5.1328	1.7595
Neutralization	0.0000	0.0000	5.5495
Sum	6.4005	8.4523	14.1359

4. Detailed results for the sensitive analysis

Table C5. Results for the sensitive analysis

Sensitive Analysis Factor	Valley beating route	Shear cutting route	Alkaline pretreatment route
Fossil energy consumption (MJ/kg CNF)			
Baseline	403.7334	371.4558	350.9592
Low mechanical pretreatment energy (-20%)	382.9010	367.6384	346.8453
high mechanical pretreatment energy (+20%)	424.5659	375.3824	355.1907
Low mechanical disintegration energy (-20%)	347.5622	315.2846	310.4941
High mechanical disintegration energy (+20%)	459.9047	427.6271	391.3152
CNF solid content (5%)	231.8700	171.9586	164.9966
Water recovery for neutralization (+80%)	N/A	N/A	342.8148
Global warming potential (kg CO_2 eq./kg CNF)			
Baseline	28.8359	26.4865	25.0736
Low mechanical pretreatment energy (-20%)	27.3486	26.2140	24.7799
high mechanical pretreatment energy (+20%)	30.3232	26.7668	25.3757
Low mechanical disintegration energy (-20%)	24.8257	22.4763	22.1847
High mechanical disintegration energy (+20%)	32.8461	30.4968	27.9547
CNF solid content (5%)	16.5625	12.2690	11.7919
Water recovery for neutralization (+80%)	N/A	N/A	24.3995
Water intake (Liters/kg CNF)			
Baseline	2120.8039	4319.1366	14933.4773
Low mechanical pretreatment energy (-20%)	2120.8039	4319.1366	14933.4773
high mechanical pretreatment energy (+20%)	2120.8039	4319.1366	14933.4773
Low mechanical disintegration energy (-20%)	2120.8039	4319.1366	14933.4773
High mechanical disintegration energy (+20%)	2120.8039	4319.1366	14933.4773
CNF solid content (5%)	1805.7648	2782.6256	6994.3662
Water recovery for neutralization (+80%)	N/A	N/A	6709.7832
Eutrophication potential (g N eq./kg CNF)			
Baseline	6.4005	8.4523	14.1359
Low mechanical pretreatment energy (-20%)	6.2191	8.4190	14.1001
high mechanical pretreatment energy (+20%)	6.5820	8.4865	14.1728
Low mechanical disintegration energy (-20%)	5.9113	7.9630	13.7834
High mechanical disintegration energy (+20%)	6.8898	8.9415	14.4874
CNF solid content (5%)	4.7363	5.3172	7.6830
Water recovery for neutralization (+80%)	N/A	N/A	9.6996